INDIVIDUAL SYNAPTIC VESICLES FROM THE ELECTROPLAQUE OF TORPEDO CALIFORNICA, A CLASSIC CHOLINERGIC SYNAPSE, CONTAIN MUTLPLE NEUROTRANSMITTER TRANSPORTERS AND SMALL RIBONUCLEIC ACIDS (SRNAS)

A Dissertation

by

HUINAN LI

Submitted to the Office of Graduate and Professional Studies of
Texas A&M University
in partial fulfillment of the requirements for the degree of

DOCTOR OF PHILOSOPHY

Chair of Committee,	Mark L. Harlow
Committee Members,	U. J. McMahan
	Arne C. Lekven
	Mendell Rimer
Head of Department,	Thomas McKnight

May 2016

Major Subject: Biology

ABSTRACT

Large-scale proteomic analyses of heterogeneous CNS preparations, such as isolated CNS synaptic vesicles, have provided a wealth of information related to synapse specific proteins and synaptic signaling pathways. However, these studies under-represent, or lack entirely, many vesicle and neurotransmitter signaling pathways. In particular, the neuromodulatory adrenergic and cholinergic pathways are often under-represented. In order to better understand the molecules and signaling pathways involved at cholinergic synapses, I have focused on the classic preparation of the electric lobe and electric organ of *Torpedo californica*. Many lines of evidence support the idea that in addition to acetylcholine, glutamate and ATP are also released from cholinergic synapses. Utilizing a single-vesicle imaging approach, I have found that individual synaptic vesicles from the electric ray possess neurotransmitter transporters for glutamate, ATP, and acetylcholine. These results help to explain neurotransmitter co-release at cholinergic terminals. In addition to classic neurotransmitter, I have discovered that synaptic vesicles in the peripheral nervous system (PNS) and the central nervous system (CNS) possess small ribonucleic acids, including transfer RNA fragments and microRNAs. This discovery suggests that, in addition to releasing neurotransmitters that can induce local changes in postsynaptic membrane polarization, synaptic vesicles may also release small RNAs that can directly regulate local protein synthesis at the postsynaptic cell.

DEDICATION

This thesis is dedicated to my parents who have supported me all the way since the beginning of my education and my decision to come to the U.S.

Also, this thesis is dedicated to all my teachers who help me constantly improve.

Finally, this thesis is dedicated to all those who firmly have faith in themselves and know that they will realize their dreams even when the chance seems slim…

ACKNOWLEDGEMENTS

I would like to express my deepest appreciation for my committee chair, my advisor Prof. Mark L. Harlow. Thank you for having faith in me, someone without much neuroscience background, giving me these exciting, yet challenging projects, and training me from how to use a pipettor to how to operate a transmission electron microscope. Thanks for sharing with me, and teaching me from the very basic neuroscience knowledge to what is unknown in the field. Thanks for bearing with me, and guiding me from how to present a paper in a journal club to how to write up this thesis. My achievements during my graduate school are true reflections of your inexhaustible passion for science and thoughtful training. As a mentor, you care about both my experiment progress and how I grow as an independently thinking scientist. Over the years, I have recognized the transition from you teaching me basic lab techniques to you letting me design experiments myself. Meanwhile, I have recognized the transition from you rehearsing with me line by line for presentation to only making several remarks before a talk. I would never forget the first time you said the negative stain picture I made was fantastic. I looked for the protocol myself and followed some of your instruction, and I made it. During the *in situ* hybridization using microRNA probes, you just asked me to list the chemicals I needed and then you ordered everything as I suggested without questions. To me, that couple of months were really stressful, and it was a great feeling that I made it work as well. Thank you for caring about my life as an international student as well. I appreciate you telling me to file for a tax refund,

explaining to me many English words and giving me rides after transit hours in the first year I joined the lab. I will always remember your enthusiasm for science and interest in research made known by your nonstop talking and loud laugh over many expensive international phone calls in winter of 2009. Mark, whatever I do in the future and wherever I am, my way of thinking about science and approaching a scientific problem will always be engraved by your style and I will tell whoever appreciates my way of thinking, I have been your Ph.D. student, your very first Ph.D. student. This five-year grad school has been the best time of my life, and if I could start all over, I would choose you as my mentor over and over again!

I also would like to give thanks to my committee members, U. J. McMahan, Arne Lekven and Mendell Rimer. Jack, thank you for your encouragement after nearly every talk I gave; thank you for allowing me to audit your and Wes' synapses class, it was my dream-come-true listening to someone's lifetime research; thank you for your suggestions and insights for my research and future career; thank you for inviting me to your home for several social events. Arne, thank you for the training during my rotation in your lab and eventually becoming my committee member, and thank you for all the communications regarding *in situ* hybridization and working in the U.S. as a scientist. Mendell, thank your for your critical comments during every committee meeting and my presentations, and thank you for the wonderful principles of neuroscience I lectures and your recommendation letters.

I would also like to thank several people who have been helpful and supportive. My former lab member Maya Stavrianakou was a respectful colleague and a good

friend. I will remember all her kindness. I appreciate the ever-positive support, great encouragement from Wesley Thompson and his recommendations for award application, as well as future jobs. I would also thank Joseph Szule and Jae Hoon Jung for their friendship and sharing their knowledge with me. I am also thankful to Yong il (Matt) Lee, who helped me with his expertise in light microscopy and mouse dissection, and Robert Hastings, who helped me with my mice colony. I am also grateful for Roula Mouneimne for her help with the microscopes. I appreciate Matt Sachs and his lab member Cheng Wu for the collaboration on some parts of my project. I am grateful for Darrell Pilling's help with protein chemistry related questions.

I am fortunate enough to have my friends and family, without whom I would not be where I am today. My dad has been supporting my education both mentally and financially since elementary school and giving me advice for my whole life. I have made lifelong friends with other graduate students from the Department of Biology, especially Allison Wilkes St.Clair, Lynn Dudinsky, Ying Fang, Mary Janecka, Liusuo Zhang (Postdoc), Emily Rose and Michael White. They make me realize that I am not alone in this Ph.D. program. Rongfeng (Ray) Cui and Nehemiah Cox have been great role model graduate students for me and keep me aware of the timeline of requirements for the Ph.D. program. I have also accumulated some friends in different ways outside grad school that are fun and helpful companions, especially my former roommate Zachary Gaston and current roommate Philipp Tesch, my friend Daniel Divine, Andrew Campomizzi, Nick Sears, Andrea Muschenborn, Austin Buchanan, Matthew Spencer, Randall Reed and Holly Gibbs. I give special thanks to James Reed and Scott Bertinetti

for their sincere advice for many decision-making moments and document editing over the years. I am grateful for having all of you in my life and thank you all for putting up with me, and sharing part of your life with me, and being helpful, patient, inspirational, genuine and honest with me.

Finally, I would like to give thanks to every single member in Department of Biology and Institute for Neuroscience. Thank you all for the interaction and the conversation. I will always keep this wonderful memory all my life.

My research was made possible by the start-up fund for Dr. Mark Harlow and teaching assistantship provided by the Department of Biology of Texas A&M University.

In the end, I sincerely appreciate the United States of America for giving me this opportunity to come and study.

NOMENCLATURE

SV	Synaptic Vesicles
ACh	Acetylcholine
VAChT	Vesicular AcetylCholine Transporter
VNUT	Vesicular NUcleotide Transporter
VMAT	Vesicular MonoAmine Transporter
VGLUT1, 2, 3	Vesicular Glutamate Transporter 1, 2, 3
ATP	Adenosine Tri-Phosphate
GABA	γ-Aminobutyric acid
SLC	SoLute Carrier
TIRF	Total Internal Reflection Fluorescence
5-HT	5-hydroxytryptamine
NO	Nitric Oxide
sRNA	small RiboNucleic Acid
miRNA	micro RiboNucleic Acid
CNS	Central Nervous System
PNS	Peripheral Nervous System
LTP	Long Term Potentiation
LTD	Long Term Depression
trfRNA	Transfer RNA Fragment

SNARE	Soluble N-ethylmaleimide sensitive fusion protein Attachment Protein REceptor
VIAAT	Vesicular inhibitory amino acid transporter
nAChR	nicotinic AcetylCholine Receptor
BDNF	Brain-derived Neurotrophic Factor

TABLE OF CONTENTS

Page

LIST OF FIGURES

Page

LIST OF TABLES

Page

1. INTRODUCTION

Synaptic transmission is the fundamental process through which neurons in the brain communicate with each other, and neurons in the spinal cord control the contraction of skeletal and smooth muscles and secretory glands in the periphery. This process occurs at specialized cell-to-cell adhesion sites termed synapses[1]. There are two types of synapses, electrical synapses and chemical synapses.

Chemical synaptic transmission is the process by which neurotransmitter is released by a presynaptic neuron, in order to ultimately bind postsynaptic receptors on target cell membranes. Early observations of neurotransmitter release laid the foundation for the quantal hypothesis[2]. That is, neurotransmitter is released in discreet packets. The biophysical mechanism responsible for the quantal release of neurotransmitter remained undetermined until the discovery of vesicular organelles in the presynaptic terminal[3,4]. These vesicles, termed synaptic vesicles, are abundant in the presynaptic terminal of all chemical synapses. Some of these synaptic vesicles are docked on the presynaptic membrane, adjacent to a protein dense area called the Active Zone Material (AZM), just opposite to dense patches of receptors on the postsynaptic membrane. When an action potential arrives at the presynaptic terminal, exogenous calcium enters the terminal through electrically - gated calcium channels, and triggers the exocytosis of some of the docked synaptic vesicles. The process of exocytosis is calcium activated, but ultimately exocytosis is mediated by proteins in both the vesicle and presynaptic membranes. Protein conformational changes fuse the opposing membranes and release the vesicle's

neurotransmitter. The fused vesicle's membrane and proteins detach from the AZM, and are eventually recovered through a clathrin-mediated process termed endocytosis. Recycled synaptic vesicles can be reloaded with neurotransmitter for subsequent rounds of exocytosis[5], a topic I will expand on in a subsequent section.

Synaptic Vesicle Proteins

All synaptic vesicles are expected to share a core group of proteins, either integral to or associated with, the vesicle membrane. They are essential for vesicle trafficking to the active zone, vesicle exocytosis and endocytosis[6]. A brief list of the most important proteins, along with their proposed functional role in neurotransmission, can be found in **Table 1**[7,8]. For example, synaptotagmin is a synaptic vesicle integral membrane protein and acts as the calcium sensor during calcium influx; the putative fusigenic SNARE core complex consists of cytosolic SNAP-25, presynaptic membrane anchored syntaxin and the synaptic vesicle integral protein synaptobrevin, and during endocytosis the cytoplasmic protein clathrin polymerizes to form a coat around the synaptic vesicle.

The vesicular neurotransmitter transporters are a group of synaptic vesicle proteins that are responsible for transporting neurotransmitter across the vesicle membrane, utilizing the electrochemical gradient provided by the VATPase in the vesicle membrane as a driving force[9]. The membrane transporters present in a synaptic vesicle, along with available cytosolic neurotransmitter (see **Table 2**), dictate the type of neurotransmitter loaded and released by a neuron. In this dissertation, I discuss 3 SoLute Carrier (SLC)

Official Name	Other Name	Transmembrane Domains	Mass (kDa)	Proposed Function
Synaptotagmin	P65	1	65	Ca^{2+} sensor: C_2A and C_2B domains bind Ca^{2+}
SV2	Synaptic vesicle protein 2	12	82-110	No clear function; possess many glycosylation sites.
Synaptobrevin	VAMP/V-SNARE	1	12	SV part of SNARE complex, important for synaptic vesicle fusion with presynaptic membrane
Synaptophysin	P38	4	38	No clear function; widely used as synaptic vesicle marker
Rab	Smg p25A	/	25	Functions in vesicle sorting and trafficking
NSF	N-ethylmaleimide sensitive fusion proteins	/	76	ATPase required for SNARE complex recycling.
Dynamin	/	/	100	Essential for vesicle formation in receptor-mediated endocytosis, vesicle recycling, caveolae internalization
SNAP-25	Synaptosomal-associated protein 25	/	23	1 of 2 plasma membrane associated SNARE complex, involved in membrane fusion
Syntaxin	Q-SNARE/ T-SNARE	/	38	1 of 2 plasma membrane associated SNARE complex, provides one helixs
Clathrin	/	/	180/tri-skeleton	Forms a clathrin coat around a vesicle for endocytosis
Synapsin I/IIa	Protein I	/	83	Tethers synaptic vesicles together, also links to cytoskeleton
Complexin	CPLX	/	16	Proposed to inhibit spontaneous release at the stage of membrane fusion, promote synchronous release at the stage of membrane fusion
α/β/γ - SNAP	Alpha/ beta/gamma soluble NSF attachment protein	/	35	NSF adaptors to disassociate SNARE complex
Munc - 18	Mammalian uncoordinated-18	/	68	Participates in the SNARE formation

Table 1. Summary of proteins involved in synaptic vesicle exocytosis and endocytosis. (/ means not applicable)

Neurotransmitter types	Examples	Receptors	Neuron types
Amino acids	Aspartate, glutamate, D-serine, GABA (γ-Aminobutyric acid) and glycine	NMDA (N-methyl-D-aspartate receptor), AMPA (α-Amino-3-hydroxy-5-methyl-4-isoxazolepropionic acid), $GABA_{A\ and\ B}$ receptors	Glutamatergic neurons, GABAergic neurons
Monoamine	Dopamine, norepinephrine, epinephrine, histamine and serotonin (5-HydroxyTryptamine)	Dopamine receptors, adrenergic receptors, histamine receptors and serotonin receptors	Dopaminergic neurons, adrenergic neurons, noradrenergic neurons and serotonergic neurons
Peptides	Substance P, neuropeptide Y	Neurokinin receptors, neuropeptide Y receptors	Often found associated with serotonergic and noadrenergic neurons
Gasotransmitters	NO (Nitric Oxide)	Soluble guanylyl cyclase	/
Others	ACh, ATP (Adenosine TriphosPhate)	nAChR (nicotinic ACh Receptor), mAChR (muscarinic ACh Receptor) and purinergic receptors	Cholinergic neurons, purinergi neurons

c

Table 2. A summary of major neurotransmitters, neuromodulators and their receptors.

families, known to transport neurotransmitters across the synaptic vesicle membrane. The three families are the SLC17, the SLC18, and the SLC32 families of proteins:

1. **SLC17 family** members include the Vesicular Glutamate Transporters (VGLUTs) 1, 2, 3. Three isoforms, VGLUT1, 2 and 3 transport glutamate into the vesicle lumen[10]. VGLUT 1 is primarily expressed in glutamatergic neurons residing in the cerebral cortex, the hippocampus and the cerebellar cortex[11], whereas VGLUT 2 is primarily expressed in glutamatergic neurons residing in the thalamus, the brainstem and the deep cerebellar nuclei[12]. VGLUT 3 is not necessarily expressed in glutamatergic neurons. It is often expressed in glial cells and serotonergic, cholinergic and GABAergic neurons[13]. SLC17 family also include the Vesicular Nucleotide Transporter (VNUT). VNUT transports ATP into the vesicle lumen[14]. VNUT is primarily expressed in purinergic neurons in the brain and adrenal gland[14].
2. **SLC18 family** members include Vesicular MonoAmine Transporter (VMAT 1 and 2) and the Vesicular Acetylcholine Transporter (VAChT). VMAT 1 and 2 transport monoamine neurotransmitters including dopamine, serotonin, norepinephrine, epinephrine and histamine into the vesicle lumen[15]. VAChT transports acetylcholine (ACh) into vesicle lumen[16]. VMAT 1 is mainly expressed in large dense-core vesicles of the Peripheral Nervous System (PNS), as well as sympathetic neurons and blood platelets[17], VMAT 2 is expressed in the

Vesicular Transporter	Family	Location	Ion Coupling	Loss of function synaptic phenotype
VGLUT1	SLC17	Glutamate neurons	Glu^- exchange nH^+ Cl^- dependent	No glutamate release at certain synapses[18,19]
VGLUT2	SLC17	Glutamate neurons	Glu^- exchange nH^+ Cl^- dependent	No glutamate release at certain synapses[20,21]
VGLUT3	SLC17	Non-glutamate neurons	Glu^- exchange nH^+ Cl^- dependent	ACh storage decrease in cholinergic synapse[22]
VMAT2	SLC18	Monoamine neurons	$Amine^+$ exchange $2H^+$ (VMAT1)[23,24]	Monoamine storage decrease, no release[25-27]
VAChT	SLC18	Cholinergic neurons	ACh^+ exchange $2H^+$ [28]	Partial reduction: reduced ACh release[29]
VGAT/VIAAT	SLC32	Inhibitory neurons	GABA/glycine exchange nH^+	No release of GABA or glycine[30]

Table 3. Summary of expression, ion coupling and synaptic phenotype by loss of function studies (Modified from Edwards Review[31])

Central Nervous System (CNS) aminergic neurons, the sympathetic nervous system and mast cells[15]. VAChT is expressed in cholinergic neurons in both CNS and PNS[32].

3. **SLC32 family** members include the Vesicular Inhibitory Amino Acid Transporter (VIAAT), also named the Vesicular GABA Transporter (VGAT). VIAAT transports GABA, glycine and β-alanine into the vesicle lumen[9]. VIAAT is expressed in both GABAergic neurons and glycinergic neurons in the CNS[30,33,34].

Further information about vesicular transporter expression, ion coupling and synaptic phenotype in loss of function studies is provided in **Table 3**.

Neurotransmitter Loading

Dale's principle states that neurons can be classified by the chemical neurotransmitter(s) they release from their nerve terminals[35]. In 1953, John Eccles proposed a simple and pragmatic interpretation of Dale's principle, proposing that, to begin with, we assume that each neuron releases only one type of small molecule neurotransmitter at all of its synapses[36]. Based on this principle, chemical synapses have been identified based upon their sensitivity to pharmacological agents, their possession of the presynaptic molecular machinery to synthesize and load certain neurotransmitters, or the postsynaptic identification specific types of chemical receptors.

Many synapses appear to follow Dale's principle; however, some neurons possess the enzymatic machinery necessary for the production of more than one neurotransmitter

and produce more than one type of neurotransmitter transporter. From a physiological perspective, the type of neurotransmitter stored and released at a terminal is determined by the enzymatic machinery and neurotransmitter transporter cofactors present in the presynaptic terminal, and ultimately the neurotransmitter transporters present on the synaptic vesicles. Thus one would expect that these terminals might release more than one neurotransmitter, and indeed, these neurons have been shown to co-release more than one type of neurotransmitter at their synaptic terminals[37]. The first observation of such a terminal was the PNS electric organ from *Torpedo californica*, where it was demonstrated that both ATP and ACh were loaded into synaptic vesicles and released from the terminals[38,39,40]. Additionally, synaptosomes isolated from the electric organs have been shown to co-release glutamate under stimulation[41]. In the CNS, there are many examples of neurons that possess multiple classes of neurotransmitter transporters, and a few well-controlled studies demonstrating the co-release of multiple types of neurotransmitter. Below is a table (**Table 4**) summarizing some examples of the neurotransmitter co-release in the CNS[37].

To be classified as a neurotransmitter, small molecules must be loaded into synaptic vesicles and released from presynaptic terminals in a calcium dependent manner. In addition, the small molecules must bind ligand-activated receptors at or near the site of release. As stated in the previous paragraph, vertebrate NMJs release, in addition to ACh, ATP and glutamate. The evidence that ACh acts as a neurotransmitter at the vertebrate NMJ is substantial. The top surface of the postsynaptic endplate us densely populated by the nicotinic ACh receptors[42,43]. Released ACh binds to the

nicotinic ACh receptors at neuromuscular junction, which in turn open and help depolarize the muscle endplate, ultimately initiating the contraction of the muscle[44-46]. The evidence that ATP acts as a neurotransmitter at the NMJ is supported by the accumulation of the purinergic receptors P2X and P2Y at the endplate[47]. P2X receptors are expressed by neurons and Schwann cells[48]. Released ATP binds to the P2 receptors on Schwann cells P2 receptors and increase intracellular Ca^{2+} from either releasing the internal store or regulating Ca^{2+} entry[49], and ultimately affects fast synaptic transmission[50], modulating transmitter release. In addition, after ATP degraded to adenosine, adenosine can bind to P1 receptors on Schwann cells[51]. The evidence that glutamate acts as a neurotransmitter is localization of AMPA (α-amino-3-hydroxy-5-methyl-4-isoxazolepropionic acid) and NMDA (N-Methyl-D-aspartic acid) receptors are receptors for glutamate on the muscle membrane[52]. In addition, excitatory amino acid transporters (EAATs), also known as glutamate transporters localize to the junctional folds of the endplate[53]. The application of glutamate to the endplate, triggers the release of nitric oxide, which has been shown to modulate the rate of synaptic vesicle endocytosis, the non-quantal release of ACh, and alter the probability of synaptic vesicle fusion[54-56].

One important question that needs to be addressed in order to explain the many examples of multiple neurotransmitter transporters in the same neuron and/or the co-release of multiple neurotransmitters at individual synaptic terminals is whether individual synaptic vesicles can possess multiple types of vesicle transporters. Two scenarios could explain the experimental observations of neurotransmitter co-release

(**Figure 1**) One, at a specific terminal, there is a heterogeneous population of synaptic vesicles, where each synaptic vesicle has only one type of neurotransmitter transporter, or two, there is homogeneous population of synaptic vesicles, where each synaptic vesicle has two or more kinds of neurotransmitter transporters. Some physiological experiments support the hypothesis that cholinergic vesicles possess at least two kinds of neurotransmitter transporters[13], and therefore, should be capable of co-transmitter release. If synaptic vesicles cannot possess more than one type of transporter and transmitter, then a mechanism to regulate individual vesicle timing and release may be necessary to explain neurotransmitter co-release.

As a step toward making direct tests of the hypothesis that synaptic vesicles contain multiple neurotransmitter transporters, I isolated synaptic vesicles from the cholinergic electric organ from the marine ray *Torpedo californica.* This is a classic cholinergic preparation like the neuromuscular junction, and it is an abundant source of cholinergic synaptic vesicles[57]. I utilized a single-molecule imaging approach based upon Total Internal Reflection Florescence Microscopy (TIRFM). TIRFM imaging is widely used in cell and molecular biology to observe cellular events happening on the surface of cells, including membrane receptor binding, endocytosis and exocytosis, actin myosin trafficking and so forth[58]. Conventional fluorescent microscope illuminates and excites fluorophores at multiple depths of the visual field of specimen, which results in high background of fluorescence and photobleaching of the fluorophores. TIRFM imaging makes use of an evanescent wave, and only illuminates the specimen adjacent

Co-release neurotransmitters	Location
GABA and ACh	Starburst amacrine cells[59]
GABA and glutamate	GABAergic neurons at Medial nucleus of the trapezoid body during development co-release glutamate[60]; hippocampal mossy fiber glutamatergic synapse co-release GABA[61]
ACh and glutamate	Cholinergic neurons from medial hebenula nuclei[62,63]; lower motor neurons onto Renshaw cells[64,65]
Monoamine and glutamate	Ventral Tegmental Area and prefrontal cortex dopaminergic neurons[66,67]

Table 4. Summary of known incidences of neurotransmitter co-release in the CNS.

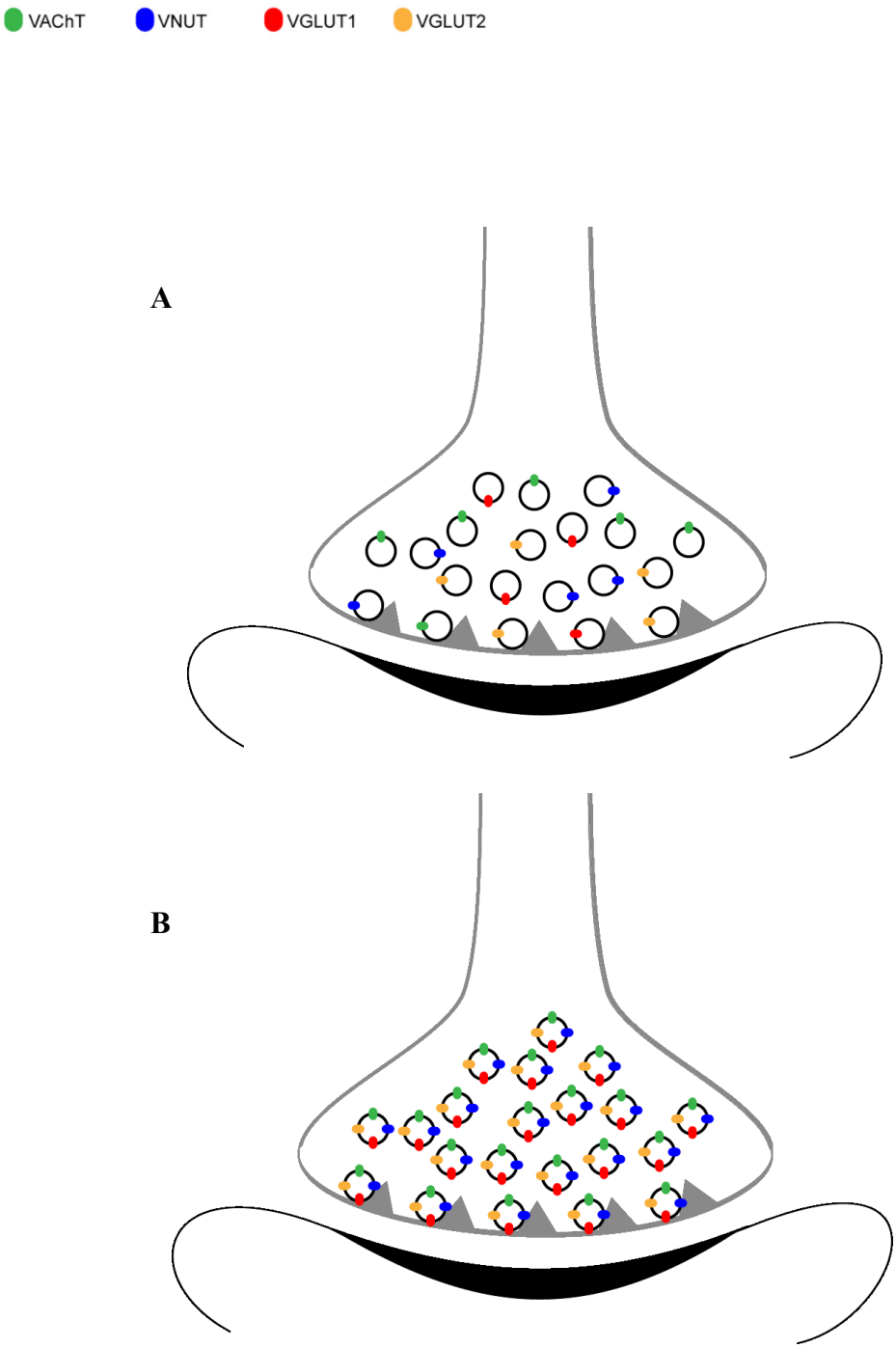

Figure 1. Two proposed models of cholinergic synapse neurotransmitter transporter. A. Cholinergic synapse has heterogeneous population of synaptic vesicles; each has one type of neurotransmitter transporter. B. Cholinergic synapse has homogenous population of synaptic vesicles; each has at least four types of neurotransmitter transporters.

to the coverslip and specimen surface region, a depth of approximately 100 nm into the specimen. Synaptic vesicles isolated from electric organs of the electric ray are around 70nm in diameter. In this case, synaptic vesicles from *Torpedo californica* preparation were examined under a glass coverslip. Only the surface, where single layer of fluorescently labeled synaptic vesicles in the solutions (1mg/ml protein content) is present, is illuminated. My evidence supporting the hypothesis that synaptic vesicles can contain multiple neurotransmitter transporters can be found in the second section of my thesis.

Synaptic Vesicles Contain Small RNAs (sRNAs)

The rate and timing at which neurotransmitter is released drives the post-synaptic activity at a synapse. That activity can have a profound effect on both the size and stability of a given synapse because it regulates not only the stability of proteins at the synapse that were synthesized within the cell body, but it also regulates the synthesis of proteins locally in the presynaptic and postsynaptic terminals. Current models strongly suggest that activity at the synapse regulates local protein synthesis[68,69]. In this model the release of neurotransmitter from the presynaptic terminal modulates postsynaptic levels of calcium, and via modulation of calcium levels indirectly controls local protein synthesis[70]. Changes in local protein synthesis then lead to changes in the post-synaptic structure such as receptor remodeling - either by synthesizing and stabilizing additional receptor proteins, or by the degradation of receptor proteins residing within the post synaptic membrane. This process is known as activity dependent synaptic plasticity, and

it is essential for dendritic outgrowth, synapse maturation, and synapse elimination during development and synaptic plasticity[70].

Protein translation is a complex process in which the information encoded in a messenger RNA (mRNA) sequence is used as a template in order to synthesize an amino-acid polypeptide chain, or protein[71,72]. Protein synthesis involves many types of macromolecules, including ribosomes, mRNAs, and transfer - RNAs (tRNAs)[73]. The translation process is tightly regulated by translation initiation factors, elongation factors, releasing factors and their regulators. Other factors regulating protein translation include the stability of individual mRNA transcripts and the rate at which translation occurs.

Given the importance of local protein synthesis at the synapse, and its dependence on local activity, I hypothesized that synaptic vesicles might, in addition to neurotransmitter, contain small molecules that can directly regulate translation. One such class of small molecules includes short strands of non-coding ribonucleic acids (RNA; < 50 nucleotides in length) that have been shown to have profound effects on transcription and translation. Short non-coding RNAs, or small RNAs (sRNAs) are a broad class of molecules that include RNA species such as micro-RNAs (miRNAs), small interfering RNAs (siRNAs), and transfer RNA fragments (trfRNAs). The different classes of sRNAs can alter transcription and translation through distinct mechanisms[74]. For instance, sRNAs can, along with certain proteins, form a RNA-induced silencing complex (RISC). These ribonucleoprotein complexes can cleave specific mRNA based upon the template provided by the sRNA. In addition, RISC complexes can also repress

protein translation by modulating the loading of ribosomes and by associating with other regulatory factors. sRNAs such as trfRNAs affect translation through alternative, non-RISC pathways. One such pathway is by binding directly to an elongation factor necessary for protein translation[75].

As a first step towards testing whether synaptic vesicles might store and release sRNAs in order to affect local protein synthesis, I tested and demonstrated that sRNAs are associated with synaptic vesicles. In addition to being associated with synaptic vesicles I also demonstrated that the vesicles protect the sRNAs from degradation by Ribonuclease (RNase). In this dissertation, I discuss three sRNA families that I find associated with synaptic vesicles. The three families are the miRNAs, the trfRNAs, and the YRNAs:

1. Mature miRNAs are around 21 nucleotides in length. The biogenesis of miRNA has been extensively studied for the last decade. Briefly, longer and intramolecular double strand RNA, also known as pri-miRNAs (primary miRNAs), are produced by a specialized ribonuclease III[76] - in animals, pri-miRNAs are cleaved by RNA polymerase III Drosha into pre-miRNAs (precursor miRNAs)[77]. A second RNase III, Dicer, cleaves pre-miRNAs into miRNA-miRNA duplexes. One miRNA strand is preferentially bound to the protein Argonaute (AGO), and loaded into an AGO-containing RNA-induced silencing complex (RISC)[78 79], while the other strand gets degraded[80]. The miRNA in the RISC complex acts as a guide to target the RISC complex to specific mRNAs. Once bound by a RISC complex, targeted mRNAs can

either be cleaved and degraded or target mRNA translation can be repressed[81,82]. Thus, miRNAs play important roles in posttranslational gene regulation by translational inhibition and mRNA destabilization.

2. Mature trfRNAs range in size from 28-34 nt, and are approximately half the size of mature transfer-RNAs (tRNAs; 76-90 nt). The biogenesis of at least some trfRNAs begins with the cleavage of a mature tRNA near the anticodon loop by the RNase angiogenin[83]. Full length tRNAs have a well defined role in protein synthesis – they can be charged with specific amino acids in order to assist with translation, or interact with a series of proteins, including elongation factors and amnoactyl-tRNA ligases[84]. The functional roles of trfRNAs are not fully elucidated; however, some are induced under stress conditions, and may be involved in the assembly of stress granules. One class of trfRNA can inhibit protein translation in a eukaryotic translation Initiation Factor 2α (eIF2α) dependent manner, and promote an integrated stress response program[75,83,85,86].
3. Y RNAs are a group of small non-coding RNAs (83-122 nucleotides)[87]. They are found in cytoplasmic extracts (Y1, Y3, and Y4) and nuclear extracts(Y5)[88]. The biogenesis of Y RNAs is not well defined. Metazoan Y RNAs are transcribed by RNA polymerase III from distinct promoters, independent of the miRNA pathway[89,90]. Y RNAs are identified as the RNA component of soluble ribonucleoproteins (RNPs) termed Ro RNPs, which have been detected in the sera of patients suffering from systemic lupus

erythematosus (SLE), a systemic autoimmune disease (or autoimmune connective tissue disease) in which the body's immune system mistakenly attacks healthy tissues[87,91]. The Y1 RNA is the RNA component of the Ro RNP complex, and is associated with the autoimmune antigen proteins Ro60 and La[92]. The functional role of Y RNAs, or their fragments, is still not known. It has been hypothesized that the Y RNAs affect DNA replication, and/or are involved in the regulation of cellular stress response and proliferation[87].

2. INDIVIDUAL SYNAPTIC VESICLES FROM THE ELECTROPLAQUE OF TORPEDO CALIFORNA, A CLASSIC CHOLINERGIC SYNAPSE, ALSO CONTAIN TRANSPORTERS FOR GLUTAMATE AND ATP*

Overview

The type of neurotransmitter secreted by a neuron is a product of the vesicular transporters present on its synaptic vesicle membranes and the available transmitters in the local cytosolic environment where the synaptic vesicles reside. Synaptic vesicles isolated from electroplaques of the marine ray, *Torpedo californica*, have served as model vesicles for cholinergic neurotransmission. Many lines of evidence support the idea that in addition to acetylcholine, additional neurotransmitters and or neuromodulators are also released from cholinergic synapses. We identified the types of vesicular neurotransmitter transporters present at the electroplaque using immunoblot and immunofluoresence techniques with antibodies against the vesicle acetylcholine transporter (VAChT), the vesicular glutamate transporters (VGLUT 1, 2, and 3), and the vesicular nucleotide transporter (VNUT). We found that VAChT, VNUT, VGLUT 1 and 2, but not 3 were present by immunoblot, and confirmed that the antibodies were specific to proteins of the axons and terminals of the electroplaque. We used a single vesicle imaging technique to determine whether these neurotransmitter transporters were

*Reprinted with permission from 'Individual synaptic vesicles from the electroplaque of *Torpedo californica*, a classic cholinergic synapse, also contain transporters for glutamate and ATP' by Huinan Li and Mark L. Harlow, 2014. Physiological Reports, Volume 2, e00206, 1-11, Copyright 2014 by Wiley Online Library.

present on the same or different populations of synaptic vesicles. We found that greater than 85% of vesicles that labeled for VAChT co - labeled with VGLUT 1 or VGLUT 2, and approximately 70% co-labeled with VNUT. Based upon confidence intervals, at least 52% of cholinergic vesicles isolated are likely to contain all four transporters. The presence of multiple types of neurotransmitter transporters - and potentially neurotransmitters – in individual synaptic vesicles raises fundamental questions about the role of co-transmitter release and neurotransmitter synergy at cholinergic synapses.

Introduction

Neurons are often classified by the small molecule neurotransmitters they release from synaptic vesicles along their axons and axon terminals. The type of neurotransmitter loaded into a synaptic vesicle is a product of the neurotransmitter transporters present in a vesicles membrane, combined with the local concentration of neurotransmitter and availability of cofactors necessary for active transport. Thus at a cholinergic synapse, the presynaptic bouton will contain the precursors and enzyme machinery to produce acetylcholine (ACh), and the synaptic vesicles present will contain the vesicular acetylcholine transporter (VAChT)[94].

The simple idea that each neuron secretes only one type of neurotransmitter has been thrown into doubt with examples of cholinergic, GABAergic and noradrenergic neurons that appear to co-release glutamate[37,63]. However, whether this co-release involves packaging of multiple transmitters into single synaptic vesicles is less clear. This is an important issue because it impacts how one thinks about the communication occurring at the synapse. Synaptic vesicles isolated from electroplaques of the marine

ray, *Torpedo californica*, have previously been shown to contain the vesicular acetylcholine transporter, as well as load and release the neurotransmitters (ACh) and adenosine triphosphate (ATP)[40]. Thus, in the case of the electroplaque, ACh and ATP are either in the same synaptic vesicles, or two populations of vesicles reside in the terminals. Additionally it has been demonstrated that synaptosomes from electroplaque release glutamate[41], in agreement with studies that show some cholinergic neurons within the central nervous system (CNS) synthesize one or more vesicular glutamate transporters (VGLUT 1,2,3) and release glutamate at their terminals[22,64,95]. Two non-mutually exclusive possibilities could account for cases where co-release has been demonstrated. Either these neurons have a heterogeneous population of two or more distinct types of vesicles containing different neurotransmitter transporters, or these neurons possess a homogenous population of synaptic vesicles that contain multiple types of neurotransmitter transporters.

To address the question of whether at one type of synapse the synaptic vesicles are heterogeneous or homogenous we have chosen to use vesicles isolated from the electroplaques of *T. californica*. The electroplaque is a classic preparation that provides an abundance of cholinergic synaptic vesicles from one class of motor neuron[57]. Two types of neurotransmitter are stored in and released from vesicles at these terminals - acetylcholine and ATP. In addition to the neurotransmitter transporters for acetylcholine and ATP[14], we tested for the presence of glutamate transporters VGLUT 1, 2 and 3[11,96-99]; which are co-expressed in other cholinergic neurons. Western blot analysis confirms the presence of four neurotransmitter transporters in the isolated vesicle preparation,

immunofluorescence labeling on cryostat tissue sections of electroplaques is consistent with the immunogenic epitopes of the four neurotransmitter transporters residing in the "cholinergic" axons and presynaptic terminals, and total internal reflection fluorescence (TIRF)[100] experiments on single vesicles[101] provide evidence that individual synaptic vesicles likely contain four types of neurotransmitter transporters. Therefore we conclude that vesicles in the axon and axon terminals of the electroplaque are a homogenous population containing at least four types of neurotransmitter transporters and three different neurotransmitter/neuromodulators including acetylcholine, ATP and glutamate.

Materials and Methods

Reagents

Mouse monoclonal antibodies to VGLUT1 (N28/9), VGLUT2 (N29/29), VGLUT3 (N34/34), as well as the mouse monoclonal antibody for VAChT (N6/38) were purchased from Antibodies Incorporated (UC Davis/NIH NeuroMab Facility; Davis, Ca). Additional antibodies included VNUT rabbit polyclonal (ABN110), synaptophysin rabbit polyclonal (MAB5258), Goat Anti-Rabbit HRP, and Goat anti-muse HRP (Millipore; Billerica, MS), and VAChT rabbit polyclonal ab68986 (Abcam; Cambridge, England) Fluorescently tagged secondary antibodies included Pacific Blue Goat anti-mouse (P31582), Alexa 488 Goat anti-rabbit (A-11034), Alexa 488 Goat anti-Mouse (A-10667) (Invitrogen/ Life Technologies; Carlsbad, CA). Alexa 594 α-bungarotoxin (B-13423), and FM 4-64 (T-13320) were used to label AChR and vesicles, respectively (Invitrogen). Pro-long gold anti-fade (P36934) was used to mount

specimens (Invitrogen). Blue/green calibration beads (100 nm) were from Zeiss (Carl Zeiss; Oberkochen, Germany). All other reagents were purchased from Sigma-Aldrich (St. Louis, MO) unless otherwise noted.

All figures were adjusted using Image J (NIH; Bethesda, MS). Schematic drawings and figure layout and labeling were done with Adobe Illustrator and Photoshop. (Adobe Systems Inc.; San Jose, CA.)

Isolation and enrichment of cholinergic vesicles

Methods were adapted from Ohsawa[102]. A Spex Freezer Mill 6800 (Spex Sample Prep; Metuchen, NJ) was cooled to -180^{o} C and ~25 g of frozen electric organ from *Torpedo californica* (Aquatic Research Consultants; San Pedro, CA), containing abundant stacks of electroplaque was ground with 25 g of frozen buffer pellets (320 mM Sucrose, 10 mM TRIS-Cl, pH 7.4). The resulting powder of buffer and electric organ was placed in a beaker and warmed to 4°C with 50 ml of buffer solution (320 mM Sucrose, 10 mM Tris-Cl, pH 7.4, 4°C). The resulting slurry (100 ml) was centrifuged at 20,000 rpm for 10 minutes (Beckman Coulter JA-20 rotor - Avanti J25 centrifuge) (Beckman Coulter; Brea, CA). The resulting supernatant was centrifuged at 34,000 rpm for 40 minutes (Beckman Coulter 70ti rotor - Optima X80 centrifuge). The supernatant from this last centrifugation was loaded onto an 8 ml 0.6 M/1.2 M sucrose step gradient (10 mM Tris-Cl, pH 7.4), then centrifuged at 48,000 rpm for 2 hours (Beckman Coulter 70ti rotor - Optima X80 centrifuge). The 4-5ml fluffy layer, enriched in vesicles, was collected. A 2 ml sample of enriched vesicles was filtered using a 0.22 μm spin column (Spin-x, Corning; Corning, NY) to remove any large debris or clusters of vesicles. The

resulting filtrate was injected into a Pharmacia LC500 plus FPLC, and run through a 25 cm 4% agarose bead column (Bioscience Beads; West Warwick, RI). The FPLC was eluted with a buffer solution (0.2 M NaCl, 10 mM HEPES, pH 7.4) at a flow rate of 1.0 ml/min. The second major peak was collected, and the vesicles concentrated to a protein concentration of 1 mg/mL or 8 mg/ml (measured by Bradford Assay – Bio-Rad)(Bio-Rad Laboratories, Inc.; Hercules, CA) using a Stirred Cell apparatus with a 100 kDa filter (PLHK02510, Millipore).

Electron microscopy

A 5µl sample of enriched synaptic vesicles (20 mg/ml as determined by Bradford assay) was pipetted onto a slot grid that had been treated by glow discharge. Excess sample was removed by filter paper, and the grid was briefly washed in deionized water, followed by 2 s staining with uranyl acetate (Ted Pella; Redding, CA), followed by another wash[103]. The slot grid was viewed with a JEOL 1200 JEOL Ltd., Akishima-Shi, TKY Japan) operated at 100 kV. Images collected at 30,000 X and 50,000 X magnifications on a bottom-mounted 3072 x 3072, slow scan, lens-coupled CCD camera SIA 15C (SIA; Dulith, GA).

Immunoblotting

Four micrograms of vesicle protein was diluted 1:1 with Laemmli buffer (Bio Rad). The samples were loaded onto a 4 –20% Mini-Protein TGX gel (Bio Rad) and resolved for 35 min at 200 V. Proteins were transferred to a PVDF membrane (Bio Rad) and probed with antibodies to synaptophysin, VAChT, VNUT, VGLUT 1,2, or 3. Antibody binding was detected with horseradish peroxidase-conjugated secondary

antibodies and ECL Prime (GE Healthcare; Fairfield, CT). Chemiluminescence was quantified using a Chemicdoc XRS+ imager (Bio Rad).

Fluorescent immunohistochemical labeling of frozen sections of electroplaque and wide-field fluorescence

Sections (30 microns thick) of electroplaque were cut with a cryostat (Leica; Solms, Germany), collected on slides, and stored at -80°C until processed for labeling. For labeling, slides were removed from the freezer and dried within a vacuum desiccator (Savant – Thermo Fisher Scientific; Waltham, MA) for 5 minutes. The slices were then fixed in 4% paraformaldehyde for 5 minutes, rinsed with phosphate buffer solution (PBS), and washed in 0.1 M glycine in PBS for 1 hour. Slides were extracted in 0.5% Triton PBS for 15 minutes on ice, and rinsed 3X for 10 minute in PBS. The samples were then blocked in 3% bovine serum albumin (BSA) in PBS for 1 hour. Primary antibodies were diluted 1:250 in 3% BSA PBS and incubated overnight at 4^{O}C. After washing 3 X 15 minutes in 3% BSA 0.1% Tween-20 PBS, the secondary antibodies (Alexa 488 Goat anti-Mouse or Alexa 488 Goat anti-rabbit) were diluted 1:1000 in 3% BSA and a 1:1000 Alexa 594 α-bungarotoxin added and incubated for 2 hours. The slides were washed 3 X 15 minutes in 3% BSA PBS, blotted, and mounted on a coverslip in Pro-long Gold for imaging.

Images of the electroplaque were acquired using a Leica (Nussloch, Germany) epifluorescence microscope and a 40X (NA, 1.0) oil immersion objective, a CoolSnap HQ integrating CCD camera (PhotoMetrics, Huntington Beach, CA), and IPLab3.5 software (BioVision, Exton, PA) using a Macintosh computer (Apple Computer,

Cupertino, CA). Filter sets used were standard HQ sets (#41001 for Alexa 488, and #41002 for Alexa 594; Chroma Technology, Rockingham, VT).

Fluorescent immunohistochemical labeling of isolated synaptic vesicles and TIRF imaging of single vesicles

After a final pass through a 0.22 μm spin column (Spin-x, Corning; Corning, NY) to remove any vesicles that may have become clustered during the stirred cell concentration step, 100 μl of synaptic vesicles (1 mg/ml) were transferred into 300 μl PBS (pH 7.4), and labeled with two rounds of primary and secondary antibodies following the procedure [101]. Briefly, the vesicles were incubated for 4 hours with 1 μg of primary mouse antibody, incubated for 30 min with 20 μl anti-mouse IgG beads, briefly centrifuged, and the vesicle containing supernatant was then incubated with 0.5 μg goat anti-mouse secondary antibody labeled with Pacific Blue for 4 hours. The vesicles were then incubated with 1 μg primary rabbit antibody for 4 hours, incubated for 4 hour with 0.5 μg goat-anti-rabbit secondary labeled with Alexa 488, and finally incubated with 20 μl anti-goat IgG beads. The beads were pelleted and the supernatant collected for imaging. The pairings of primaries were the following: VAChT mouse monoclonal and VNUT polyclonal, VGLUT1 mouse monoclonal and VAChT rabbit polyclonal, and VGLUT2 mouse monoclonal and VAChT rabbit polyclonal.

FM4-64 [104] was added to the labeled vesicles (final concentration 1 μM), and the samples were incubated on a glass bottom culture dish (MatTek P35G-1.5-20-C; Ashland, MA) for 1 hour prior to imaging to allow vesicles to settle on the coverslip. Culture dishes with settled vesicles were placed on a Zeiss Axio Observer Z1

Microscope with TIRF slider, 100X TIRF objective (NA 1.45). Images were acquired using AxioVision (Carl Zeiss; Oberkochen, Germany). Three separate images for each field were taken using laser lines and filter cubes paired to eliminate fluorescent cross talk between the dyes: laser line 401 with filter cube 73 HE was used for Pacific Blue, laser line 488 with filter cube 38 HE was used for Alexa 488, and laser line 561 with filter cube 74 HE was used for FM 4-64. Images were collected with a Roper S/W PVCAM EMCCD camera and analyzed using ImageJ (NIH) software. Suitable spots detected in the FM4-64 channel were marked. The other channels were then quantified for label.

Confidence intervals for the binomial proportion were calculated using two-sided Agresti-Coull confidence limits [105] providing a statistical means to combine paired labeling experiments that otherwise would have been impossible due to secondary antibody specificity and optical isolation of the three color channels used in the TIRF microscopy.

Results

Synaptic vesicle enrichment

Synaptic vesicles were isolated from the electric organ of *T. californica* using standard vesicle isolation techniques. In order to verify that the synaptic vesicles were uniform and structurally intact, a sample of the vesicles was concentrated to 20 mg/ml, negatively stained[103] and viewed with an electron microscope (**Figure 2A**). In agreement

Figure 2. Synaptic vesicles can be enriched from electroplaques of *T. californica* and shown to contain 4 neurotransmitter transporters. A) Electron micrograph image (30,000 magnification) of negatively stained vesicles isolated and enriched from electroplaque tissue. Sample contains abundant ~80 nm vesicles (some marked with single arrowheads) and occasional large clusters of vesicles and debris (double arrowheads). A insert) Higher magnification (50,000) negative stain image shows characteristic profile of membrane vesicles, Scale bar = 100 nm. B) Immunoblot of the 38 kD protein synaptophysin demonstrates isolation and enrichment of synaptic vesicles during the isolation procedure. Synaptophysin was seen in the tissue (T), and discarded pellets (P1, and P2), however during isolation the majority of vesicles are maintained in the much larger by volume supernatant (S1 and S2) until the final centrifugation. In the final centrifugation the vesicles move through the supernatant (S3) and collect on the fluffy layer (FL). The fluffy layer was collected, and the synaptic vesicles were further enriched by size exclusion chromatography (SV). Purified vesicles were tested by immunoblot and found to be positive for the ~60 kD transporter proteins: VAChT, VNUT, VGLUT1, VGLUT2. Extra bands are possibly due to differences in protein glycosylation. No signal was detected for the transporter protein VGLUT3.

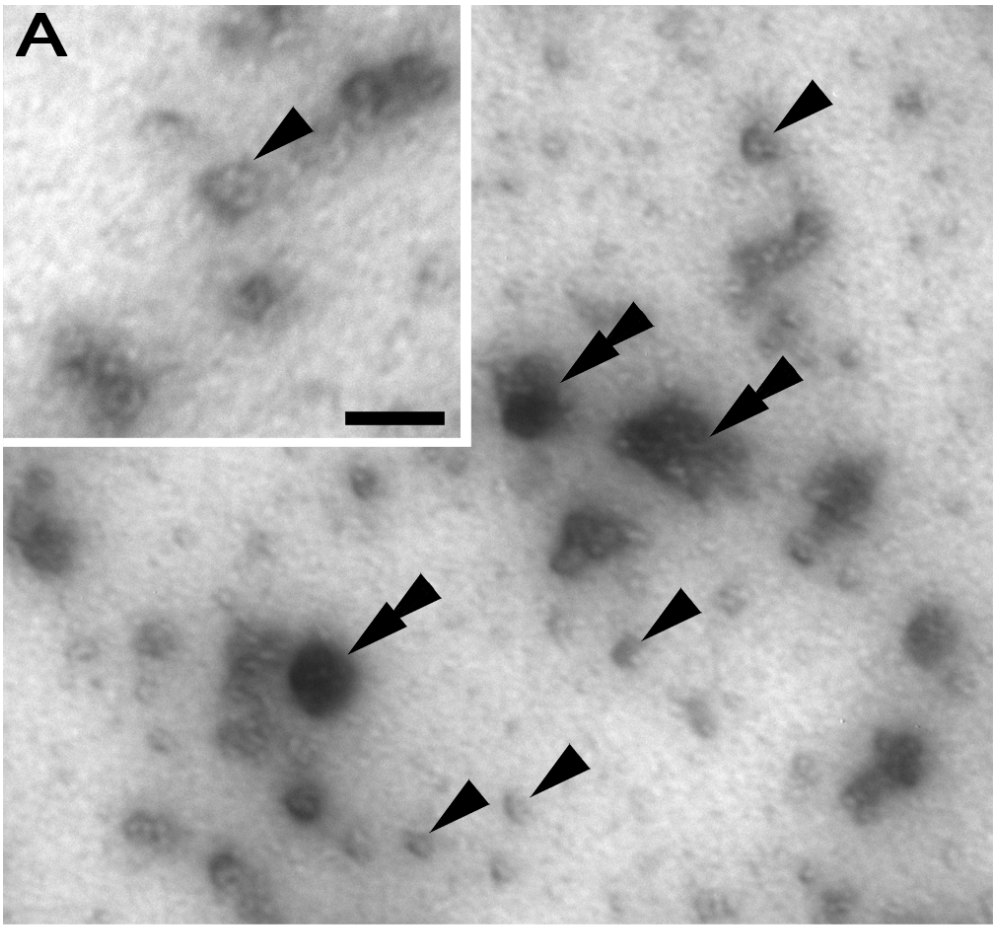
A

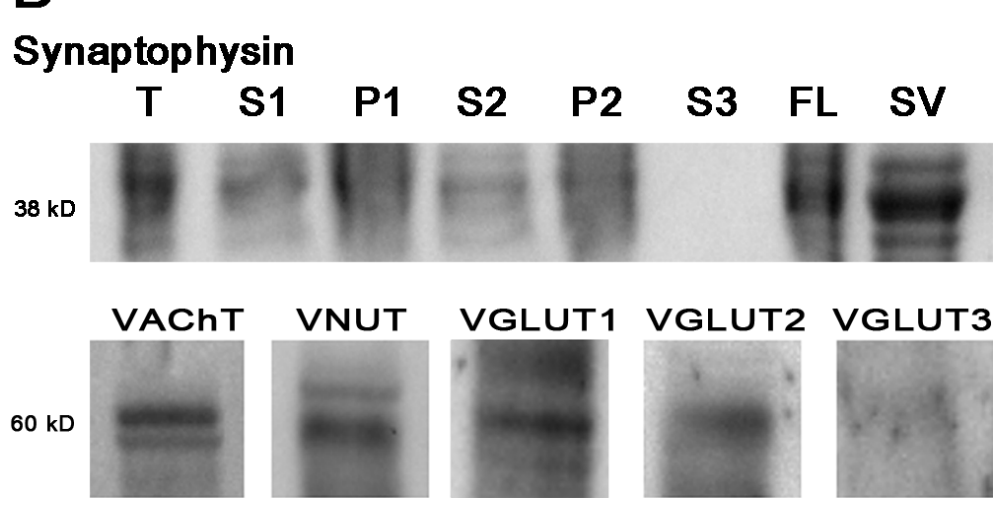
B
Synaptophysin
T
S1
P1
S2
P2
S3
FL
SV
38 kD
VAChT
VNUT
VGLUT1
VGLUT2
VGLUT3
60 kD

with previous studies, the vesicles of *T. californica* are larger (80-120 nm)[106] than vesicles found at neuromuscular synapses in *T californica*[107], or at neuromuscular synapses at other vertebrates (45-60 nm)[108]. Although single vesicle profiles were the dominant structure seen, some larger clusters were also present, and perhaps a result of the concentration procedure (**Figure 2A**).

Immunoblotting of neurotransmitter transporters

The electric organ of *T. californica* is derived from muscle fibers during development, and like all electrocytes, is a non-contractile muscle organ innervated by cholinergic neurons from the electric lobe. Fractions collected during the isolation procedure were immunoblotted for the synaptic vesicle protein synaptophysin to verify the isolation and enrichment procedure. Each lane contained the same amount of protein by Bradford Assay, however pellet and supernatant volumes were not equal. As the isolation procedure advanced, synaptophysin was maintained and ultimately enriched in the final steps (**Figure 2B**), providing further confirmation that the vesicular profiles seen by negative stain are from isolated synaptic vesicles[109].

Immunoblotting was used to determine whether each of five types of neurotransmitter transporters representative of three types of neurotransmitters were present in the synaptic vesicles. As expected, synaptic vesicles isolated from the electric organ possess the cholinergic transporter VAChT (**Figure 2B**). In addition to acetylcholine, it has previously been demonstrated that ATP is loaded and released by synaptic vesicles isolated from the electric organ[38]. We tested for the presence of the purinergic ATP transporter in the vesicle preparation, and found it labeled for VNUT

(**Figure 2B**). In addition to testing for the transporters of known neurotransmitters at the electric organ, we probed for the three known glutamatergic transporters. Previous studies have demonstrated glutamatergic transporter expression in cholinergic neurons[22,64], and in some cases glutamatergic signaling[95]. By immunoblot, VGLUT 1 and 2, but not 3 was shown to be present in the synaptic vesicle preparation (**Figure 2B**; **Figure 3**).

As a further verification of antibody specificity we labeled cryostat sections of the electric organ. An electric organ, present on either side of the ray, is made up of pancake-like stacks of non-contractile, muscle derived, cells termed electroplaques (**Figure 4A**). On the top surface of each electroplaque is a high concentration of nicotinic acetylcholine receptors. Four large nerve bundles originate from the electric lobe, and axons from these nerves travel between the stacks of electroplaque cells before turning 90 degrees and innervating the entire surface of the electroplaque cell with presynaptic boutons. We found that VNUT, VGLUT 1 and 2, and VAChT labeled the axons (**Figure 4B,C; E-G**). In addition, we found labeling for each of the transporters was present above the postsynaptic surface of the electroplaque (labeled with α-Bungarotoxin) (**Figure 4B,C; E-H**).

Single vesicle imaging with TIRF microscopy

Very little is known about the molecular components residing within individual synaptic vesicles, and virtually no information exists about the molecular homogeneity of vesicles within a nerve terminal. Recently a single molecule technique based upon total-internal-reflection-fluorescence (TIRF) microscopy[100] has been developed that

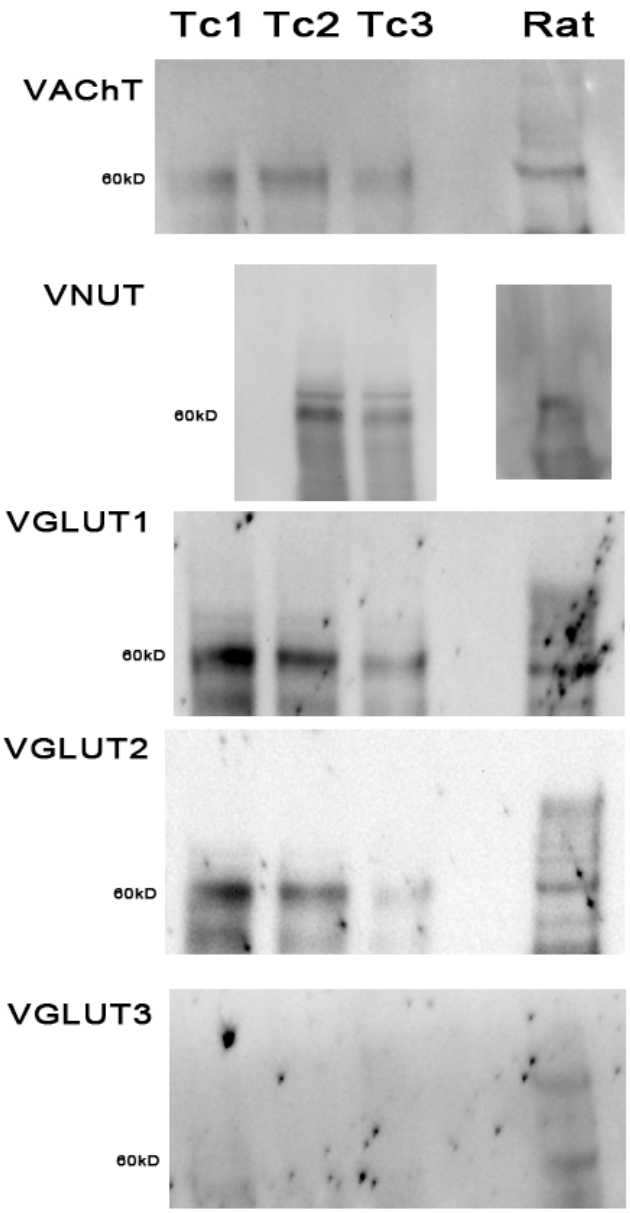

Figure 3. Immunoblot of purified vesicles from rat CNS and *Torpedo californica* electric organ. Rat synaptic vesicles were isolated from rat brains purchased from Pel-Freez Biologicals (Rogers, AR) by the isolation procedure in the methods section. Three lanes of Torpedo electric organ vesicles were loaded in decreasing concentrations (only two lanes of torpedo vesicles were blotted against VNUT). The lanes are Tc1 = 4 mg, Tc2 = 2 mg, and Tc3 = 1 mg. One blank lane separated the lane loaded with 2 mg of isolated rat vesicles. For each blot, the approximate location of the 60 kD marker was marked. The following antibodies were tested: VAChT, VNUT, VGLUT1, VGLUT2, VGLUT3. All antibodies were positive against the vesicles isolated from rat brain.

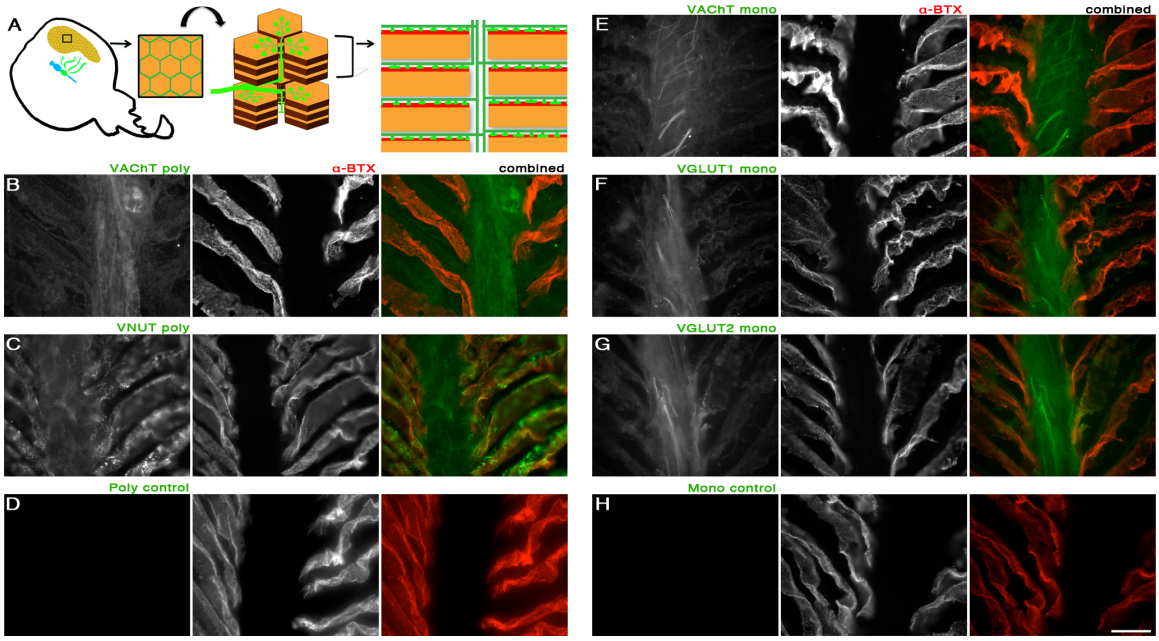

Figure 4. Antibodies against VAChT, VNUT, VGLUT1 and VGLUT2 stain axons and presynaptic boutons residing within the electric organ. A) Cartoon depicting the electric organ of T. californica (1 side of the paired organ shown) and its innervation by four electromotor nerves that project from the electric lobe of the central nervous system (green). From the surface, the electroplaque cells of the electric lobe appear as a honeycomb. Viewed from the side the electroplaque cells appear as large, pancake-like stacks. Each individual electroplaque has a top surface covered in nicotinic-acetylcholine receptors (red surface). That surface is richly innervated with presynaptic boutons and axons. Axons run in between the pancake stacks before entering the target electroplaque and forming synapses. The drawing to the far right in A illustrates the view shown in the remainder of the figure; however in the immunostains, the receptor rich surface of each electroplaque commonly runs at an angle to the central core containing only axons. B-H) Labeling with each of the neurotransmitter transporter antibodies was done in conjunction with α-Bungarotoxin to mark the postsynaptic surface on the electroplaque cells. B) VAChT polyclonal antibody, and C) VNUT polyclonal antibody. D) Application of a secondary antibody to tissue to which no primary polyclonal was applied. E) VAChT monoclonal antibody, F) VGLUT1 monoclonal antibody G) VGLUT2 monoclonal antibody, and H) secondary antibody in a control to which no primary monoclonal antibody was applied. Axons and presynaptic labeling can be seen in B, C and E-G, but no appreciable label was detected in the controls (D and H). Scale bar = 5 microns.

allows for the quantification of protein copy numbers present on single vesicles[110]. In the CNS, the smaller glutamatergic vesicles (35nm) were shown to possess four VGLUT1 transporters per vesicle[110]. We chose to use this technique on vesicles isolated from the electric organ to address the question of whether single synaptic vesicles could have multiple classes of neurotransmitter transporters. Because the terminal is cholinergic, we chose to test the three other transporters VNUT, VGLUT1, and VGLUT2 in a pair-wise labeling with the VAChT. The vesicle isolation procedure was designed to minimize vesicle clusters and larger cellular debris (**Figure 2A**). In addition, the plating density was tittered to reduce the probability of two vesicles residing within a sub-diffraction limited spot. In order to verify that single vesicles were imaged, the lipophilic dye FM4-64[104] was added for two additional checks. For the first check, the resulting fluorescent spots (single vesicles) were checked to ensure they possessed a similar fluorescent profile as 100 nm fluorescent control beads (**Figure 5A**). For the second check, the fluorescence intensity of each spot was quantified in order to verify that each sub-diffraction limited spot did not contain multiple vesicles (**Figure 5B**). Although it was a rare event due to the titer density, we did occasionally find spots that had double or even triple the intensity expected for a single vesicle. Fluorescent profiles from the 4-64 channel that did not match the shape of a single molecule event (simple point spread function), or that possessed multiple quanta of lipid stain (as measured by fluorescence) were excluded from this study. Sites of FM4-64 label that met the above criteria were then examined for the presence of secondary label in the two additional channels. One channel was optimized for the secondary label (Goat anti-mouse) Pacific

Figure 5. TIRF microscope images of vesicles labeled with FM4-64 were used to verify the size and intensity of the spots matched that of a single vesicle. A) Fluorescent images were collected from 51 fluorescent beads (100 nm diameter) and compared to 51 synaptic vesicles labeled with FM4-64 from each of the fluorescent pairings in this study. Although the fluorescent beads are brighter, the beads and the vesicles possess similar sized diameters and point spread function widths. Scale bar = 1 micron. B) The fluorescence intensity of each putative vesicle was quantified in order to verify that each sub-diffraction limited spot did not contain multiple vesicles. If two vesicles reside adjacent to one another they may still appear as single spot with a similar cross sectional width in the X-axis; however, the photon count in the FM4-64 channel would equal the sum of the two vesicles. Cross sections along the X-axis were taken of four vesicles (marked a the site of the line labeled by a diamond, square, circle or triangle), The diamond and square spots contain twice the intensity of labeling as the circle and triangle spots in the image, and are thus likely to be two adjacent vesicles within the same sub-diffraction labeled spot.

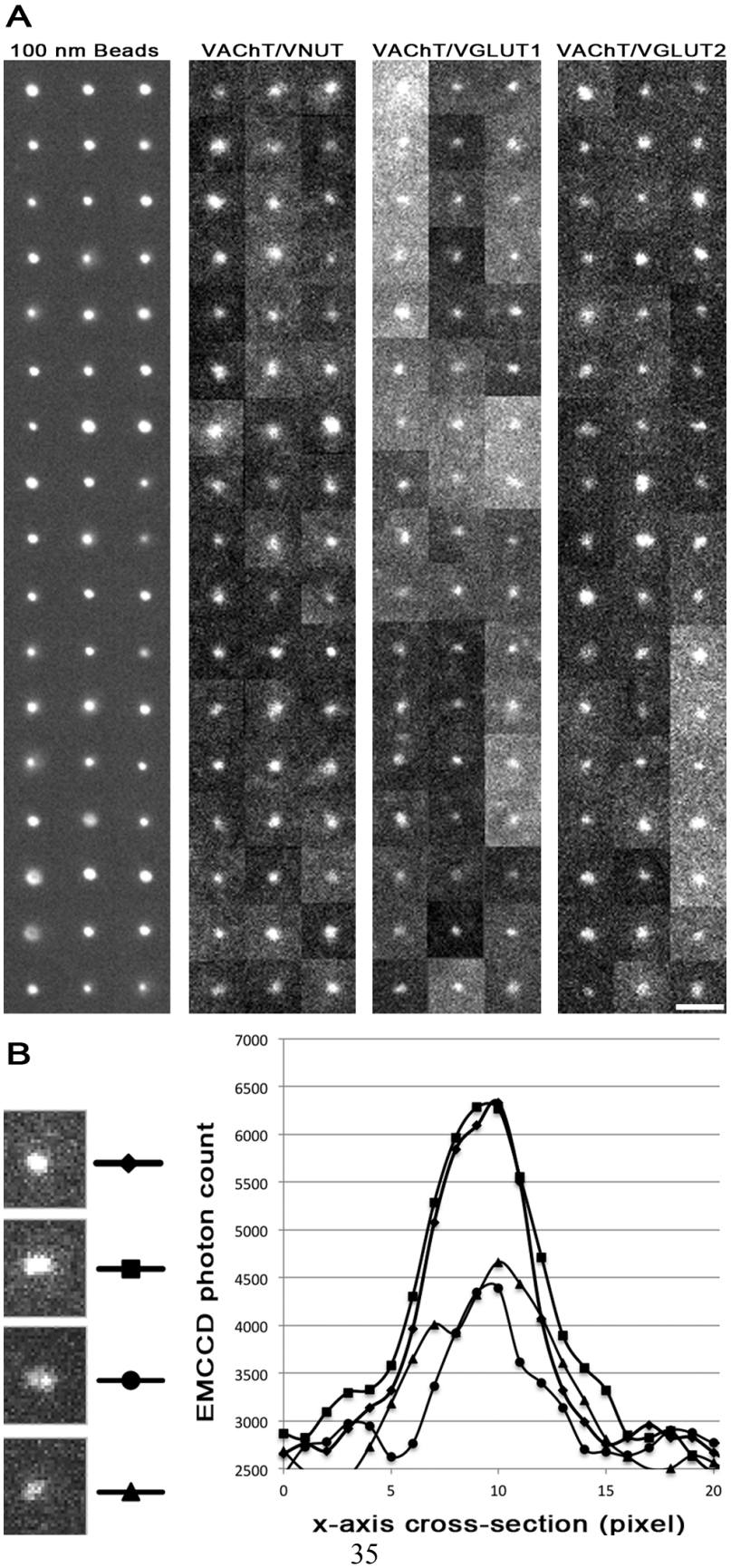
A
100 nm Beads
VAChT/VNUT
VAChT/VGLUT1
VAChT/VGLUT2
B
EMCCD photon count
7000
6500
6000
5500
5000
4500
4000
3500
3000
2500
0
5
10
15
20
x-axis cross-section (pixel)

Blue, and the other secondary channel was optimized for the secondary label (Goat anti-rabbit) Alexa 488. The types of possible outcomes are diagramed in **Figure 6 A-H**. Instances of FM4-64 label with no additional label in either of the other channels were not quantified. Instances of single channel label (Pacific Blue or Alexa 488), or instances of dual channel label (Pacific Blue and Alexa 488) were quantified, examples of which can be seen in **Figure 6 I-K**.

Statistical analysis of the VAChT labeled vesicles found a high degree of pairing in the second label channel, with a majority of the vesicles that labeled with VAChT also labeled with VNUT (69%), VGLUT1 (86%), or VGLUT2 (88%). Further statistical groupings can be quantified based on pairwise comparisons using Agresti Coull confidence limits[105]. In addition to containing a VAChT, 59% of vesicles are likely to contain VNUT and VGLUT1, 61% of VAChT vesicles are likely to contain VNUT and VGLUT2, 75% of VAChT vesicles are likely to contain VGLUT1 and VGLUT2, and 52% of the single VAChT vesicles are expected to contain VNUT, VGLUT1, and VGLUT2 (**Figure 7**).

Discussion

In this study we used single vesicle imaging to examine whether cholinergic synaptic vesicles possess additional types of neurotransmitter transporters. As observed by electron tomography, cholinergic vesicles at the frog's neuromuscular junction possess a stereotypic structure and arrangement of transmembrane molecules and appear homogenous[111]. We found that cholinergic vesicles isolated from the electric organ of *T. californica* have at least four different neurotransmitter transporters. In addition to the

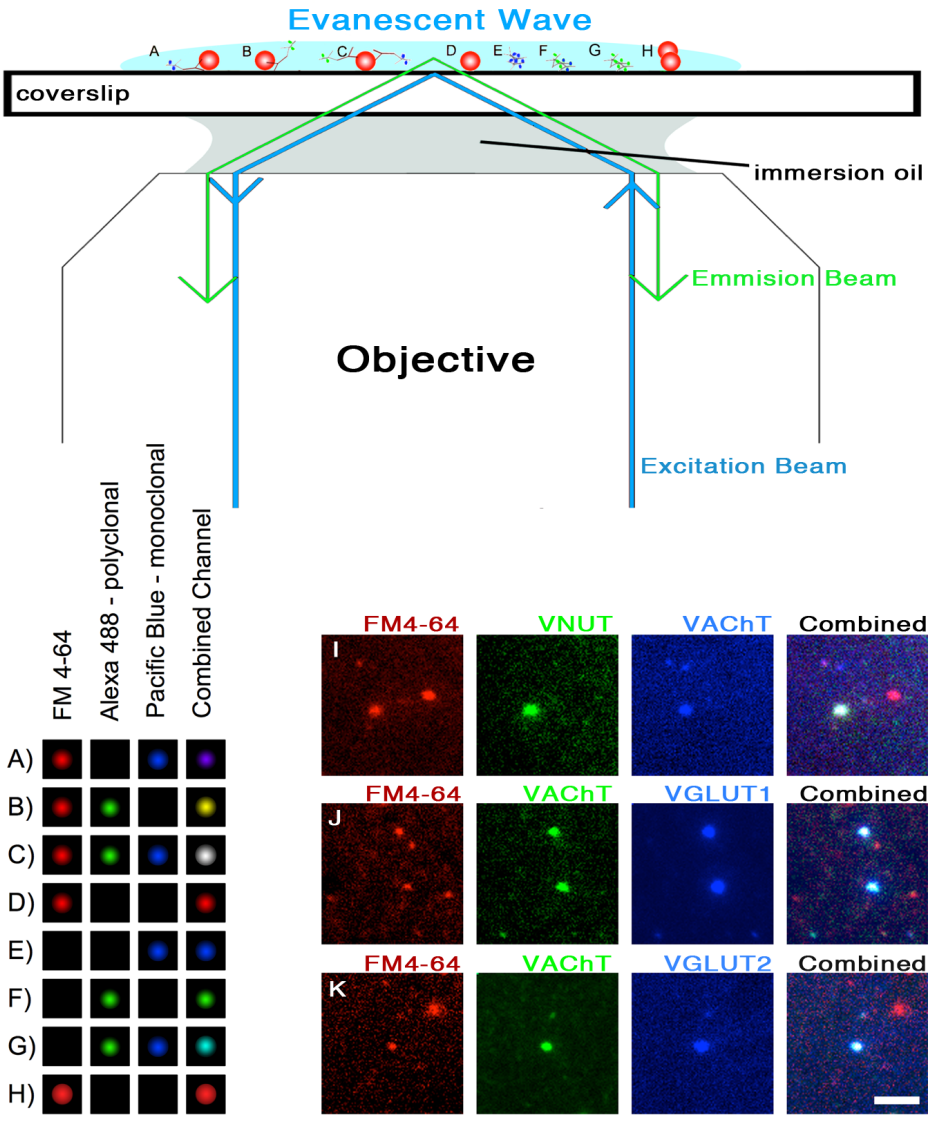

Figure 6. **TIRF microscope images of single synaptic vesicles.** During TIRF illumination, the excitation beam travels off-axis through the microscope objective causing the beam's incident angle at the coverslip to be too shallow to allow the beam to pass into the sample, thus leading to the total internal reflection of the beam back into the objective. An evanescent field of illumination, approximately 100 nm in depth, is created at the surface of the coverslip, allowing for selective illumination of single molecules residing on the coverslip. A diagram of expected observations could include singly label vesicles A, B or dually labeled vesicles C. FM4-64 was used in order to control for three possible scenarios: D) Non-labeled vesicles or debris, E-G) fluorescent secondary on the coverslip not associated with any synaptic vesicles, or H) spots that contained brighter than standard labeling in the FM4-64 channel, as discussed in Fig 3B, and were thus unlikely to be single vesicle events. Example TIRF images of dual labeled, single vesicle events for I) VAChT and VNUT, J) VAChT and VGLUT1, and K) VAChT and VGLUT2. Scale bar = 1 micron.

cholinergic transporter VAChT, a purinergic transporter VNUT and two glutamatergic transporters VGLUT1 and VGLUT2 were shown to co-localize with VAChT to individual vesicles.

Until recently, the stimulated release of acetylcholine and ATP from the motor neurons of the electric lobe[40] stood as one of the few exceptions to Eccels'[36] interpretation of Dale's hypothesis[35] - one neuron, one neurotransmitter. Not only are the two neurotransmitters released from the presynaptic terminals in a stimulation dependent manner, ensemble measurements of synaptic vesicles isolated from *T. californica* clearly demonstrate that both neurotransmitters actively load into the synaptic vesicles. Subsequent work has demonstrated that ATP acts on specific purinergic receptors at terminals[112], and the transporter responsible for loading ATP into the vesicles, VNUT, has been cloned and characterized[14]. However, prior to this study, whether individual synaptic vesicles contained both cholinergic and purinergic transporters was unknown. Using single vesicle imaging we demonstrate that at least 69% of the VAChT containing vesicles also possess VNUT, indicating that indeed individual vesicles do contain both cholinergic and purinergic transporters and are therefore most likely filled with and secrete both ACh and ATP simultaneously.

Glutamate is perhaps the most abundant neurotransmitter in the nervous system of vertebrates. Based upon our initial transcriptome of the electric lobe we believe homologs for all three glutamate transporters are present in T. californica (data not shown). However, neuromuscular junctions in vertebrates like *T. californica* utilize acetylcholine as their primary excitatory neurotransmitter. Still, many of the conditions

for considering glutamate as a neurotransmitter, or at least a neuromodulator, at cholinergic motor neurons have been met. Glutamate plasma membrane transporters used to remove glutamate after release are present in muscle cells, and in fact concentrated in the folds of the neuromuscular junction just opposite the presynaptic release site[53]. Glutamate has been shown to activate a nitric oxide signaling pathway in muscle cells[113] that in turn modulates both the number of vesicles released presynaptically[114] and the amount of acetylcholine released by non-quantal means [56]. Glutamate release from the presynaptic terminal has not been demonstrated at the vertebrate neuromuscular junction, although glutamate release has been demonstrated from lower motor neurons onto Renshaw cells[64], and from synaptosomes isolated from *T. californica*[41]. We find that at least 86% of the VAChT containing vesicles also possess VGLUT1, and 89% possess VGLUT2. At this time we cannot exclude the possibility that VGLUT3 might be present in these vesicles, and that the antibody used in this study was not specific to the homolog in *T. californica*. While the synapses at electroplaque cells are not contractile, the possibility that a vesicular glutamate transporter may also be present at vertebrate neuromuscular junctions warrants further study.

The results presented in this paper show single synaptic vesicles that possess two or more neurotransmitter transporters – with at least 52% of vesicles possessing all four neurotransmitter transporters (**Figure 7**). Assuming more than one type of neurotransmitter to be present in the terminal, fusion of one of these vesicles with the plasma membrane would produce co-release of two or more neurotransmitters. In

VAChT paired single vesicle counts

	Only VAChT	W/O VAChT	Paired	Ttl VAChT	% VAChT Paired	95% Lower CI	95% Upper CI
VNUT	141	48	309	450	68.67	64.24	72.78
VGLUT1	38	40	224	262	85.50	80.72	89.25
VGLUT2	29	32	222	251	88.45	83.90	91.83

VAChT statistical pairs

	From VAChT % pairings	95% Lower CI	95% Upper CI
VAChT, VNUT, & VGLUT1	58.71	51.85	64.95
VAChT, VNUT, & VGLUT2	60.73	53.90	66.84
VAChT, VGLUT1, & VGLUT2	75.62	67.82	81.96
VAChT, VNUT, VGLUT1, & VGLUT2	51.92	43.50	59.65

Figure 7. Single synaptic vesicle observations of vesicular transporters (VNUT, VGLUT1, or VGLUT2) co-labeled with VAChT, and confidence intervals of statistically paired transporters calculated using two-sided Agresti - Coull confidence limits.

addition to the ability to load more than one neurotransmitter, the transporters, and the neurotransmitters themselves, may alter the proton gradient (ΔpH) and membrane potential ΔΨ across the vesicle membrane, and in fact may work in a synergistic manner [37,63]. Ensemble measurements of acetylcholine loading into isolated CNS cholinergic vesicles show a marked increase in the presence of glutamate [22]. Glutamate is known to increase the ΔpH across the vesicle membrane, and ΔpH is the most important driving force for VAChT activity. With a negative charge at cytosolic pH, ATP would also provide an increase in ΔpH, although an exact measurement of that activity would be difficult given the requirement of ATP for the vesicular proton pump. The presence of multiple types of neurotransmitter transporters, taken as a whole, provide a mechanism to explain co-transmitter release, and in the case of cholinergic vesicles, synergistic neurotransmitter loading effects.

3. SYNAPTIC VESICLES CONTAIN SMALL RIBONUCLEIC ACIDS (SRNAS) INCLUDING TRANSFER RNA FRAGMENTS (TRFRNAS) AND MICRORNAS (MIRNAS)*

Overview

Synaptic vesicles (SVs) are neuronal presynaptic organelles that load and release neurotransmitter at chemical synapses. In addition to classic neurotransmitters, we have found that synaptic vesicles isolated from the electric organ of *Torpedo californica,* a model cholinergic synapse, contain small ribonucleic acids (sRNAs), primarily the 5' ends of transfer RNAs (tRNAs) termed tRNA fragments (trfRNAs). To test the evolutionary conservation of SV sRNAs we examined isolated SVs from the mouse central nervous system (CNS). We found abundant levels of sRNAs in mouse SVs, including trfRNAs and micro RNAs (miRNAs) known to be involved in transcriptional and translational regulation. This discovery suggests that, in addition to inducing changes in local dendritic excitability through the release of neurotransmitters, SVs may, through the release of specific trfRNAs and miRNAs, directly regulate local protein synthesis. We believe these findings have broad implications for the study of chemical synaptic transmission.

---

*Reprinted with permission from 'Synaptic vesicles contain small ribonucleic acids (sRNAs) including transfer RNA fragments (trfRNA) and microRNAs (miRNA)' by Huinan Li, Cheng Wu, Rodolfo Aramayo, Matthew Sachs and Mark L. Harlow, 2015. Scientific Reports, Volume 5, 14918, 1-14, Copyright 2014 by MacMillan Publisher International Limited.

Introduction

Multiple downstream events occur upon the activity-dependent release of neurotransmitter at chemical synapses. Most obviously, the presynaptic release of neurotransmitter leads to a stereotypic electrical change across a postsynaptic cell membrane. Thus at vertebrate neuromuscular junctions the release of acetylcholine leads to the activation of nicotinic acetylcholine receptors on the muscle membrane, membrane depolarization and subsequent muscle contraction[115-117]. More dynamically, the presynaptic release of neurotransmitter coupled with coincident local postsynaptic membrane depolarization leads to a change in synaptic physiology that can persist for minutes, hours or days[118]. These long term changes have been best characterized at central nervous system (CNS) synapses, and can lead to long term potentiation (LTP) or depression (LTD) of the synaptic coupling between the two cells. In the short-term (minutes) both LTP and LTD rely upon changes in calcium, but for these synaptic changes to be consolidated for the long-term (hours and days) requires, in addition to calcium influx, local protein synthesis[119].

Local protein synthesis at the synapse requires a host of mRNAs, translation factors, and ribosomes[69,120-122]. In addition, it is suspected that microRNA (miRNA) and other non-coding RNA (ncRNA) that include, but are not restricted to, endogenous small interfering RNA (esiRNA), piwi-interacting RNA (piRNA), antisense and long-ncRNA, play a key role in regulating translation[123]. Mechanistically, the release of neurotransmitter presynaptically has been thought to indirectly drive the selective

control of postsynaptic protein synthesis through activity-based modulation of calcium[124].

We hypothesized that the presynaptic terminal might play a more direct role in the regulation of postsynaptic transcription and translation. Previous studies have identified sRNAs that are associated with synaptosomes, as well as sRNAs that are released from and taken into synaptosomes and sRNAs that associate with SV fractions[125,126]. As a first step to test the hypothesis that the presynaptic terminal might play a more active role in local protein synthesis, we looked for the presence of, and ultimately sequenced, small molecule RNAs (sRNAs) that not only associate with synaptosomes and SVs, but localize within the SVs. We first chose SVs isolated from the electroplaques of *Torpedo californica*, a classic peripheral nervous system (PNS) preparation that provides an abundance of cholinergic synaptic vesicles from one class of motor neuron[57]. We treated the SVs with RNase to remove any exogenous cytoplasmic RNA from the preparation, and after RNA extraction, found an abundance of sRNAs protected from degradation. Sequencing of the sRNAs derived from affinity purified SVs revealed the presence of 5' tRNA fragments, with a 5'-fragment of glutamyl-tRNA ($tRNA^{Glu}$) sequence constituting the most abundant of the sequences. We verified by northern blot that the 5' fragments were not a result of the RNase treatment of the vesicles, and that the fragments were protected from degradation in the absence of (but not the presence of) detergent. *In situ* hybridization of the most abundant fragment sequence confirmed the presence of the fragment in the axons and presynaptic terminals of the electroplaque. We extended the results to SVs isolated from

the mouse CNS. As with the electroplaque, we found an abundance of sRNA species that were co-enriched with SVs and were resistant to RNase degradation. The 5'-fragment of $tRNA^{Glu}$ that was most abundant in cholinergic *T. californica* SVs was the second most abundant species of sRNA found in SVs isolated from the mouse brain. Other species of sRNAs were found to be abundant in mouse CNS vesicles, including known miRNAs, and most abundantly, 5' RNA fragments of the Ro ribonucleoprotein associated Y1 RNA (RNY1)[127]. Together these observations not only support the idea that sRNAs are present within SVs, they also suggest that these sRNAs play key roles regulating local protein synthesis at the synapse.

Results

Cholinergic vesicles isolated from the electric organ contain RNA

We isolated synaptic vesicles from the electric organ of the Pacific ray *T. californica* in order to provide an abundant, homogenous preparation of cholinergic SVs[57]. We chose a freeze grinding method of isolation that has been shown by others to retain more of the SV neurotransmitter content while offering a similar SV enrichment (~20 fold; **Table 5**) as other isolation procedures[128,129]. In addition, we wanted to isolate SVs residing within classic synaptosomal boutons as well as those present at less structured synaptic varicosities. SVs were collected from the middle of the 0.6 M (1.07 g/ml density) sucrose gradient layer, well above the 1.2 M (1.17 g/ml) sucrose layer used to isolate exosomes[130,131] or detect exosome markers[132,133]. The size of the vesicles we isolated averaged ~80nm (**Figure 8a**), larger than SVs within the vertebrate CNS

RNA totals

Electric organ SVs fish 1

	SV	pH10	DM	RNase	pHDR
SV starting material protein (mg)	.75	.75	.75	.75	.75
RNA recovered after treatment (ng)	8142	10092	8958	450	372
Amount of RNA loaded into gel (ng) **Fig 1c**	452	560	498	375	310
Average sample RNA (SV,pH10,DM) (ng)	9064				
After RNAse RNA (ng)	450				
Fraction RNA RNase resistant	0.05				

Electric organ SVs fish 2

	SV	pH10	DM	RNase	pHDR
SV starting material protein (mg)	.81	.81	.81	.81	.81
RNA recovered after treatment (ng)	4926	5598	5874	258	258
Average sample RNA (SV,pH10,DM) (ng)	5466				
After RNAse RNA (ng)	258				
Fraction RNA RNase resistant	0.05				

Electric organ SVs fish 3

	SV	pH10	DM	RNase	pHDR
SV starting material protein (mg)	.63	.63	.63	.63	.63
RNA recovered after treatment (ng)	10284	10716	9492	372	486
Amount of RNA loaded into gel (ng) **Fig 2b**	285	298	264	206	270
Average sample RNA (SV,pH10,DM) (ng)	10164				
After RNAse RNA (ng)	372				
Fraction RNA RNase resistant	0.04				

Table 5. Quantification of RNA from *Torpedo californica* experiments.

Figure 8. **Cholinergic SVs from the electric organ of *Torpedo californica* contain RNA.** a) Electron micrograph of negatively stained SVs isolated and enriched from electroplaque tissue. Sample contains abundant ~80 nm vesicles (some marked with arrows). b) Western-blot analysis of the synaptic vesicles during purification. The SV protein synaptophysin was used as a marker during the enrichment. The isolation procedure includes the collection of the original slurry (Sl), two centrifugation supernatants and pellets (S1, P1 and S2, P2), followed by a sucrose density gradient centrifugation and collection of the SV fluffy layer (FL). Further purification using size exclusion chromatography yields the final, enriched sample of SVs (SV). Purified vesicles were tested by immunoblot and found to be positive for the ~60 kD vesicle acetylcholine transporter (VAChT). c) Abundant sRNAs co-enrich with the synaptic vesicles (SV). These sRNAs are stable under high pH (pH10), or in the presence of detergent (DM). After addition of RNase much of the RNA is degraded; however an RNase resistant ~32 nt band persists (RNAse). The RNAse resistant band of RNA can be degraded in the presence of high pH, detergent, and RNAse (pHDR). Bands of gel underlined (_) indicate a 20-fold reduction of sample loaded. d) TIRF microscope images of SVs reveals that single SVs contain RNA, as demonstrated by triple-labeling of the SVs with the steryl dye FM4-64, VAChT, and the RNA dye Syto12. Five representative vesicles shown from a total of 307. Scale bar = 1 μm.

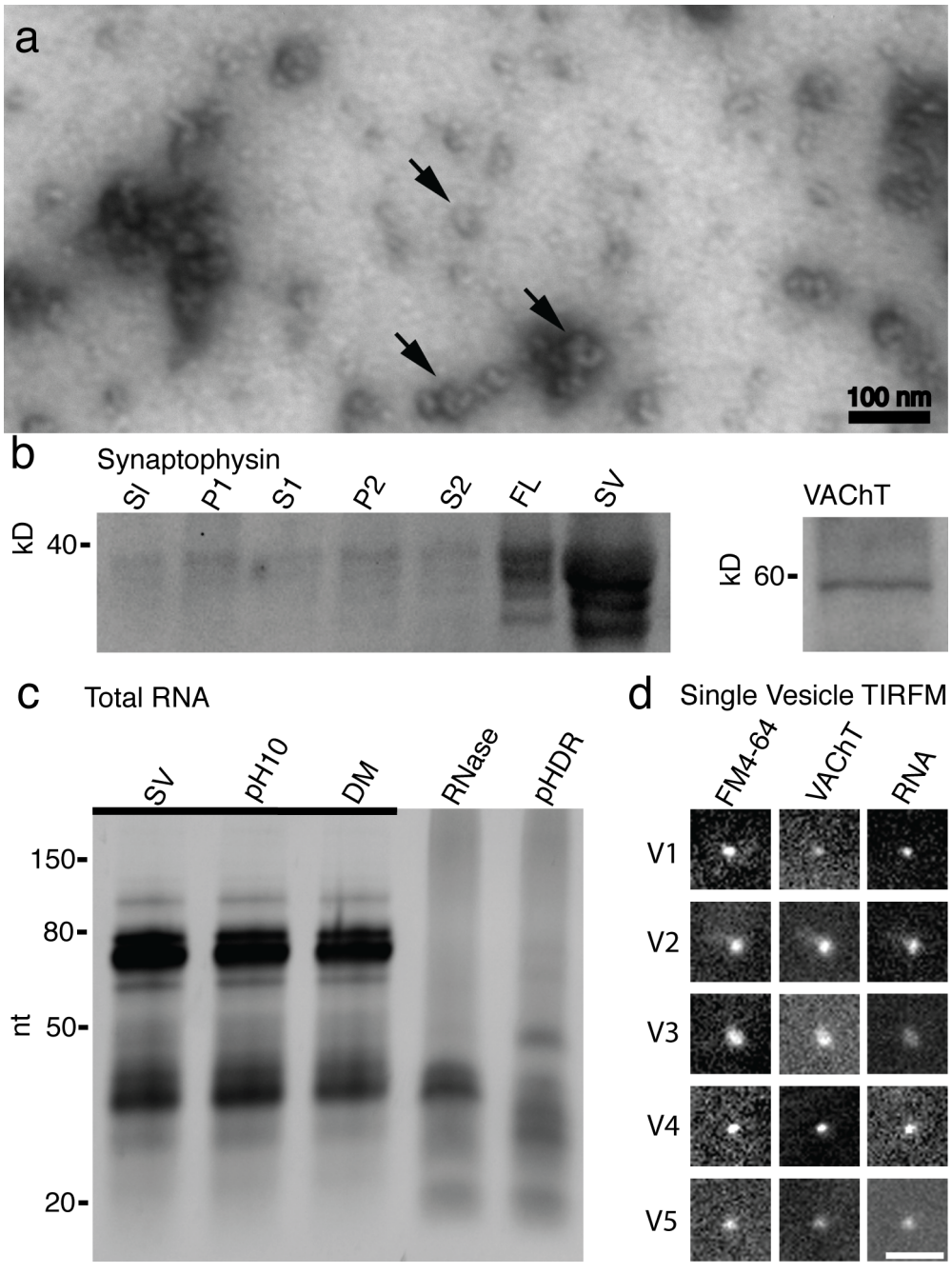
a
100 nm
b
Synaptophysin
Sl
P1
S1
P2
S2
FL
SV
kD
40
VAChT
kD
60
c
Total RNA
SV
pH10
DM
RNase
pHDR
150
80
nt
50
20
d
Single Vesicle TIRFM
FM4-64
VAChT
RNA
V1
V2
V3
V4
V5

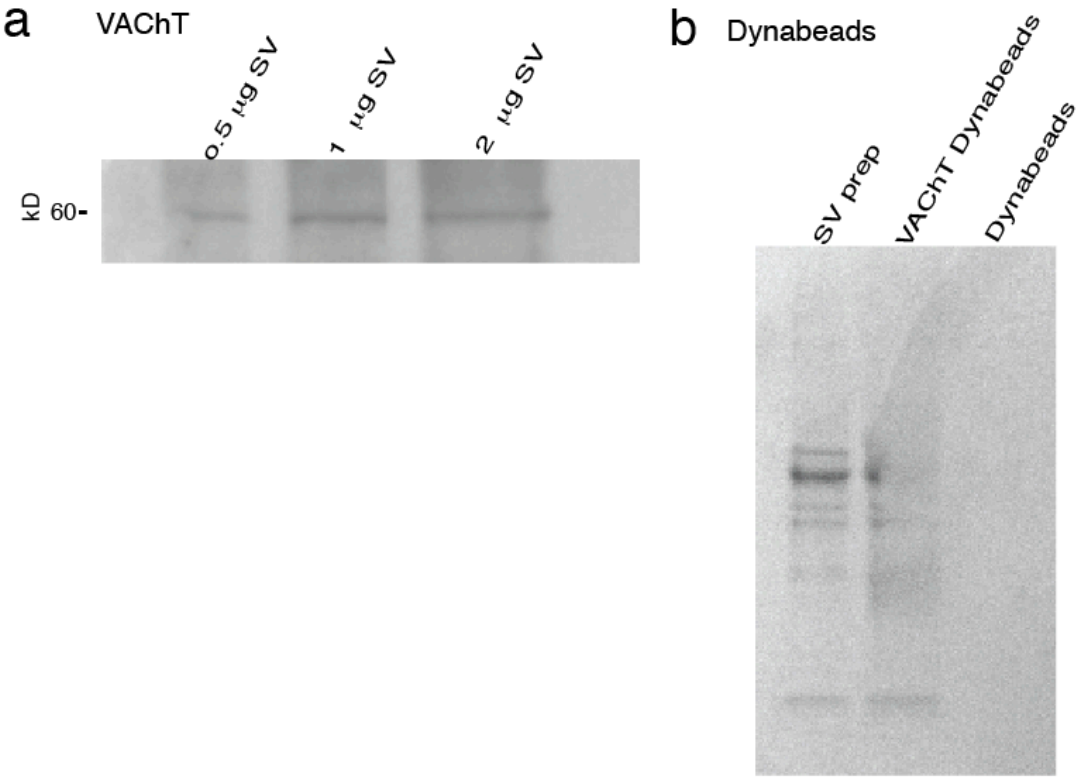

Figure 9. Western blot analysis of purified synaptic vesicles from the electric organ of *Torpedo californica* and Ponceau staining of synaptic vesicles isolated with Dynabeads. a) The ~60 kd Vesicular AcetylCholine Transporter (VAChT) is shown in three lanes. Lane 1) 0.5 µg SV loaded 2) 1 µg SV loaded and 3) 2 µg of SV loaded. Further verification of antibody with this preparation described in Li & Harlow, 2014[31]. b) A protein gel containing three lanes of samples were transferred to a membrane and total protein was imaged with Panceau stain (G-Biosciences; St Louis, MO). SV lane shows 5 µg of purified synaptic vesicles, VAChT Dynabeads lane shows resulting affinity purified synaptic vesicles isolated with VAChT conjugated dynabeads, and Dynabeads lane shows parallel experiment demonstrating dynabeads without antibody conjugated do not isolate SVs or other material.

(~40nm)[103] or SVs found at vertebrate neuromuscular junctions (~50nm)[107,108], but normal for vesicles from this preparation[106]. As further verification that the isolated vesicles were neuronal in origin, we found by western blot analysis that the synaptic vesicle marker synaptophysin[109] was enriched during isolation and that the vesicular acetylcholine transporter (VAChT)[94] was present in the final preparation (**Figure 8b; Figure 9**). We hypothesized that, in addition to neurotransmitter, SVs might contain RNA. To test this hypothesis we extracted RNA from the SV enriched preparation using a TRIzol extraction method and found abundant small molecule RNAs (**Figure 8c**). The cytoplasm of presynaptic terminals likely contains RNA molecules that might co-enrich with the SVs. In order to test whether the sRNAs were exogenous to or resided within the SVs we hypothesized that the vesicle membranes would provide protection from RNase degradation, thus allowing us to separate the cytoplasmic associated RNA from any vesicular protected RNA. We tested the preparation under five conditions. In the presence of high pH buffer (pH 10 – known to disrupt RNA secondary and tertiary structure[134]) we observed no difference between the RNA isolated from the pH 7.4 SV preparations and the RNA isolated from the pH 10 SV preparation. We next chose, along with high pH, to add membrane detergent (DM; n-Decyl-β-D-Maltopyranoside) to disrupt the SV membranes without denaturing proteins[135]. Once again in the presence of pH 10 and DM we found no difference between the RNA we isolated from the untreated SV preparation. Next we added RNase to the SVs. In the presence of RNase we found a substantial (~20 fold; Supplemental table 1) reduction in RNA, suggesting that

exogenous RNA does co-enrich with SVs. After RNase treatment a specific band of sRNAs of approximately ~32 nucleotide (nt) persisted. It was only when we combined pH 10, DM, and RNAse that we observed degradation of the ~32nt band (**Figure 8c**).

We have previously used a single vesicle imaging approach to study the co-localization of multiple types of vesicular transporters to single vesicles in the cholinergic SV preparation[110,136]. As an initial step to verify that the sRNAs not degraded by RNase resided within cholinergic synaptic vesicles, and were not the result of RNA co-enriching with the SVs during the isolation procedure, we triple labeled isolated SVs in the presence of RNase (**Figure 8d**). Isolated SVs were labeled by immunofluorescence with a polyclonal antibody against VAChT, the nucleic acid dye SYTO12, and the membrane steryl dye FM4-64. Because SVs are smaller than the diffraction limit, cholinergic vesicles were identified as small diffraction-limited dots visible in the FM4-64 channel that co-labeled for VAChT. Almost all cholinergic SVs co-labeled for RNA (96.1%; N=307)

Cholinergic vesicles isolated from the electric organ contain tRNA fragments

We sequenced the RNase resistant cholinergic SV's sRNA. As a further step beyond size and density based purification methods, magnetic beads with conjugated antibodies against VAChT were used in the purification procedure (Supplemental Fig. 1)[131,137]. SV non-luminal RNA was removed by treatment with RNase before luminal RNA was extracted by TRIzol. Five primary sequences with slight variations of length dominated the next generation sequencing reads, accounting for 60% of the total reads

(**Table 6**). The most abundant primary sequence was that of a 5' fragment of a $tRNA^{Glu}$ with the anticodon CUC ($tRNA^{Glu}_{CUC}$) that is conserved across vertebrates (**Figure 10a**)

	Sequence	NT	Copy #	Identity
1	UCCCUGGUGGUCUAGUGGUUAGGAUUCGGCGC	32	2988724	5'-trfRNA^{Glu}
	UCCCUGGUGGUCUAGUGGUUAGGAUUCGGCGCUC	34	475743	
	UCCCUGGUGGUCUAGUGGUUAGGAUUCGGCGCU	33	402173	
	UCCCUGGUGGUCUAGUGGUUAGGAUUCGGCG	31	249273	
	UCCCUGGUGGUCUAGUGGUUAGGAUUCGGC	30	80234	
			4196147	
2	GCAUUGGUGGUUCAGUGGUAGAAUUCUCGCC	31	829169	5'-trfRNA^{Gly}
	GCAUUGGUGGUUCAGUGGUAGAAUUCUCGCCU	32	412080	
	GCAUUGGUGGUUCAGUGGUAGAAUUCUCGCCUG	33	299964	
	GCAUUGGUGGUUCAGUGGUAGAAUUCUCGCCUGC	34	205669	
	GCAUUGGUGGUUCAGUGGUAGAAUUCUCGC	30	172506	
			1919388	
3	GCAUCGGUGGUUCAGUGGUAGAAUUCUCGCC	31	200366	5'-trfRNA^{Gly}
	GCAUCGGUGGUUCAGUGGUAGAAUUCUCGCCUGC	34	115460	
	GCAUCGGUGGUUCAGUGGUAGAAUUCUCGCCUG	33	79351	
			395177	
4	GUUUCCGUAGUGUAGUGGUUAUCACGUUCGCC	32	219845	5'-trfRNA^{Val}
5	GCCCGGAUAGCUCAGUCGGUAGAGCAUCAGAC	32	130889	5'-trfRNA^{Lys}

Table 6. sRNAs identified through next-generation sequencing of affinity purified SVs from the electroplaque of *T. californica*

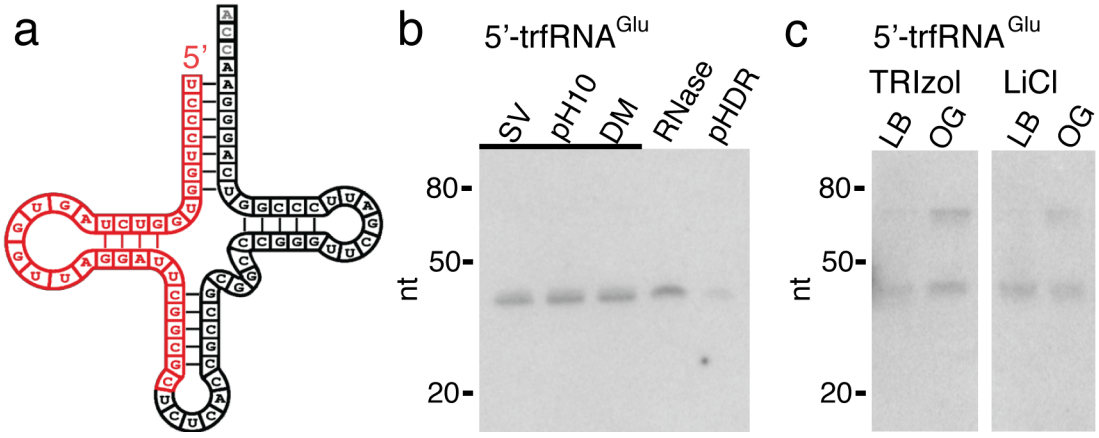

Figure 10. Cholinergic vesicles isolated from the electric organ of *T. californica* contain 5'-tRNA fragments. a) Next-generation sequencing of RNA isolated from RNAse treated SVs enriched and affinity purified against VAChT reveals that cholinergic SVs contain 5' fragments of tRNA. The most abundant fragment (5'-trfRNA^{Glu}) shown in red mapped onto the complete tRNA glutamate (tRNA$^{Glu}_{CUC}$) shown in black. b) Northern analysis of RNA isolated from SVs verifies that the 5'-trfRNA^{Glu} sequence was not a product of RNase treatment. RNA isolated from SVs purely isolated (SV), at pH10 (pH10), in detergent (DM), treated with RNase (RNase), and treated simultaneously with pH10, detergent, and RNase (pHDR). Bands of gel underlined (_) indicate a 20-fold reduction of sample loaded. c) Northern analysis of total RNA (Trizol) and tRNA enriched RNA (LiCl) isolated from the electric lobe (LB) and electric organ (OG) of T. californica reveals full length tRNA$^{Glu}_{CUC}$ and 5'-trfRNA^{Glu} were found in near equal abundance in the electric organ, whereas 5'-trfRNA^{Glu} was more abundant than tRNA$^{Glu}_{CUC}$ in the electric lobe.

followed by 5' fragments of two different tRNAs specifying glycine ($tRNA^{Gly}_{CCC}$), a 5' fragment of tRNA Valine (5'-$trfRNA^{Val}_{CAC}$), and a 5' fragment of tRNA Lysine ($trfRNA^{Lys}_{UUU}$). Fragments of tRNA, both 5' and 3', are signaling molecules cleaved by the vertebrate RNase angiogenin[86,138,139], and are designated 5'- and 3'- trfRNAs (for stress-induced tRNA fragment). We verified that the 5'-trfRNAs were not a result of the RNase treatment used in the isolation procedure by northern analysis of the most abundant 5'-$trfRNA^{Glu}$ sequence (**Figure 10b; Figure 11; Table 7**). The northerns were conducted three times, each with RNA isolated from SVs prepared from separate fish. Only a ~32nt band was observed in samples of the isolated SVs, pH 10 treated SVs, membrane detergent (DM) treated SVs, and RNase treated SVs. RNAs from the SV sample treated with pH 10-DM-RNase were degraded, providing further evidence that the 5'-trfRNAs reside within the cholinergic SVs, and are not a product of the RNAse treatment (**Figure 8b**).

To test whether the full-length $tRNA^{Glu}_{CUC}$ could be found in the presynaptic electric lobe and/or the postsynaptic electric organ we extracted total RNA from the two tissues for northern anaylsis. Full-length $tRNA^{Glu}_{CUC}$ and 5'-$trfRNA^{Glu}$ were found in near equal abundance in the electric organ, whereas 5'-$trfRNA^{Glu}$ was more abundant than $tRNA^{Glu}_{CUC}$ in the electric lobe (**Figure 10c; Figure 11; Table 7**). We further enriched for tRNA from total RNA preparations using sodium acetate and LiCl extraction[140], and observed a similar pattern of $tRNA^{Glu}_{CUC}$ and 5'-$trfRNA^{Glu}$ abundance in the tissues (**Figure 10c; Figure 11; Table 7**).

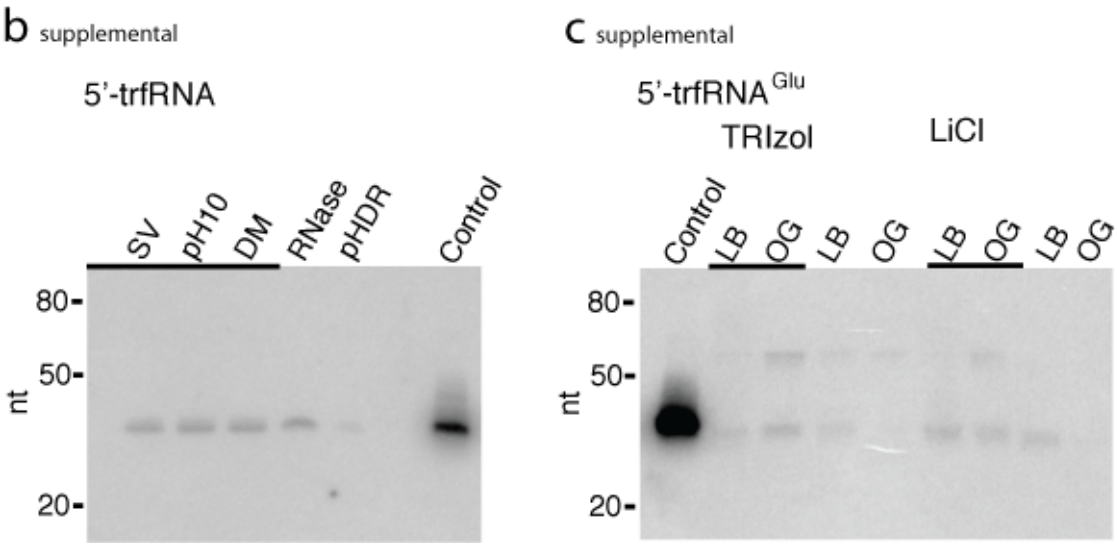

Figure 11. (b and c) Northern quantification based upon comparison to positive control and quantified using Imagequant.

Table 7. Calculations of 5'-trfRNA^{Glu} found in the SV preparation shown in Figure 11b and 11c. Calculation of full-length tRNA$^{Glu}_{CUC}$ and 5'-trfRNA^{Glu} found in the electric lobe and organ of *T. californica* shown in Fig. 11c. TRIzol = total RNA preparation; LiCl = tRNA enriched preparation. First two lanes of LB and OG from each extraction method loaded with 80% sample (indicated by LB and OG); adjacent lanes of LB and OG loaded with 20% sample (4-fold dilution).

11b supplemental

	SV	pH10	DM	RNase	pHDR
Total RNA (ng) from preparation	10266	10716	9492	372	486
Amount of RNA (ng) loaded in Fig 11b lane	285	298	264	206	270

Northern Analysis - Calculation of 5'-trfRNA^{Glu}

Amount of trfRNA in Northern (ng)	13	17	17	14	3
Calculated amount of trfRNA from preparation (ng)	468	612	612	25	5
Average sample ttl trfRNA (SV,pH10,DM) (ng)	564				
After RNAse (ng)	25				
Fraction of 5'-trfRNA^{Glu} RNAse resistant	0.04				

11c supplemental – total RNA and LiCl sRNA enrichments from three *T. californica* rays.

0.1 gram of tissue used from each organ	Trizol		LiCl	
	Lobe (ng)	Organ (ng)	Lobe (ng)	Organ (ng)
Fish 1 Tissue	4872	1632	4987	4685
Fish 2 Tissue	4416	1957	5362	3343
Fish 3 Tissue	4459	1964	5388	3527
total	13747	5553	15737	11555

	TRIzol				LiCl			
	LB	OG	LB	OG	LB	OG	LB	OG
Sample total and loaded RNA (ng) in Fig 11c lane	10998	4443	2749	1111	12590	9244	3147	2311

	TRIzol				LiCl			
Northern Analysis	LB	OG	LB	OG	LB	OG	LB	OG
Calculated amount of tRNA in Northern (ng)	0	4	0	0	0	2	0	0
Calculated amount of trfRNA in Northern	6	5	3	0	5	3	3	0
(ng)								

5'-trfRNA^{Glu} localizes to axons and presynaptic nerve terminals

To confirm that 5'-trfRNAs are presynaptic SV-associated species, we performed fluorescent *in situ* hybridization on cryostat sections of the *T. californica* electric organ. Probes for 5'-trfRNA^{Glu} or the SV transporter VAChT were used in association with fluorescently labeled α-Bungarotoxin, a postsynaptic marker for the nicotinic receptors that cover the surface of the electric organ. Nerve axons run perpendicular to the pancake stacked electric organ electrocytes before turning 90 degrees and innervating the entire surface of each cell. We found that the probe for 5'-trfRNA^{Glu,} but not a scrambled control probe, labeled the axons and surface of the electrocytes in a similar pattern as the presynaptic SV marker VAChT (**Figure 12 a,b; Figure 13**), suggesting that the 5'-trfRNA^{Glu} is associated with axons and presynaptic nerve terminals rather than the postsynaptic electric organ.

Synaptic vesicles isolated from mouse CNS contain RNA

We hypothesized that synaptic vesicles residing in the CNS might also contain sRNAs. To test this, we isolated SVs from the mouse brain of Swiss Webster mice. As expected, the mouse brain SVs were ~40nm in diameter (**Figure 14a**) and the synaptic vesicle marker synaptophysin co-purified with SVs during isolation (**Figure 14b; Figure 15**). Once again, SVs were collected from the middle of the 0.6 M (1.07 g/ml density) sucrose gradient layer, well above the 1.2 M (1.17 g/ml) sucrose layer used to isolate exosomes[130,131] or detect exosome markers[132]. We treated the mouse SVs with TRIzol and found that the preparation was enriched in sRNAs (**Figure 14c**). As with the

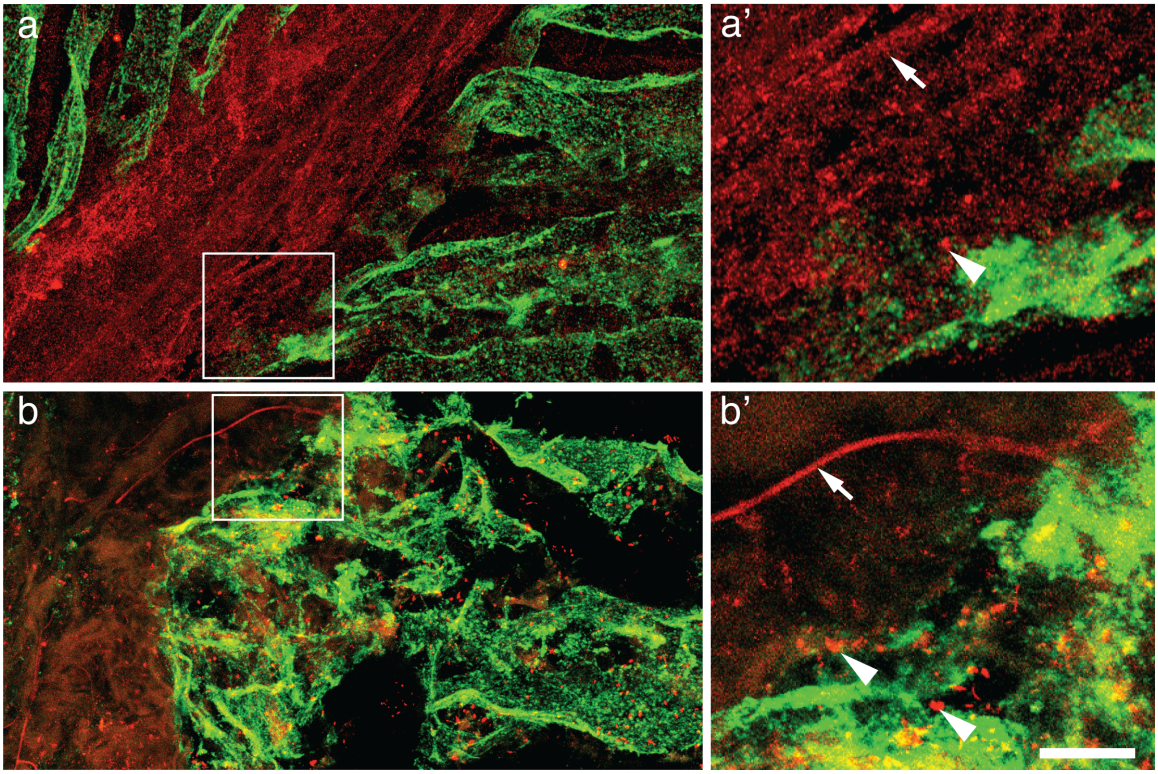

Figure 12. **5'-trfRNA^{Glu} localize to axons and presynaptic nerve terminals of the electric organ of *T. californica*.** a) Immunohistochemical labeling of 20-micron thick cryostat sections of the electric organ. Axons and presynaptic terminals labeled with polyclonal antibodies against VAChT (red). The nicotinic acetylcholine receptor rich surface of the electrocyte cells labeled with α-Bungarotoxin (green). a') Enlarged region from A, axon marked with white arrow and presynaptic bouton white arrowhead b) A similar pattern of labeling is present within *in situ* hybridization samples of the same tissue. Axons and presynaptic boutons labeled with a probe for 5'-trfRNA^{Glu} (red), and the surface of the electrocyte cells labeled with α-Bungarotoxin (green). b') Enlarged region from B, axon marked with white arrow and presynaptic boutons white arrowheads a' and b' scale bar = 5 μm.

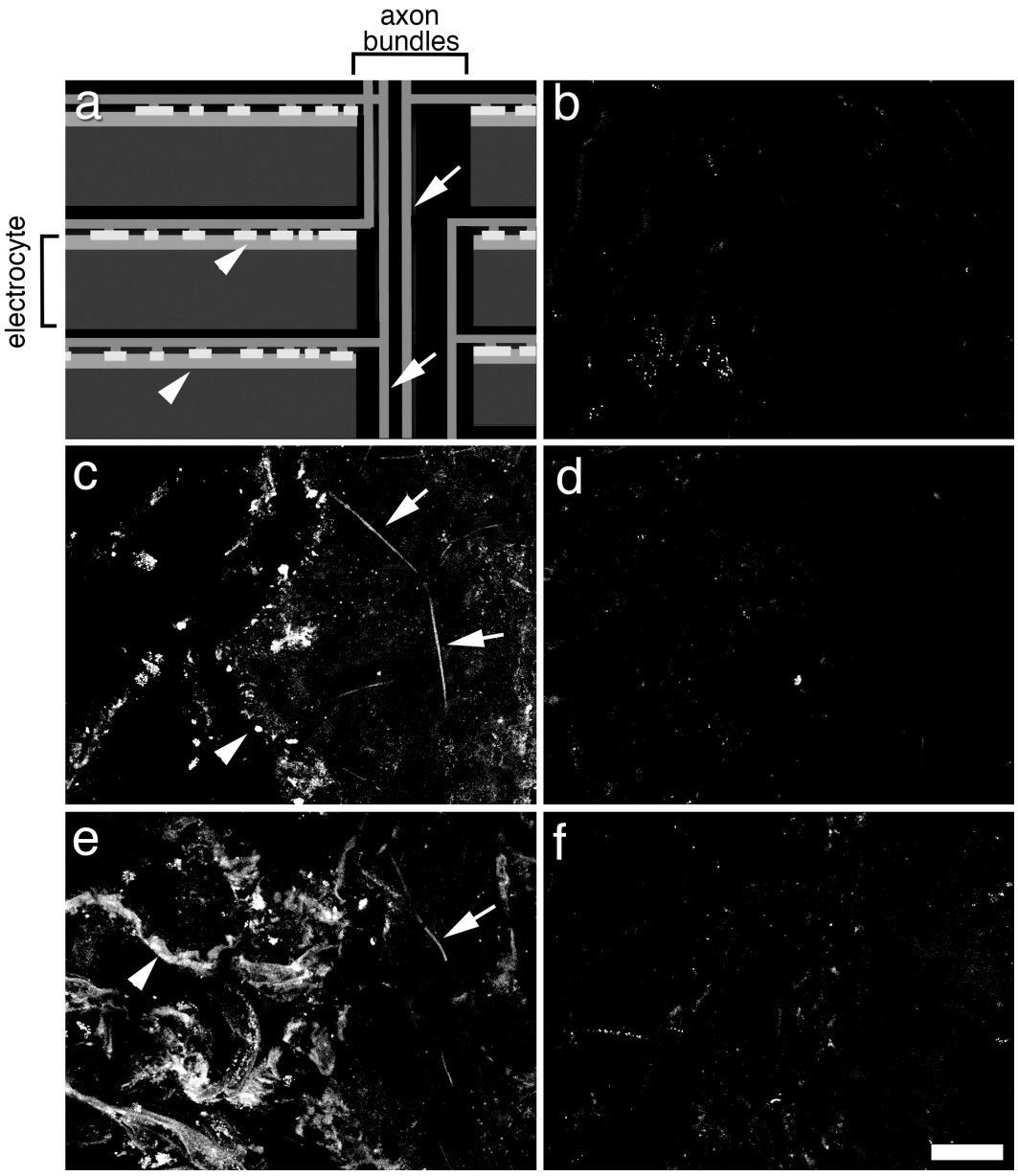

Figure 13. ***In situ*** **hybridization control demonstrating specificity of the 5'-trfRNA^{Glu} probe versus scrambled probe.** a) Cartoon depicting the orientation of cryostat sections of the electric organ shown in b-f. Stacks of electrocyte cells are on the left sides of each image, with the axon bundles and a small amount of an adjacent stack of electrocytes shown on the right side of each panel. Right side panels (b,d,f) show three *in situ* preparations labeled with the scrambled probe. No appreciable labeling can be found on tissue sections. Left panels c,e show two additional *in situ* preparations labeled with the probe for 5'-trfRNA^{Glu}. Axons, running nearly perpendicular to electrocyte cells are visible (arrowheads), and strong staining of electrocyte surfaces (arrowhead) can be seen. All images taken and balanced under identical conditions. Scale bar = 5 microns.

RNA totals

Electric organ SVs fish 1

	SV	pH10	DM	RNase	pHDR
SV starting material protein (mg)	.75	.75	.75	.75	.75
RNA recovered after treatment (ng)	8142	10092	8958	450	372
Amount of RNA loaded into gel (ng) **Fig 8c**	452	560	498	375	310
Average sample RNA (SV,pH10,DM) (ng)	9064				
After RNAse RNA (ng)	450				
Fraction RNA RNase resistant	0.05				

Electric organ SVs fish 2

	SV	pH10	DM	RNase	pHDR
SV starting material protein (mg)	.81	.81	.81	.81	.81
RNA recovered after treatment (ng)	4926	5598	5874	258	258
Average sample RNA (SV,pH10,DM) (ng)	5466				
After RNAse RNA (ng)	258				
Fraction RNA RNase resistant	0.05				

Electric organ SVs fish 3

	SV	pH10	DM	RNase	pHDR
SV starting material protein (mg)	.63	.63	.63	.63	.63
RNA recovered after treatment (ng)	10284	10716	9492	372	486
Amount of RNA loaded into gel (ng) **Fig 2b**	285	298	264	206	270
Average sample RNA (SV,pH10,DM) (ng)	10164				
After RNAse RNA (ng)	372				
Fraction RNA RNase resistant	0.04				

Table 8. Quantification of RNA from *Torpedo californica* experiment

T. californica SVs, we tested the mouse SV RNA under three conditions. We raised the buffer to pH 10, but saw little difference. Next we added the detergent DM (also at pH 10) and observed little difference between the RNA we isolated from the SV prep. When we added RNase to the SV prep we had a dramatic reduction (~38 fold; **Table 8**) in the amount of total RNA extracted; however, two bands of resistant RNA at ~32 and ~21 nt remained. These bands appear to be partially degraded when we combined pH 10, membrane detergent (DM), and RNase (**Figure 14c**).

We sequenced the RNase resistant mouse SV sRNA using next generation sequencing. Two classes of sequences with slight variations of length dominated the reads, with the top ten sequences accounting for 40% of the total reads (**Table 9**). The most abundant set of sequences mapped to a 5' fragment of a Y RNA: Ro-associated Y1 (RNY1)[127]. The 5' fragment of RNY1 (5'-fRNY1) is part of the stem loop of RNY1, and like the 5'-trfRNAs, exists as multiple copies of similar length (~32nt). The second most abundant set of sRNAs in the mouse CNS SVs was the most abundant sequence found in the *T. californica* SVs: the 5'-trfRNA^{Glu} (~32nt). The third, fourth, seventh, eighth and ninth mapped to neuronal associated microRNAs, including miR128, miR99, miR100, miR22, and miR127 (21-22nt). Fragments of other tRNA^{Glu} species accounted for the fifth and sixth most abundant sequences. The fifth sequence does not map perfectly to any known mouse genomic sequence for a tRNA, perhaps as a result of a splice variation or mouse genomic strain difference, and the sixth most abundant sequence mapped to a fragment of tRNA$^{Glu}_{TTC}$. The tenth most abundant sequence mapped to the 5'-terminal fragment of the 28s ribosomal RNA (20nt). These

	Sequence	NT	Copy #	Identity
1	GGCUGGUCCGAAGGUAGUGAGUUAUCUCAAUU	32	4491149	RNA, Ro-associated Y1
	GGCUGGUCCGAAGGUAGUGAGUUAUCUCAAU	31	3921692	
	GGCUGGUCCGAAGGUAGUGAGUU	23	799788	
	GGCUGGUCCGAAGGUAGUGAGUUAUCUCA	29	347449	
	GGCUGGUCCGAAGGUAGUGAGUUAUCUCAA	30	338822	
	GGCUGGUCCGAAGGUAGUG	19	314918	
			10213818	
2	UCCCUGGUGGUCUAGUGGUUAGGAUUCGGCG	31	2289788	5'-trfRNA^{Glu}
	UCCCUGGUGGUCUAGUGGUUAGGAUUCGGCGC	32	2039321	
	UCCCUGGUGGUCUAGUGGUUAGGAUUCGGC	30	882725	
	UCCCUGGUGGUCUAGUGGUUAGGAUU	26	576141	
	UCCCUGGUGGUCUAGUGGUUAGGAUUCGG	29	333204	
			6121179	
3	UCACAGUGAACCGGUCUCUUU	21	2581783	MIR-128-1
	UCACAGUGAACCGGUCUCUUUU	22	1857626	
	UCACAGUGAACCGGUCUCUUUUU	23	427156	
			4866565	
4	AACCCGUAGAUCCGAUCUUGU	21	2055063	MIR-99a
	AACCCGUAGAUCCGAUCUUGUG	22	346662	
			2401725	
5	UCCCUGUGGUCUAGUGGUUAGGAUUCGGCG		1488662	5'-trfRNA^{Glu}
6	UCCCACAUGGUCUAGCGGUUAGGAUUCCUGGUU	33	1087820	5'-trfNA^{Glu}
7	AACCCGUAGAUCCGAACUUGUG	22	545334	MIR-100
	AACCCGUAGAUCCGAACUUGU	21	350473	
			895807	
8	AAGCUGCCAGUUGAAGAACUGU	22	716387	MIR-22
9	UCGGAUCCGUCUGAGCUUGG	20	687125	MIR-127
10	CGCGACCUCAGAUCAGACGU	20	609557	rRNA-RNA, 28S ribosomal 5

Table 9. sRNAs identified through next-generation sequencing of SVs isolated from the mouse CNS.

nucleotides, along with the last 20nt of the 5.8s RNA, form the eukaryotic expansion segment known as $ES4^{L}$, a double-stranded complex of the 60s ribosomal subunit[141].

We verified that the 5'-trfRNAs were not a result of the RNase treatment used in the isolation procedure by northern analysis with the 5'-$trfRNA^{Glu}$ sequence. The northerns were conducted three times, each with RNA isolated from a different preparation of mouse SVs. As with the *T. californica*, the 32nt 5'-$trfRNA^{Glu}$ is present in the mouse SV preparations before RNase treatment (**Figure 14d**). Unlike the *T. californica* SV preparation, full-length ~ 80 nt $trfRNA^{Glu}$ does appear to associate with synaptic vesicles prior to RNase degradation. In addition, we did not see an appreciable decline in signal for the 5'-$trfRNA^{Glu}$ after pH 10-DM-RNase treatment (**Figure 14d; Figure 15**). We can quantify the number of 5'-$trfRNA^{Glu}$ per SV from the mouse CNS using the weight of an average mouse SV (25.6×10^{-18} g/vesicle)[142] and the amount of 5'-$trfRNA^{Glu}$ detected in our northern analysis. We found that on average, 15 vesicles per 1000 would contain a 5'-$trfRNA^{Glu}$ if the sRNAs were evenly distributed (**Figure 16**). In the northern analyses of the 5' -fRNY1 RNA, multiple sizes representing full length and partial fragments of the RNY1 are associated with the SVs before RNAse treatment – ranging from shorter than 30nt to the full length 112 nt (**Figure 14e; Figure 17**). However, only the 32-nt 5'-fRNY1 RNA fragment is substantially enriched inside the SV and thus protected from RNase degradation. We found that on average, 142 vesicles per 1000 would contain a 5'-fRNY1 if the sRNAs were evenly distributed (Supplemental Fig. 6). As with the 5'-$trfRNA^{Glu}$, we did not see an appreciable degradation of the 5'-fRNY1 after pH 10-DM-RNase treatment. We verified that the

Figure 14. SVs isolated from the mouse CNS contain sRNAs. a) Electron micrograph image of negatively stained vesicles isolated from the mouse CNS. Sample contains abundant ~40 nm vesicles (some marked with arrows). b) Western-blot analysis of the synaptic vesicles during purification. The SV protein synaptophysin was used as a marker during isolation. The isolation procedure includes the collection of the orginal slurry (Sl), two centrifugation supernatants and pellets (S1, P1 and S2, P2), followed by a sucrose density gradient centrifugation and collection of the SV fluffy layer (FL). Further purification using size exclusion chromatography yields the final, isolated sample of SVs (SV). c) Abundant sRNAs co-enrich with the synaptic vesicles (SV). These sRNAs are stable under high pH (pH10), or in the presence of detergent (DM). After addition of RNase much of the RNA is degraded; however an RNase resistant ~32 nt and lower ~20 nt band persists (RNAse). The RNAse resistant band of RNA can be partially degraded in the presence of high pH, detergent, and RNAse (pHDR). d) Northern analysis of RNA isolated from SVs verifies that the 5'-trfRNA^{Glu} sequence, the second most abundant sequence in mouse CNS SV, was not a product of RNase treatment. RNA isolated from SVs purely isolated (SV), at pH10 (pH10), in detergent (DM), treated with RNase (RNase), and treated simultaneously with pH10, detergent, and RNase (pHDR). In the mouse CNS, both full-length tRNA$^{Glu}_{CUC}$ and 5'-trfRNA^{Glu} co-enrich with the SVs, but only 5'-trfRNA^{Glu} is resistant to RNase treatment. e) The most abundant species of sRNA in mouse was a 5' fragment of a Y RNA: Ro-associated Y1 (RNY1): 5'-fRNY1. Like the 5'-trfRNA^{Glu}, full length and precursor sequences of RNY1 co-enrich with the SVs. c-e) Bands of gel underlined (_) indicate a 20-fold reduction of sample loaded. f) The miRNA and RISC associated protein AGO2 co-enriches with SVs, however it is susceptible to trypsin degradation (0-20 minute exposure) indicating it does not reside within the lumen of the SVs. The SV protein synaptophysin, which has trypsin cleavage domains residing within the lumen of the SVs, is not degraded.

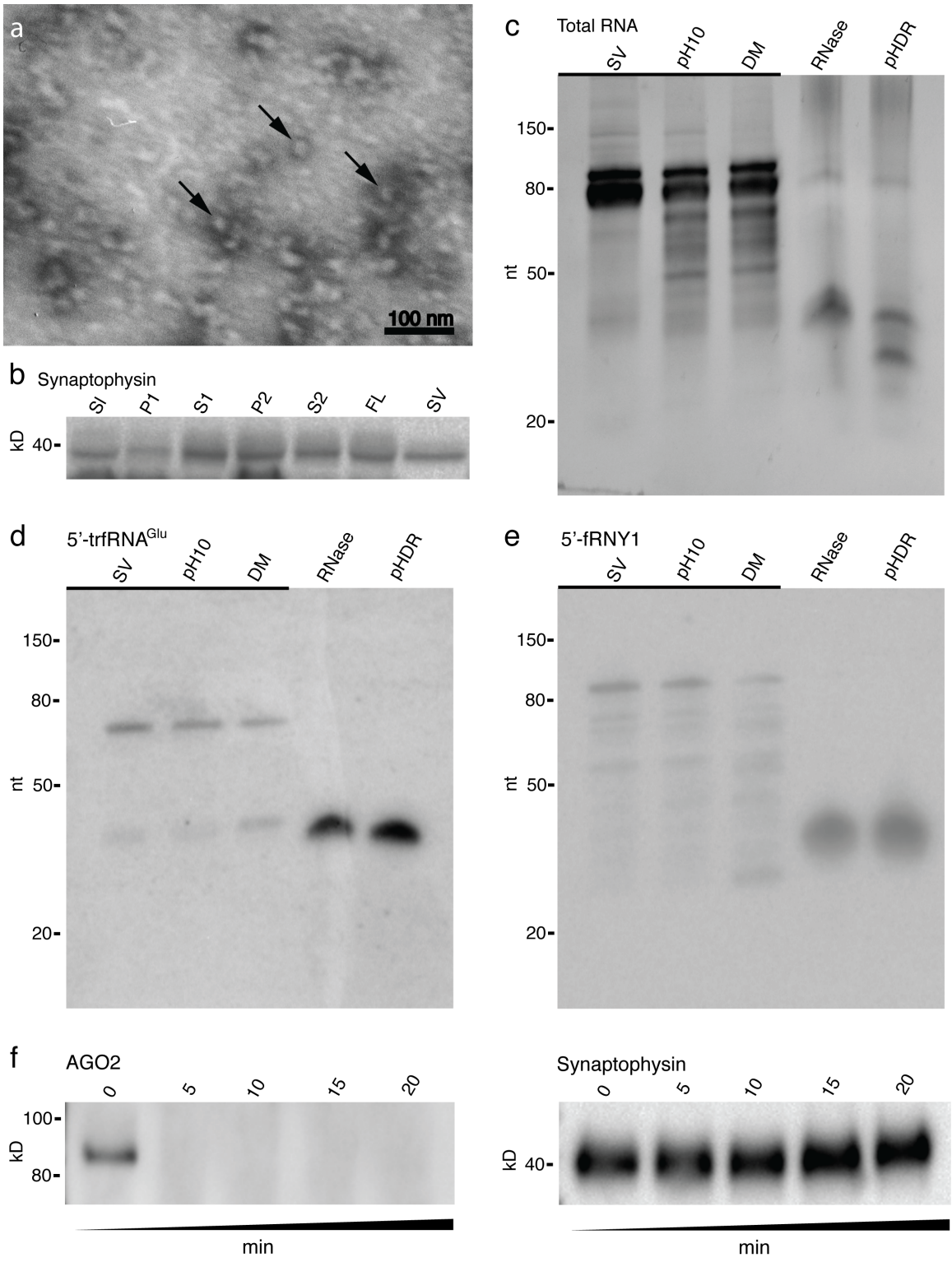
a
100 nm
b
Synaptophysin
SI
P1
S1
P2
S2
FL
SV
kD
40
c
Total RNA
SV
pH10
DM
RNase
pHDR
150
80
nt
50
20
d
5'-trfRNA^Glu
SV
pH10
DM
RNase
pHDR
150
80
nt
50
20
e
5'-fRNY1
SV
pH10
DM
RNase
pHDR
150
80
nt
50
20
f
AGO2
0
5
10
15
20
100
kD
80
min
Synaptophysin
0
5
10
15
20
kD
40
min

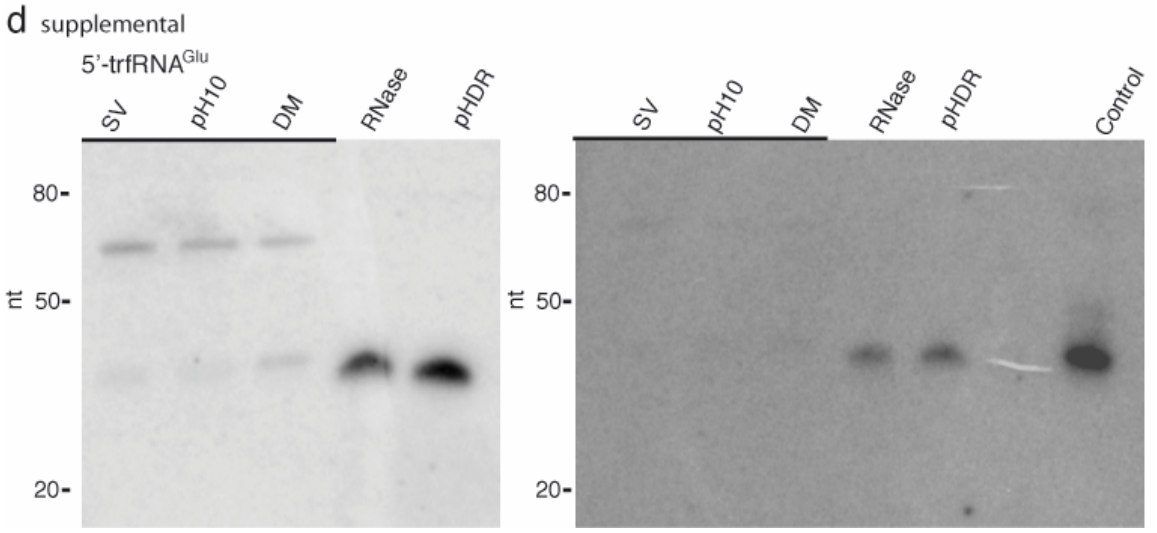

Figure 15. Northern quantification based upon positive control of the 5'-trfRNA^{Glu}. Control and quantified using ImageQuant. Left Figure – Used for publication; no control fragment was loaded in gel. Right Figure. Gel with similar loaded volume and control used as a basis for quantification.

	SV	pH10	DM	RNase	pHDR
RNA recovered after treatment (ng)	9114	11910	11136	300	324
Amount of RNA loaded into gel (ng)	253	330	309	200	165

Northern Analysis

Amount of tRNA in northern (ng)	1.5	0.7	1	0	0
Calculated amount of tRNA after isolation (ng)	36	16.8	24	0	0
Amount of 5'-trfRNA^{Glu} in northern (ng)	1.2	2	2.5	10	14
Calculated amount of 5'-trfRNA^{Glu} after isolation (ng)	29	28	60	15	27

Amount of tRNA before RNAse	25.6
Amount of 5'-trfRNA^{Glu} before RNAse	39
Fraction of 5'-trfRNA^{Glu} RNAse resistant	0.25

Amount of SVs (g)	8.4×10^{-4}
Number of Vesicles	3.28×10^{13}
Number of 5'-trfRNA^{Glu} (10ng)	3.73×10^{11}
Copies of 5'-trfRNA^{Glu} per vesicle	0.015

Table 10. The number of synaptic vesicles in Figure 15 can be estimated based upon the amount of vesicles used in the preparation (grams) and the published molecular weight of mouse CNS synaptic vesicles (25.6×10^{-18} g/vesicle)[142]. Likewise the amount of RNAse resistant copies of 5'-trfRNA^{Glu} per vesicle can be estimated based upon molecular mass of 5'-trfRNA^{Glu} and the amount found in the northern.

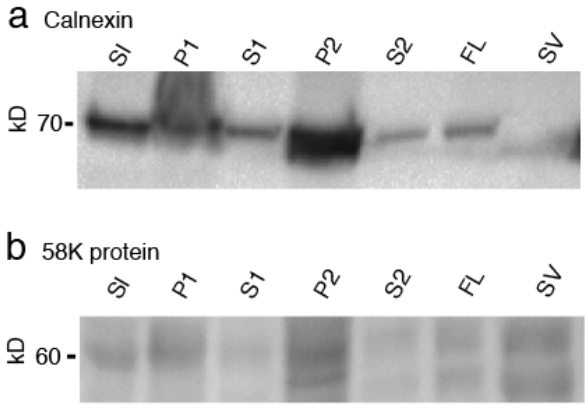

Figure 16. Western-blot analysis of the synaptic vesicles during purification. The Endoplasmic reticulum protein Calnexin and the Golgi apparatus marker 58k protein were used as markers during the purification. The isolation procedure includes the collection of the original slurry (Sl), two centrifugation supernatants and pellets (S1, P1 and S2, P2), followed by a sucrose density gradient centrifugation and collection of the SV fluffy layer (FL). Further purification using size exclusion chromatography yields the final, enriched sample of SVs (SV). Vesicle preparation appears to contain little to no Calnexin or 58K protein. As a further control, SVs were isolated using an alternative, synaptosomal-based strategy, and found to contain sRNAs of similar length (Figure 18b).

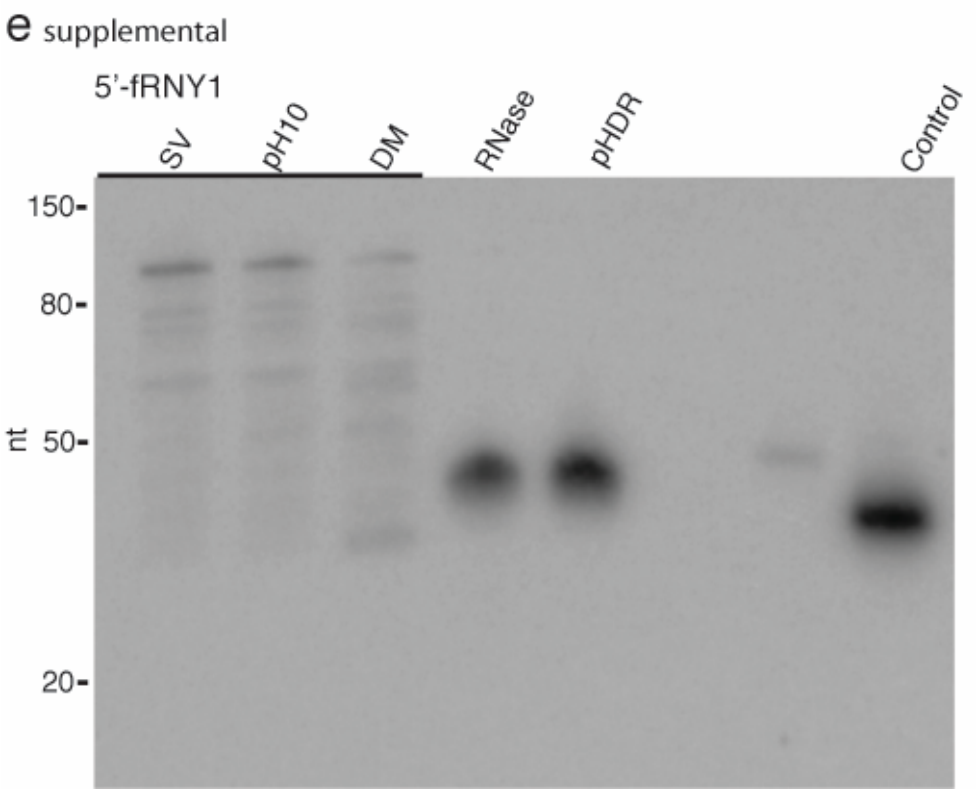

Figure 17. Northern quantification of 5'- fRNY1 in sample based upon positive control of the 5'-fRN Control loaded into the gel and quantified using ImageQuant.

	SV	pH10	DM	RNase	pHDR
Sample total (ng)	9114	11910	11136	330	408
Sample loaded (ng)	253	330	309	183	226

Northern Analysis

Amount of 5'fRNY (ng) in northern	n/a	n/a	n/a	71	113
Calculated amount of 5'-fRNY after isolation (ng)	n/a	n/a	n/a	129	205

Amount of SVs (g) – see Sup Table 2	8.4×10^{-4}
Number of Vesicles	3.28×10^{13}
Number of 5'- fRNY1 (129ng)	4.65×10^{12}
Copies of 5'- fRNY1 per vesicle	0.142

Table 11. Quantification of Figure 17 using ImageQuant. The number of synaptic vesicles can be estimated based upon the amount of vesicles used in the preparation (grams) and the published molecular weight of mouse CNS synaptic vesicles (25.6×10^{-18} g/vesicle)[142]. Likewise the amount of RNAse resistant copies of of 5'- fRNY1 per vesicle can be estimated based upon molecular mass of of 5'- fRNY1 and the amount found in the northern.

RNAse cocktail was capable of degrading all of the sRNA in the sample by first isolating the RNase resistant RNA with Trizol followed by a treatment of RNase. Once separated from the SV, all of the sRNAs were degraded (**Figure 18**). We did not find any complementary sequences to the 20-21 nt miRNAs found within the SVs, suggesting the miRNAs present are single stranded. We tested whether the miRNAs that reside within the SVs might be associated with argonaute-2 (AGO2), as a previous study found AGO2 associated with enriched SVs [126]. AGO2 bound to miRNAs can form the minimal RNA-induced silencing complex (RISC)[143]. We found that AGO2 was associated with our SV preparation. To test whether AGO2 resided within the SVs, or was associated with the exterior of the SVs, we treated the sample with the protease trypsin. We hypothesized that much like the RNase resistant sRNAs, AGO2 would be protected from degradation if it resided within the SVs. AGO2 was not protected from degradation, suggesting the miRNAs present are not associated with AGO2 (**Figure 14f**). To verify that we were not inducing the degradation of the vesicles with the application of trypsin we also tested for the degradation of synaptophysin. Synaptophysin can be cleaved by trypsin, but the trypsin cleavage sites reside within the lumen of the SVs. Synaptophysin was not degraded in the trypsin treated samples (**Figure 14f**). That AGO2 is associated with the isolated SVs raised the possibility that some of the RNase and detergent resistant sRNAs might be in an AGO2 associated complex. To test that hypothesis we treated SVs with trypsin for 20 minutes, followed by trpsin inhibitor and RNase. The sRNAs were resistant to the trypsin treatment (**Figure 18**). As an additional test we

Figure 18. RNase and Trypsin sensitivity, and alternative SV isolation procedure. a) Abundant sRNAs co-enrich with the synaptic vesicles (SV). After addition of RNase much of the RNA is degraded; however an RNase resistant ~32 nt band persists (RNAse). If the RNAse resistant RNA is isolated by TRIzol first, and then subjected to another round of RNase treatment, the RNA shows sensitivity to RNase and is degraded (Isolated RNA RNase). Bands of gel underlined (_), 20-fold reduction in loading b) SVs isolated by an alternative isolation procedure possess sRNAs. Vesicles were isolated following the synaptosomal isolation procedure following Ahmed et al.[144] Isolated SVs were then treated with RNase as described - sRNAs of similar nt length can be seen (RNAse). c) sRNAs are resistant to trypsin treatment. SVs untreated shown in (SV), after trypsin treatment for 20 minutes (Trypsin), trypsin treatment for 20 minutes Trypsin followed by trypsin inhibitor and RNase (Trypsin and RNase), or trypsin treatment for 20 minutes in the presence of the membrane detergent DM, followed by trypsin inhibitor and RNase (Trypsin & RNase and DM). The RNase resistant sRNAs persisted - northerns for both (d) 5'-trfRNA^{Glu} and (e) 5'-fRNY1 demonstrate that the sRNAs were not affected by prior treatment with trypsin, and the addition of DM did not lead to degradation of either sRNA. The PBS perfused mouse brains used in (b) were kindly provided by Matthew Lee and Mendell Rimer under protocols approved by the IACUC of Texas A&M University.

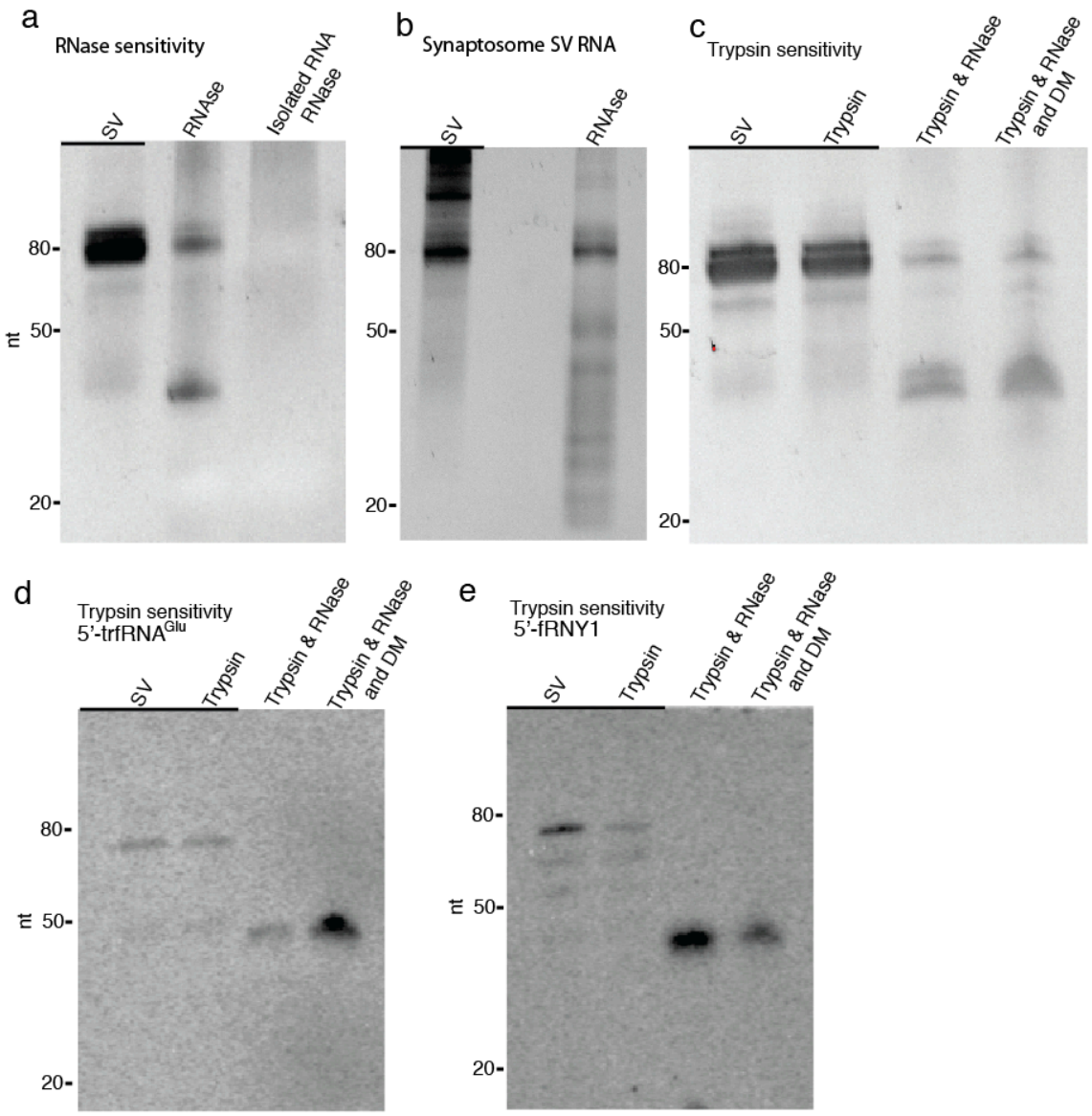
a
RNase sensitivity
SV
RNAse
Isolated RNA RNase
80
50
20
nt
b
Synaptosome SV RNA
SV
RNAse
80
50
20
c
Trypsin sensitivity
SV
Trypsin
Trypsin & RNase
Trypsin & RNase and DM
80
50
20
d
Trypsin sensitivity
5'-trfRNA^Glu
SV
Trypsin
Trypsin & RNase
Trypsin & RNase and DM
80
50
20
nt
e
Trypsin sensitivity
5'-fRNY1
SV
Trypsin
Trypsin & RNase
Trypsin & RNase and DM
80
50
20
nt

treated the SVs with trypsin in association with the membrane detergent DM for 20 minutes before addition of trypsin inhibitor and RNase treatment. The RNase resistant sRNAs persisted - northerns for both 5'-fRNY1 and 5'-trfRNA^{Glu} demonstrated that the sRNAs were not affected by prior treatment with trypsin, and the addition of DM had no effect (**Figure 18**).

What is the structure of 5'-trfRNA?

In an effort to gain insight into the molecular mechanism of 5'-trfRNA^{Glu}, we examined the predicted structure of 5'-trfRNA^{Glu} through computational approaches. We used RNAfold [145] to calculate the optimal secondary structure of the minimum free energy (MFE) of the sequence (**Figure 19a**). We found that MFE of the optimized secondary structure was -5.20 kcal/mol. The free energy of the thermodynamic ensemble was -5.37 kcal/mol, with a frequency of the MFE structure in the ensemble of 76% (**Figure 19a**). A similar centroid secondary structure was calculated with a MFE of -5.20 kcal/mol. Based upon this secondary structure we calculated a tertiary structure of the 5'-trfRNA^{Glu} using RNACOMPOSER [146]. Surprisingly, the stem and loop structure determined in this manner closely resembled known crystal structures of the tRNA anticodon stem and loop, particularly at the anticodon region (**Figure 19d**), even though the tRNA^{Glu} anticodon from the full-length tRNA is not in the 5' tRNA fragment. The sequence of this pseudo-anticodon is GGU and thus would recognize threonine codons, a codon not present in vertebrate genomes.

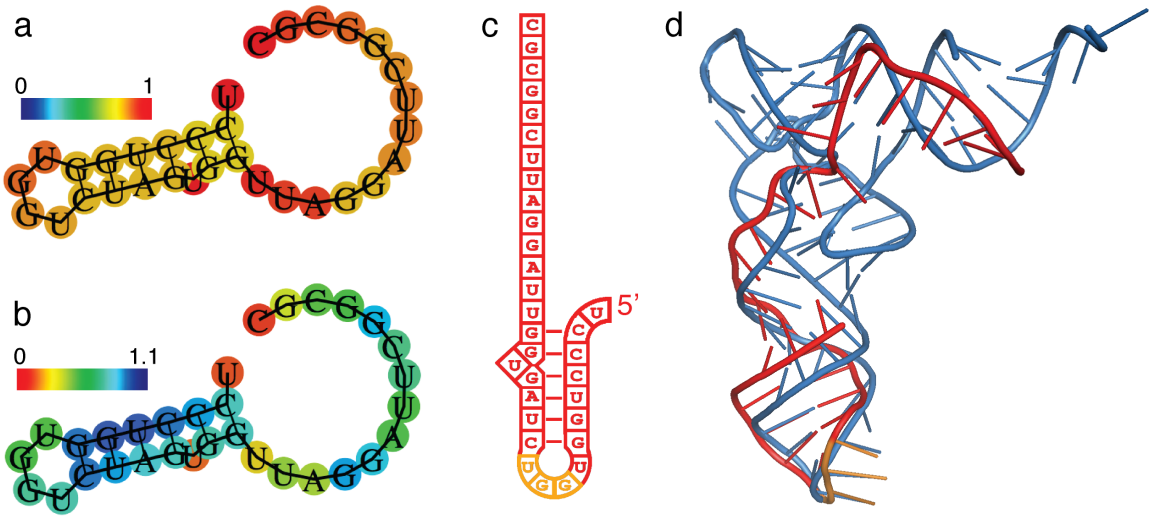

Figure 19. Tertiary structure of 5'-trfRNA^{GLU} mimics tRNA anticodon stem and loop. a) RNAfold was used to calculate the minimum free energy secondary structure of 5'-trfRNA^{Glu}. Base-pair probabilities are shown in a heat map from 0-1; for non-paired nucleotides, heat map indicates probability of being unpaired. b) The centroid secondary structure is identical to the minimum free energy structure. The heat map shows the positional entropy (from 0 - 1.1). c) Secondary structure of 5'-trfRNA^{Glu} showing the pseudo-anticodon region in orange. d) Tertiary structure of 5'-trfRNA^{Glu} calculated using RNACOMPOSER (red and orange). The tertiary structure was aligned in pymol to a known crystal structure of a tRNA, shown in blue (yeast tRNA^{Phe} 1ehz) The stem and loop structure determined in this manner closely resembled known crystal structures of the tRNA anticodon stem and loop, particularly at the anticodon region (orange). The sequence of this pseudo-anticodon is GGU. Both RNAfold and RNACOMPOSER used with default settings.

Discussion

In this study, we demonstrated that cholinergic SVs isolated from the PNS electroplaque of *T. californica* contain sRNAs (**Figure 8c**). Single vesicle imaging of RNase treated SV preparations from *T. californica* demonstrated that membrane bound structures co-labeled with probes for membrane, for cholinergic neurotransmitter transporter VAChT, and for RNA (**Figure 8d**). We immunopurified *T. californica* SVs using antibodies against VAChT. We then isolated RNase resistant sRNAs from these vesicles. Next generation sequencing showed that these sRNAs consisted primarily of 5'-tRNA fragments, with 5'- trfRNA^{Glu} being the most abundant (**Table 5**). We demonstrated by northern analysis that the 5'- trfRNA^{Glu} was not a byproduct of RNase treatment (Figure 7b), and that it exists as both a full-length tRNA$^{Glu}_{CUC}$ and a 5'-trfRNA^{Glu} in the *T. californica* PNS, and in the electric lobe, the location within the CNS of the cell bodies of the electromotor neurons (**Figure 8c**). In addition, we demonstrated by northern analysis that the signal representing 5'- trfRNA^{Glu} in the *T. californica* SV preparation could only be reduced below detectable levels in the presence of detergent, high pH, and RNase (**Figure 8b**), suggesting that this RNA resides within the vesicles. *In situ* hybridization of the 5'- trfRNA^{Glu} sequence was consistent with immunohistochemical labeling of the SV marker VAChT in cryostat sections of the *T. californica* electric organ (**Figure 9a,b**).

We extended our findings to heterogeneous SVs isolated from the mouse brain. We found that these mouse brain SVs also contain sRNAs, the most abundant of which is a 5' fragment of the RO associated Y1 RNA, we term 5'-fRNY1 (**Table 6**). The second most abundant sRNA sequence in SVs isolated from the mouse brain is the 5'-

trfRNA^{Glu}. We demonstrated by northern analysis that the 5'-fRNY1 and the 5'-trfRNA^{Glu} were not a byproduct of RNase treatment (**Figure 14d,e**), i.e. we found that precursors for both fragments exist, but are degraded by RNase treatment, suggesting they do not reside within the SV lumens. One potential interpretation for the presence of the precursors in association with the SVs is that the presynaptic terminal is a site of cytoplasmic maturation and cleavage of SV sRNAs. Finally, we demonstrated by northern analysis that the signals representing the 5'-fRNY1 and 5'- trfRNA^{Glu} in the mouse CNS SV preparation were RNase resistant (**Figure 14d,e**) - even if the SVs were treated with trypsin (**Figure 15**). We do not have an explanation for the persistence of the mouse sRNAs in detergent and RNase compared to the *T. californica* sRNAs sensitivity to the same treatment. The smaller size of the mouse SVs may make them less soluble in detergent, or the sRNAs are in a trypsin resistant complex in the mouse SVs.

The most abundant sRNA present in *T. californica* SVs, as well as a large percentage of the sRNAs present in mouse SVs (second, fifth and sixth most abundant), were previously identified as stress-induced tRNA fragments (**Table 5, 6**). Two pathways are known to produce these fragments in vertebrates. 5'-trfRNA^{Tyr} arises by induced RNA pol III transcription in response to H_2O_2 [147]. A second pathway for the production of 5'-trfRNAs is by the stress-induced RNase angiogenin[138,139,148]. Angiogenin has been shown to be involved in the fragmentation of tRNA$^{Glu}_{CUC}$ into 5'-trfRNA^{Glu} in airway epithelial cells after viral infection and induce stress granule formation and suppress protein translation in a miRNA and siRNA independent manner

[86]. Whether a similar mechanism occurs at the synapse, or in other tissues shown to be enriched in 5'-trfRNA^{Glu} and 5'-trfRNA^{Gly} is not known[149]. We calculated a tertiary structure of the 5'-trfRNA^{Glu} using RNACOMPOSER [146], which predicted a stem and loop structure that closely resembled known crystal structures of the tRNA anticodon stem and loop (Figure 10d). If 5'-trfRNA^{Glu} does alter translation in a miRNA and small interfering RNA (siRNA) independent manner, perhaps it does so by directly interacting with the protein translation machinery by mimicking the anti-codon stem loop of a tRNA.

In this paper we focused on the isolation and localization of sRNAs isolated from SVs of two different organisms, the PNS of *T. californica* and the CNS of mouse. The most abundant sequences of sRNAs isolated and sequenced were over 30nt; however, we did isolate and sequence miRNAs in the 20-21nt range, including miR128, miR99a, miR100, miR22, and miR127. The most abundant miRNA, and the third most abundant class of sequences was miR128, a miRNA important for neuronal development, synaptogenesis, and post-mitotic neuronal functioning[150]. Members of the miR-99 family (miR99a, and miR100, the fourth and seventh most abundant mouse sRNAs) are miRNAs that have been shown to co-enrich with polyribosomes in mammalian neurons, and regulate the mammalian target of rapamycin (mTOR) pathway[151]. miR22, the eighth most abundant mouse sRNA, is important for cerebellar development, and in adults has been shown to protect neurons from neurodegeneration, and is down regulated in both Huntington's and Alzheimer's disease [152]. miR127, along with a cluster of miRNAs found on chromosome14q32, is maternally expressed, and the down regulation of

miRNAs within this cluster (including miR127) has been linked to schizophrenia[153]. The mechanism by which miRNAs are taken in at the synapse is not known. However, a previous study has demonstrated that miR99a is released from synaptosomes in an activity and calcium dependent manner, consistent with the release from SVs, and synthetic miRNAs were taken up by synaptosomes via an unspecified endocytic pathway[126].

Long-term changes in synaptic plasticity require protein synthesis, the local dendritic regulation of which is still an active area of research [69,120-122]. One common, and critical component of every model of local protein synthesis is the role activity plays in up-regulation and down-regulation of translation. Activity at a local synapse is driven by the presynaptic fusion of synaptic vesicles with the plasma membrane, and the subsequent release of the contents residing within the SV lumen. Currently most of our understanding of SV content release has focused on small molecule neurotransmitters that rapidly bind metabotropic and ionotropic receptors leading to near instantaneous changes in target membrane excitability. Given the immense specificity and wide ranging effects that sRNAs can exert on transcription and translation[123,154,155], the precise molecular control with which SVs link presynaptic activity to SV content release, and the developmental precision with which the pre and postsynaptic apparatus are spatially aligned at every type of synapse, the addition of sRNAs to the list of molecules released by SVs during exocytosis, and/or possibly taken up by SVs during endocytosis, is both powerful and exciting. It provides the potential for a direct means of controlling

translation locally, which may prove at least as important as the proposed calcium induced mechanisms for controlling translation.

Materials and Methods

Isolation and enrichment of synaptic vesicles

Methods were adapted from Ohsawa[102]. Three preparations of electric organ with tissue from 3 separate *Torpedo californica* fish (2 female, 1 male), and three preparations of mouse brains (approximately 50 mouse brains of both male and female per each preparation) were used during these studies. A Spex Freezer Mill 6800 (Spex Sample Prep; Metuchen, NJ) was cooled to -180°C and ~25 g of frozen electric organ from an individual (Aquatic Research Consultants; San Pedro, CA) or 25g frozen Swiss Webster mouse brains (BioChemed Services, Winchester, V.A.) was ground with 25 g of frozen buffer pellets (320 mM Sucrose, 10 mM TRIS-Cl, pH 7.4) (Sigma-Aldrich; St. Louis, MO). The resulting powder of buffer and electric organ/brain was warmed to 4°C with 50 ml of buffer solution (320 mM Sucrose, 10 mM Tris-Cl, pH 7.4, 4°C). The resulting slurry (100 ml) was centrifuged at 20,000 rpm for 10 minutes (Beckman Coulter JA-20 rotor - Avanti J25 centrifuge) (Beckman Coulter; Brea, CA). The resulting supernatant was centrifuged at 34,000 rpm for 40 minutes (70ti rotor - Optima X80; Beckman). The supernatant was then loaded onto a 4ml/4ml 0.6 M/1.2 M sucrose step gradient (10 mM Tris-Cl, pH 7.4), then centrifuged at 48,000 rpm for 2 hours (70ti rotor - Optima X80). The 4 ml 0.6 M (1.07 g/ml density) sucrose fluffy layer, enriched in vesicles, was collected. Heavier densities and pellet (> 0.6M sucrose), known to be

enriched in exosomes, were discarded[130],[132]. A 2 ml sample of enriched vesicles was filtered using a 0.22 μm spin column (Spin-x, Corning; Corning, NY) to remove any large debris. The filtrate was injected into a Pharmacia LC500 plus FPLC (GE Healthcare, Fairfield, CT) and run through a 25 cm 4% agarose bead column (Bioscience Beads; West Warwick, RI). Separate bead columns were prepared for electric organ and mouse brains to ensure no contamination. The FPLC was eluted with a buffer solution PBS, pH 7.4 at a flow rate of 1.0 ml/min. The second major peak was collected, and the vesicles concentrated to a protein concentration of 5 mg/mL (measured by Bradford Assay)(Bio-Rad Laboratories, Inc.; Hercules, CA) using a Stirred Cell apparatus with a 100 kDa filter (PLHK02510; Millipore, Billerica, MS).

Electron microscopy

Negative stain of isolated synaptic vesicles of *T. californica* and mouse are conducted following Jahn and Maycox[103] . Briefly, A 5 μl sample of enriched synaptic vesicles (further concentrated to 20 mg/ml with Pierce concentrator, PES, 100K MWCO (88503, Thermo Scientific) as determined by Bradford assay was pipetted onto a slot grid. Excess sample was removed by filter paper, and the grid was briefly washed in 12mM sodium phosphate buffer, followed by 2 s staining with uranyl acetate (Ted Pella; Redding, CA), followed by another wash[103]. The slot grid was viewed with a JEOL 1200 JEOL Ltd., Akishima-Shi, TKY Japan) operated at 100 kV. Image was collected at 50,000 X magnification on a bottom-mounted 3072 x 3072, slow scan, lens-coupled CCD camera SIA 15C (SIA; Dulith, GA).

Western blots

Synaptic vesicle lysates were loaded on to a 4–20% SDS-PAGE gel (456-9034; BioRad) and blotted using standard protocols. All gel lanes were loaded with equal volume (3µl) of sample. Primary antibodies against synaptophysin (1:1000; MAB5258; EMD Millipore, Billerica, MA), AGO2 (1:1000; ab186733; Abcam, Cambridge, England), VAChT (1:1000; ab68986; Abcam), 58K (1:1000; ab19072; Abcam), and Calnexin (1:1000; ab22595; Abcam). Secondary antibodies were HRP-conjugated goat-anti rabbit (1:2000; 2-348; EMD Millipore), rabbit anti-goat (1:2000; 6020-05, Southern Biotech; Birmingham, AL), and goat-anti mouse (1:2000; ab5879; Abcam). Visualization of blots was conducted with ECL Prime (RPN2232; GE Healthcare) according to manufacturer's instructions. Chemiluminescence was quantified using a Chemicdoc XRS+ Imager with Imagelab software (BioRad).

Synaptic vesicle RNA isolation and tRNA isolation

SVs were isolated and concentrated as described above. For each assay, 1 preparation of vesicles was utilized and split into 5 equal samples. Each sample consisted of 3 x 50 µl of SVs (5 mg/ml) in PBS (80 mM Na_2HPO_4 and 25 mM NaH_2PO_4, 100 mM NaCl pH 7.4; Sigma). The 5 parallel treatments conducted on the SV preparations were: 1) addition of 50 µl PBS, pH 7.4, 2) addition of 50 µl PBS pH 11 (adjusted with NaOH; Sigma), 3) addition of 50 µl PBS pH 11 and 100 mM membrane detergent DM (n-Decyl-β-D-Maltopyranoside, D322; Anatrace, Maumee, OH), 4) Addition of 50 µl PBS pH 7.4 with 1 µl RNase cocktail as instructed (RNase A (500 U/ml) and RNase T1 (20,000 U/ml), AM2286; Ambion/Life Technologies), and finally 5) addition of 50 µl combined pH 11, DM, and RNAse treatments. RNA was extracted

after the treatments using 900 µl TRIzol (Invitrogen/Life Technologies) followed by 200 µl chloroform and 400 µl isopropanol (EMD Millipore), with a final precipitation by 75% ethanol. The total SV RNA was resuspended in 6 µl of DI water, and the three samples of each treatment were quantified – Supplemental Tables show combined results.

RNA concentration was determined using QuantiFluor RNA System (E3310, Promega, Madison, WI) and Quantus Fluorometer (E6150, Promega). Briefly, 1 µl of isolated RNA is dissolved for 5 minutes in 199 µl of Master solution (20X TE Buffer, DI water, and QuantiFluor RNA dye); the solution was then read in the Quantus Fluorometer.

To isolate total RNA from the electric lobe (CNS) and electric organ (PNS) of *T. californica*, 100 mg of tissue of each organ was dissected and ground with silica beads before RNA extraction by TRIzol (described above). For further enrichment of sRNA and tRNA, samples of total RNA were resuspended in 300 µl of 10 mM sodium acetate (Sigma-Aldrich) pH 4.5 at 4°C, and mixed with 30 µl of 8 M LiCl (Sigma-Aldrich). After centrifugation at 15,000 g, 4°C, the tRNA and sRNA is collected from the resulting supernatant.

Fluorescent immunohistochemical labeling of isolated synaptic vesicles and TIRF imaging of single vesicles

Isolated SVs were passed through a 0.22 µm spin column, and 100 µl of synaptic vesicles (1 mg/ml) were transferred into 300 µl PBS (pH 7.4), and labeled with one round of primary and secondary antibody following the procedure[101]. Briefly, the

vesicles were incubated for overnight with 1 μg of VAChT antibody in 4°C, incubated for 30 min with 20 μl anti-rabbit IgG beads (Sigma-Aldrich), briefly centrifuged, and the vesicle containing supernatant was then incubated with 0.5 μg goat anti-rabbit secondary antibody labeled with Pacific Blue (P-10994, Life Technologies) for 4 hours before finally being incubated with 20 μl anti-goat IgG beads (Sigma-Aldrich). The beads were pelleted and the supernatant collected for imaging. SVs were incubated in RNase cocktail for 30 minutes.

FM4-64[104] and SYTO 12 (S7574; Life Technologies) were added to the labeled vesicles (final concentration 1 μM), and the samples were settled on a glass bottom culture dish (MatTek P35G-1.5-20-C; Ashland, MA) for at least 1 hour. Settled vesicles were imaged with a Zeiss Axio Observer Z1 Microscope with TIRF slider, 100X TIRF objective (NA 1.45). Images were acquired using AxioVision (Carl Zeiss; Oberkochen, Germany). Three separate images from each field were taken using laser lines and filter cubes paired to eliminate fluorescent cross talk between the dyes: laser line 401 with filter cube 73 HE was used for Pacific Blue, laser line 488 with filter cube 38 HE was used for SYTO 12, and laser line 561 with filter cube 74 HE was used for FM 4-64. Images were collected with a Roper S/W PVCAM EMCCD camera and analyzed using ImageJ (NIH, Bethesda, MA) software. Suitable spots detected in the FM4-64 channel were marked. The other channels were then quantified for label.

RNA gels and northern blots

Electrophoresis and blotting are previously described[140]. Denatured RNA samples were run through 10% TBE Urea precast gel (BioRad, 456-6033). Because of

resulting sample differences in yield between non-RNAse treated and RNAse treated SV RNA preparations, gel lanes loaded with non-RNase treated samples were reduced by ~20-fold to match the amount loaded in the RNase treated lanes as described in figure legends and documented in supplemental materials. Northern blots were conducted in triplicate, in order to reduce bias from any single preparation, each northern was conducted on RNA isolated from a single fish. For mouse brain SVs, three separate preparations of SV RNAs were isolated in order to perform northerns in triplicate. Northern blots were transferred to Zeta Probe Blotting Membrane (BioRad, 162-0153) in 1xTBE buffer at 20V for 90min. The membrane was rinsed with 5xSSC buffer and RNAs were crosslinked to the membrane using a Stratalink UV crosslinker (auto setting). The membrane was incubated in a hybridization tube with 15ml of prehybridization buffer at 42°C for 3 or more hours. 50 pmol of oligo was radioactively labeled using 300 μCi [gamma32-P] ATP (NEG502A; Perkin Elmer; Waltham, MA) and T4 Polynucleotide Kinase and the signal was detected by autoradiography. Denatured probe (heated at 95°C for 5 min and chilled on ice) was added to the hybridization tube, and incubated at 42°C overnight. The membrane was washed with 100ml 2xSSC/0.1% SDS and then with 100ml 0.2xSSC/0.1% SDS at room temperature for 5 min, respectively. The membrane was washed at 42°C with 100ml 0.2xSSC/0.1% SDS for 30 min and then at 68°C with 100ml 0/1xSSC/0.1% SDS for 30 min. The membrane was dried and then exposed to a storage phosphorplate (GE Healthcare) for 16 h before being scanned with a Typhoon Trio Variable Mode Imager (GE Healthcare) and quantified

based upon binding of probe to positive control loaded sample of known quantity using ImageQuant TL software (GE Healthcare).

20xSSC buffer: 3M sodium chloride, 300mM sodium citrate

prehybridization buffer: 0.75M NaCl, 50mM NaPO4, 5mM EDTA, 1%SDS, 50% formamide, 0.2% BSA, 0.2% polyvinylpyrollidone 40, 0.2% Ficoll 400 (Sigma)

trfRNA^{Glu} – probe 5'- CGCCGAATCCTAACCACTAGCCACCA

trfRNA^{Glu} – positive control *in vitro* transcription

5'-TAATACGACTCACTATAGGTCCCTGGTGGTCTAGTGGTTAGGATTCGGCGC

5'-GCGCCGAATCCTAACCACTAGACCACCAGGGACCTATAGTGAGTCGTATTA

Ro Y1 – probe 5' -AACTCACTACCTTCGGACCAGCC

Ro Y1 – positive control *in vitro* transcription

5'-TAATACGACTCACTATAGGGGCTGGTCCGAAGGTAGTGAGTT

5'- AACTCACTACCTTCGGACCAGCCCCTATAGTGAGTCGTATTA

RNA isolation and sequencing

SVs from *T. californica* and mouse whole brain were isolated and treated with RNAse cocktail (Ambion/Life Technologies) as described above. As a further enrichment, SVs from *T. californica* were affinity enriched using dynabeads (100.07D; Dynabeads; Invitrogen/ Life Technologies) with VAChT antibody[131,137]. The total RNA

was extracted following the TRIzol procedure described above. Library preparation and sequencing were performed by the Genomic Sequencing and Analysis Facility at the University of Texas, Austin. The samples were prepared for sequencing using the TruSeq small RNA sample preparation kit (Illumina; San Diego, CA). Single-end reads (100bp) were sequenced on an Illumina HiSeq 2500(Illumina).

trfRNA in situ *hybridization*

For *in situ hybridization* (ISH), frozen *T. californica* electoplaque was cryosectioned (30-40 μm) and mounted onto Superfrost Plus slides (VWR, Radnor, PA). Fluorescein-labeled anti-sense morpholino oligomer probe matching coding 5'-trfRNA^{Glu} was synthesized from Gene Tools (Philomath, OR). Control fluorescein-labeled anti-sense cRNA probes matching coding 5'-trfRNA^{Glu} and scrambled were synthesized from IDT (Coralville, IA). Probes were hybridized to sections as previously described [156], with minor modifications in amplification strategy. Following overnight hybridization, slides were incubated with alkaline phosphatase conjugated anti-fluorescein antibody (1:5000; 11426338910; Roche Life Sciences, Indianapolis, IN) for overnight at 4°C. Tissues were washed and incubated in Fast Red (11496549001; Roche Life Sciences) according to manufacturer's instructions for overnight at 4°C in dark. Confocal images were captured with a Zeiss 780 Structure Illumination microscope (Zeiss, Germany). Sequences used for probe generation are listed below.

trfRNA^{Glu} Morpholino: 5'- GCCGAATCCTAACCACTAGACCACC-fluoroscein

trfRNA^{Glu} DNA control: 5'- GCCGAATCCTAACCACTAGACCACC-fluoroscein

trfRNA^{Glu} DNA scramble: 5' - CCCGAATCGTAACGACTAGAGCAGC-fluoroscein

Trypsin sensitivity

AGO2/synaptophysin Westerns: SVs were isolated and concentrated as described above. One preparation of vesicles was split into 10 equal samples. Each sample consisted of 5 µl of SVs (6 mg/ml) in PBS, pH 7.4. Paired samples were treating in the following manner: no Trypsin treatment, 2µl Trypsin (T1426, 10mg/ml; Sigma-Aldrich) treated for 5 mins, 10 mins, 20 mins or 30 mins. Westerns were conducted using antibodies against synaptophysin or AGO2.

SV RNA sensitivity to Trypsin: SVs were isolated and concentrated as described above. For each assay, 1 preparation of vesicles was utilized, and split into 4 equal samples of 50 µl. Each sample consisted of SVs (6 mg/ml) in PBS (80 mM Na_2HPO_4 and 25 mM NaH_2PO_4, 100 mM NaCl), pH 7.4. The 4 parallel treatments conducted on the SV preparations were: 1) addition of 50 µl PBS, pH 7.4, 2) addition of 50 µl PBS pH 7.4 and 0.5 µl Trypsin (T1426,10mg/ml; Sigma-Aldrich) for 20 minutes, 3) addition of 50 µl PBS pH 7.4 and 0.5 µl Trypsin for 20 min, followed by 5 µl Trypsin Inhibitor (T9128, 6.5mg/10ml, Sigma-Aldrich) and 1µl RNAse for 30 min., 4) addition of 50 µl combined Trypsin, 200mM DM for 20 min, followed by 5 µl Trypsin Inhibitor and RNAse treatment for 30 minutes. RNA was extracted after the treatments and quantified as described above.

Prediction of 5'-trfRNA^{Glu} structure

The secondary structure of the 5'-trfRNA^{Glu} was predicted using the default settings of RNAfold [145] (ViennaRNA Package 2.0;Theoretical Biochemistry Group, University of Vienna Wien, Austria). The resulting secondary structure was used to

calculate a predicted tertiary structure using the default settings for RNACOMPOSER [146] (Institute of Computing Science, Poznan University of Technology, Poznan Poland). Visualization of the structure was conducted using the MacPymol Molecular Graphics System, Version 1.7.4 (Schrödinger, LLC; Cambridge, MA) running on a Mac Pro with OS 10.9.5 (Apple; Cupertino, CA).

4. CONCLUSIONS AND FUTURE WORK

In the previous section, I proposed that synaptic vesicles contain small ribonucleic acids (sRNAs), including transfer RNA fragments (trfRNA) and microRNAs (miRNA) known to be involved with post-transcriptional regulation. Moreover, I hypothesized that the activity-based release of these molecules, along with neurotransmitter, may be an important regulator of local protein synthesis at the synapse. In this section, I will outline several key questions about SV sRNAs and propose potential experiments that could address some of these questions.

The Biogenesis of Synaptic Vesicle sRNAs

The origins of the SV trfRNAs are currently unknown. The most prominent trfRNA I discovered is predicted to be a 5' fragment of a glutamyl-tRNA; however, whether this tRNA is ever used during protein translation is not known. Bioinformatic analysis predicts that there are multiple tRNAs with the same anti-codon region in all vertebrate genomes, but there is little experimental evidence as to which of these tRNAs are actually used to transport amino acids to the ribosome during protein translation[157]. Functional tRNAs possess multiple modifications to their chemical backbone subunit, such as 2-methyladenosine and agmatidine[158,159]. These modifications are enzymatically regulated during tRNA biogenesis. If the 5'-trfRNA^{Glu} discussed in the previous section is cleaved from a functional tRNA, it should possess post-transcriptional modifications to its chemical backbone. Thus, to address whether the 5'-trfRNA^{Glu} was ever a functional tRNA, I would test whether the trfRNAs in the isolated synaptic vesicles have

such backbone modifications. To detect these modifications, I propose the use of mass spectrometry. Mass spectrometry is an analytical technique that can identify and quantify molecules present in a sample. By combining mass spectrometry with endonuclease treated samples of our SV sRNAs, I can test for the presence of modified nucleotides. Sample preparation is summarized briefly. Isolated sRNAs can be further purified through RNA gel electrophoresis, and the specific band where the 5'-trfRNAs resides can be isolated. To detect any modifications, the sample can be digested with a RNase cocktail that will reduce the RNA molecules into individual nucleotides. Modified nucleotides will possess a unique mass-to-charge ratio, and can easily be identified. The absence of modified nucleotides would indicate the 5'-trfRNA^{Glu} does not share its biogenesis with classic tRNAs. If some modified nucleotides are detected, combining mass spectrometry with sequence specific endonucleases can identify the location of the modifications. Fragmented trfRNAs can be compared to synthetic trfRNAs, and step-by-step, the exact chemical backbone of the 5'-trfRNA^{Glu} can be deduced. Knowing the true chemical sequence of the 5'-trfRNA^{Glu} will provide important details as to its origin. Furthermore, knowing the true chemical nature will be important for future studies aimed at identifying its function.

How are sRNAs Transported into Synaptic Vesicles?

The mechanism by which sRNAs are loaded into SVs and the location within the cell that SV loading occurs are not known. As discussed in previous section, sRNAs are products of nuclear transcription followed by cytosolic maturation and cleavage to mature miRNAs [160] or 5'-trfRNAs [148]. Although not tested in this dissertation, at least

three pathways could lead to the loading of sRNAs into SVs for subsequent release into the synaptic cleft (**Figure 20**). In the first model, mature cytosolic sRNAs are loaded within the SVs during SV biogenesis and maturation, a process that also occurs within the neuronal cell body. Newly synthesized SVs would then be axonally transported to presynaptic terminals preloaded with sRNAs, and through activity driven fusion with the presynaptic membrane, lose their sRNAs in their initial fusion events (red). A second model for how sRNAs are loaded into SVs would be through an endocytotic event – either a clathrin mediated pathway in which sRNAs are captured by recycling SVs (yellow), or an endosomal mediated pathway in which sRNAs are uploaded into SVs during the SVs' passage through endosomal recycling intermediates (green). A third model resembles classic neurotransmitter loading. In this model mature sRNAs are loaded in SVs at nerve terminals. This model would require a protein or macromolecular complex, much like a neurotransmitter transporter, capable of loading SVs (blue). Once released from the presynaptic terminal, sRNAs could be taken in by the postsynaptic cell. There, in association with the RISC complex, the sRNAs could affect local mRNA stability or translation. In an alternative model to the presynaptic release of sRNAs, endocytic SVs might engulf exogenous sRNAs. These sRNAs could be transported back to the presynaptic neuron cell body via retrograde transport (yellow).

Although I did not test whether sRNAs are taken up by isolated SVs, I did detect by northern blot sRNAs and precursor sRNAs associated with isolated SVs. This finding suggests that some sRNAs might mature at the presynaptic terminal before being loaded into the lumen of the SVs. If so, there would need to be a mechanism to load sRNAs into

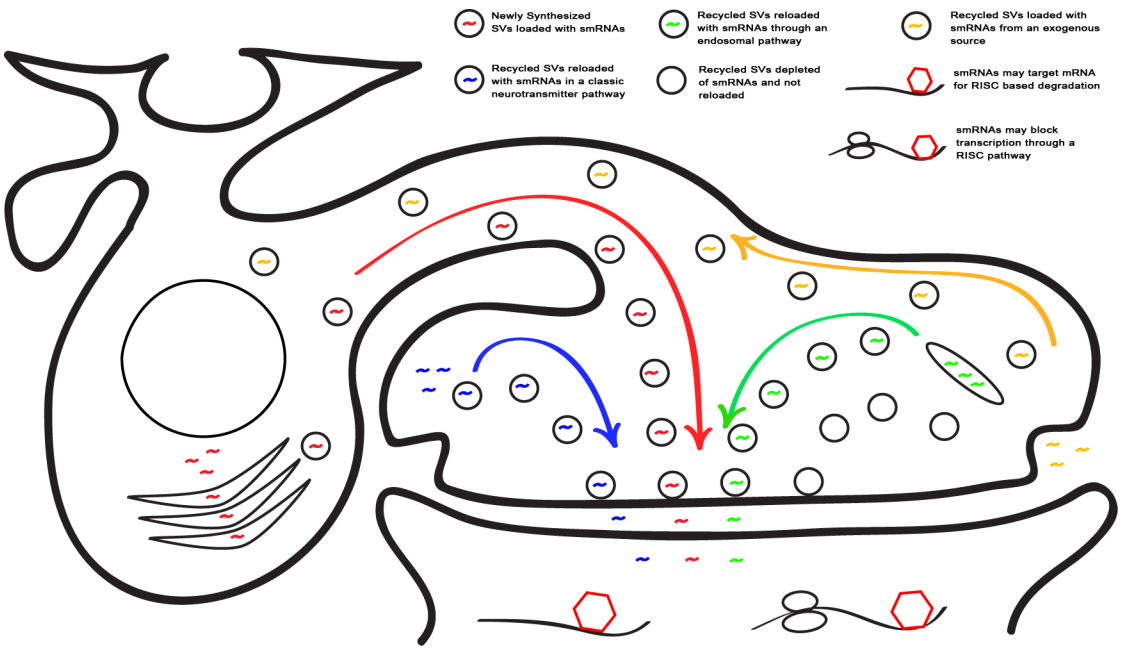

Figure 20. Potential pathways for sRNAs in the synapse.

SVs at the presynaptic terminals. One potential mechanism could be an undiscovered vesicular sRNA transporter. Although no such transporter is known, there are many SV proteins whose function remains unknown. Comparing the SV proteins to proteins capable of transporting RNA across membranes, such as the Systemic RNAi Defective (SID) family members[161,162] might offer candidate vesicle transport proteins. Independent of identifying a molecular pathway, one could test whether sRNAs are actively loaded into isolated SVs. Much like radiolabeled neurotransmitters have been shown to load into isolated SVs, one could test whether radioactive synthetic sRNAs load into isolated SVs[163]. If so, is the process ATP dependent or independent? If it is ATP dependent, that would suggest an active transport pathway similar to that of classic neurotransmitters.

Synaptic Vesicle sRNAs Co-effectors

5'-trfRNA^{Glu} has been shown to post-transcriptionally regulate protein synthesis via a siRNA and miRNA mechanism[86]. Whether 5'-trfRNA^{Glu} regulates translation independently, or requires a co-effector, is not known. Many sRNAs do require co-effectors. Proteins such as Argonaute (AGO) are known to bind RNAs, including microRNAs (miRNAs), short interfering RNAs (siRNAs) or PIWI-associated RNAs (piRNAs)[164]. AGO protein-RNA complexes can interact with other protein factors to coordinate downstream gene-silencing events[164]. In particular, AGO2 is known to bind microRNAs and further silence the target gene[165]. AGO2 bound RNA can either guide the target gene into a de-adenylation degradation pathway or form an active RNA-induced silencing complex (RISC), which can induce endonucleolytic cleavage of

targeted mRNA[165]. Proteins that associate with sRNAs can be selectively isolated for further characterization[166]. One such approach is an RNA pull down assay. Briefly, high affinity tags are used to label a specific RNA. These tagged RNA molecules are then mixed with a cell or tissue extract. If a complex forms between the tagged RNA and a co-effector, the co-effector can then be isolated via the high affinity tag. The co-effector protein portion can be detected by western blotting or mass spectrometry[167]. To confirm a co-effector other techniques, including fluorescent *in situ* hybridization for RNA probe and immunohistochemistry to label the protein complex, may be required to further confirm the co-effector. If a new co-factor is discovered, it would add to the mechanisms available for post- transcriptional regulation of protein synthesis.

Are SV sRNAs Specific for Different Neuronal Cell Types?

Neurons are classified by the types of molecules, such as neurotransmitters they release at their synapses. One question that needs to be addressed is whether neurons can be classified by the types of SV sRNAs they release. Knowing the specific types of sRNAs released by specific neurons will be of great importance in understanding synaptic transmission at specific terminals. It will also be important knowledge because it will impact the study of sRNA uptake at the synapse, which I will briefly discuss in the next section. One way of studying the different species of sRNAs at specific neurons is to isolate synaptic vesicles using immunoprecipitation against different types of vesicular transporters. Once isolated, the SV sRNAs from different classes of neurons can be sequenced. Another proposed experiment would be to apply specific synthesized sRNAs to neuronal cell cultures in order to see if there is any post synaptic effect. For

example, would the application of cholinergic specific sRNAs to a neuronal cell culture, lead to changes in the types of post-synaptic receptors found in the culture? Ultimately, it will be important to catalog the types of sRNAs found within different types of neurons, including GABAergic, glutamatergic, serotonergic and dopaminergic neurons.

sRNA Receptors and/or Cellular Uptake Mechanisms

Protein translation occurs within cellular environments; therefore, if released SV sRNAs are to have an effect on post-synaptic targets, it is likely they must bind to a receptor for selective endocytosis or be taken into the target cells by a bulk mechanism. Potential postsynaptic cellular targets include neurons and /or glial cells, including oligodendricytes in the CNS, and muscles and/or Schwann Cells in the PNS. One potential class of receptors found on the plasma membrane of neurons and glial cells are the toll like receptor (TLR) families. Many classes of TLRs exist, and some can be activated by binding DNA or RNA[168,169]. In particular, TLR 7 and 8 can bind single stranded RNAs, and they have been localized to both the plasma membrane as well as endolysosomal compartments[170]. TLR 7 and 8 are expressed by neurons in the nervous system, including layer 9 motor neurons in the spinal cord (*in situ* hybridization, Allen Brain Atlas (© 2015 Allen Institute for Brain Science. Allen Brain Atlas [Internet]. Available from: http://www.brain-map.org.)). Immunohistochemistry with antibodies against TLR 7 and 8 could be used to test if these TLR receptors are found at neuronal synapses, and therefore potential candidate receptors for trfRNAs. For co-localization studies in cholinergic neurons, ACh receptor labels can be used[136]; while for co-localization in Schwann Cells, glutamate receptors can be used[171]. To further support

this hypothesis, *in situ* hybridization on thin sections can be used as well. As further support for this hypothesis, *in situ* hybridization with sRNA antisense on thin sections can be used as well. If there is co - localization between sRNA antisense and TLR 7 or 8, it is possible they are the receptors for trfRNAs. Further tests would still be needed. Studies of neurons and glial cells of knock - out TLR 7 or 8 mice might shed further light on the pathway.

REFERENCES

1 Sherrington, C. The Integrative Action of the Nervous System. *Psychological bulletin* **4**, 198-199 (1907).

2 Katz, B. *Liverpool University Press,* The Release of Neural Transmitter Substances. (1969).

3 Palade, G. E. & Palay, S. L. Electron microscope observations of interneuronal and neuromuscular synapses. *Anat. Rec.*, 335-336 (1954).

4 Palay, S. L. Electron Microscope Study of the Cytoplasm of Neurons. *Anatomical Record* **118**, 336-336 (1954).

5 Heuser, J. E. & Reese, T. S. Structural changes after transmitter release at the frog neuromuscular junction. *J Cell Biol* **88**, 564-580 (1981).

6 Sudhof, T. C. The synaptic vesicle cycle. *Annual Review of Neuroscience* **27**, 509-547, doi:Doi 10.1146/Annurev.Neuro.26.041002.131412 (2004).

7 Pang, Z. P. & Sudhof, T. C. Cell biology of Ca2+-triggered exocytosis. *Curr Opin Cell Biol* **22**, 496-505, doi:10.1016/j.ceb.2010.05.001 (2010).

8 Jahn, R., Lang, T. & Sudhof, T. C. Membrane fusion. *Cell* **112**, 519-533 (2003).

9 Chaudhry, F. A., Edwards, R. H. & Fonnum, F. Vesicular neurotransmitter transporters as targets for endogenous and exogenous toxic substances. *Annu Rev Pharmacol* **48**, 277-301, doi:Doi 10.1146/Annurev.Pharmtox.46.120604.141146 (2008).

10 Reimer, R. J. & Edwards, R. H. Organic anion transport is the primary function of the SLC17/type I phosphate transporter family. *Pflugers Archiv : European journal of physiology* **447**, 629-635, doi:10.1007/s00424-003-1087-y (2004).

11 Takamori, S., Rhee, J. S., Rosenmund, C. & Jahn, R. Identification of a vesicular glutamate transporter that defines a glutamatergic phenotype in neurons. *Nature* **407**, 189-194, doi:10.1038/35025070 (2000).

12 Herzog, E. *et al.* The existence of a second vesicular glutamate transporter specifies subpopulations of glutamatergic neurons. *The Journal of neuroscience : the official journal of the Society for Neuroscience* **21**, RC181 (2001).

13 Gras, C. *et al.* A third vesicular glutamate transporter expressed by cholinergic and serotoninergic neurons. *The Journal of neuroscience : the official journal of the Society for Neuroscience* **22**, 5442-5451 (2002).

14 Sawada, K. *et al.* Identification of a vesicular nucleotide transporter. *Proceedings of the National Academy of Sciences of the United States of America* **105**, 5683-5686, doi:10.1073/pnas.0800141105 (2008).

15 Wimalasena, K. Vesicular monoamine transporters: structure-function, pharmacology, and medicinal chemistry. *Medicinal research reviews* **31**, 483-519, doi:10.1002/med.20187 (2011).

16 Alfonso, A., Grundahl, K., Duerr, J. S., Han, H. P. & Rand, J. B. The Caenorhabditis elegans unc-17 gene: a putative vesicular acetylcholine transporter. *Science* **261**, 617-619 (1993).

17 Brunk, I. *et al.* Regulation of vesicular monoamine and glutamate transporters by vesicle-associated trimeric G proteins: new jobs for long-known signal transduction molecules. *Handbook of experimental pharmacology*, 305-325 (2006).

18 Fremeau, R. T., Jr. *et al.* Vesicular glutamate transporters 1 and 2 target to functionally distinct synaptic release sites. *Science* **304**, 1815-1819, doi:10.1126/science.1097468 (2004).

19 Wojcik, S. M. *et al.* An essential role for vesicular glutamate transporter 1 (VGLUT1) in postnatal development and control of quantal size. *Proceedings of the National Academy of Sciences of the United States of America* **101**, 7158-7163, doi:10.1073/pnas.0401764101 (2004).

20 Wallen-Mackenzie, A. *et al.* Vesicular glutamate transporter 2 is required for central respiratory rhythm generation but not for locomotor central pattern generation. *The Journal of neuroscience : the official journal of the Society for Neuroscience* **26**, 12294-12307, doi:10.1523/JNEUROSCI.3855-06.2006 (2006).

21 Moechars, D. *et al.* Vesicular glutamate transporter VGLUT2 expression levels control quantal size and neuropathic pain. *The Journal of neuroscience : the official journal of the Society for Neuroscience* **26**, 12055-12066, doi:10.1523/JNEUROSCI.2556-06.2006 (2006).

22 Gras, C. *et al.* The vesicular glutamate transporter VGLUT3 synergizes striatal acetylcholine tone. *Nature neuroscience* **11**, 292-300, doi:10.1038/nn2052 (2008).

23 Knoth, J., Zallakian, M. & Njus, D. Stoichiometry of H+-linked dopamine transport in chromaffin granule ghosts. *Biochemistry* **20**, 6625-6629 (1981).

24 Johnson, R. G., Carty, S. E. & Scarpa, A. Proton - Substrate Stoichiometries during Active-Transport of Biogenic-Amines in Chromaffin Ghosts. *Journal of Biological Chemistry* **256**, 5773-5780 (1981).

25 Takahashi, N. *et al.* VMAT2 knockout mice: heterozygotes display reduced amphetamine-conditioned reward, enhanced amphetamine locomotion, and enhanced MPTP toxicity. *Proceedings of the National Academy of Sciences of the United States of America* **94**, 9938-9943 (1997).

26 Fon, E. A. *et al.* Vesicular transport regulates monoamine storage and release but is not essential for amphetamine action. *Neuron* **19**, 1271-1283 (1997).

27 Wang, Y. M. *et al.* Knockout of the vesicular monoamine transporter 2 gene results in neonatal death and supersensitivity to cocaine and amphetamine. *Neuron* **19**, 1285-1296 (1997).

28 Nguyen, M. L., Cox, G. D. & Parsons, S. M. Kinetic parameters for the vesicular acetylcholine transporter: two protons are exchanged for one acetylcholine. *Biochemistry* **37**, 13400-13410, doi:10.1021/bi9802263 (1998).

29 Prado, V. F. *et al.* Mice deficient for the vesicular acetylcholine transporter are myasthenic and have deficits in object and social recognition. *Neuron* **51**, 601-612, doi:Doi 10.1016/J.Neuron.2006.08.005 (2006).

30 Wojcik, S. M. *et al.* A shared vesicular carrier allows synaptic corelease of GABA and glycine. *Neuron* **50**, 575-587, doi:10.1016/j.neuron.2006.04.016 (2006).

31 Edwards, R. H. The neurotransmitter cycle and quantal size. *Neuron* **55**, 835-858, doi:10.1016/j.neuron.2007.09.001 (2007).

32 Arvidsson, U., Riedl, M., Elde, R. & Meister, B. Vesicular acetylcholine transporter (VAChT) protein: A novel and unique marker for cholinergic neurons in the central and peripheral nervous systems. *J Comp Neurol* **378**, 454-467 (1997).

33 Gasnier, B. The SLC32 transporter, a key protein for the synaptic release of inhibitory amino acids. *Pflugers Archiv : European journal of physiology* **447**, 756-759, doi:10.1007/s00424-003-1091-2 (2004).

34 Chaudhry, F. A. *et al.* The vesicular GABA transporter, VGAT, localizes to synaptic vesicles in sets of glycinergic as well as GABAergic neurons. *Journal of Neuroscience* **18**, 9733-9750 (1998).

35 Dale, H. Pharmacology and Nerve-endings (Walter Ernest Dixon Memorial Lecture): (Section of Therapeutics and Pharmacology). *Proceedings of the Royal Society of Medicine* **28**, 319-332 (1935).

36 Eccles, J. C., Fatt, P. & Koketsu, K. Cholinergic and inhibitory synapses in a pathway from motor-axon collaterals to motoneurones. *J Physiol* **126**, 524-562 (1954).

37 Hnasko, T. S. & Edwards, R. H. Neurotransmitter corelease: mechanism and physiological role. *Annual review of physiology* **74**, 225-243, doi:10.1146/annurev-physiol-020911-153315 (2012).

38 Whittaker, V. P., Dowdall, M. J. & Boyne, A. F. The storage and release of acetylcholine by cholinergic nerve terminals: recent results with non-mammalian preparations. *Biochemical Society symposium*, 49-68 (1972).

39 Wagner, J. A., Carlson, S. S. & Kelly, R. B. Chemical and physical characterization of cholinergic synaptic vesicles. *Biochemistry* **17**, 1199-1206 (1978).

40 Dowdall, M. J., Boyne, A. F. & Whittaker, V. P. Adenosine triphosphate. A constituent of cholinergic synaptic vesicles. *Biochem J* **140**, 1-12 (1974).

41 Vyas, S. & Bradford, H. F. Co-release of acetylcholine, glutamate and taurine from synaptosomes of Torpedo electric organ. *Neuroscience letters* **82**, 58-64 (1987).

42 Nirthanan, S., Garcia, G., 3rd, Chiara, D. C., Husain, S. S. & Cohen, J. B. Identification of binding sites in the nicotinic acetylcholine receptor for TDBzl-etomidate, a photoreactive positive allosteric effector. *The Journal of biological chemistry* **283**, 22051-22062, doi:10.1074/jbc.M801332200 (2008).

43 Miledi, R. Junctional and extra-junctional acetylcholine receptors in skeletal muscle fibres. *J Physiol* **151**, 24-30 (1960).

44 Kuffler, S. W. Physiology of neuro-muscular junctions; electrical aspects. *Fed Proc* **7**, 437-446 (1948).

45 Albuquerque, E. X., Pereira, E. F., Alkondon, M. & Rogers, S. W. Mammalian nicotinic acetylcholine receptors: from structure to function. *Physiol Rev* **89**, 73-120, doi:10.1152/physrev.00015.2008 (2009).

46 Dennis, M. J., Harris, A. J. & Kuffler, S. W. Synaptic transmission and its duplication by focally applied acetylcholine in parasympathetic neurons in the heart of the frog. *Proc R Soc Lond B Biol Sci* **177**, 509-539 (1971).

47 Burnstock, G. Historical review: ATP as a neurotransmitter. *Trends Pharmacol Sci* **27**, 166-176, doi:10.1016/j.tips.2006.01.005 (2006).

48 Del Puerto, A., Wandosell, F. & Garrido, J. J. Neuronal and glial purinergic receptors functions in neuron development and brain disease. *Frontiers in cellular neuroscience* **7**, 197, doi:10.3389/fncel.2013.00197 (2013).

49 Robitaille, R. Purinergic receptors and their activation by endogenous purines at perisynaptic glial cells of the frog neuromuscular junction. *The Journal of neuroscience : the official journal of the Society for Neuroscience* **15**, 7121-7131 (1995).

50 Giniatullin, A., Petrov, A. & Giniatullin, R. The involvement of P2Y12 receptors, NADPH oxidase, and lipid rafts in the action of extracellular ATP on synaptic transmission at the frog neuromuscular junction. *Neuroscience* **285**, 324-332, doi:10.1016/j.neuroscience.2014.11.039 (2015).

51 Cunha, R. A. & Ribeiro, J. A. ATP as a presynaptic modulator. *Life Sci* **68**, 119-137, doi:Doi 10.1016/S0024-3205(00)00923-1 (2000).

52 Mays, T. A., Sanford, J. L., Hanada, T., Chishti, A. H. & Rafael-Fortney, J. A. Glutamate Receptors Localize Postsynaptically at Neuromuscular Junctions in Mice. *Muscle Nerve* **39**, 343-349, doi:10.1002/mus.21099 (2009).

53 Rinholm, J. E. *et al.* Subcellular localization of the glutamate transporters GLAST and GLT at the neuromuscular junction in rodents. *Neuroscience* **145**, 579-591, doi:10.1016/j.neuroscience.2006.12.041 (2007).

54 Urazaev, A. K., Magsumov, S. T., Poletayev, G. I., Nikolsky, E. E. & Vyskocil, F. Muscle Nmda Receptors Regulate the Resting Membrane-Potential through No-Synthase. *Physiol Res* **44**, 205-208 (1995).

55 Pinard, A., Levesque, S., Vallee, J. & Robitaille, R. Glutamatergic modulation of synaptic plasticity at a PNS vertebrate cholinergic synapse. *European Journal of Neuroscience* **18**, 3241-3250, doi:10.1046/j.1460-9568.2003.03028.x (2003).

56 Malomouzh, A. I. *et al.* Glutamate regulation of non-quantal release of acetylcholine in the rat neuromuscular junction. *Journal of neurochemistry* **85**, 206-213 (2003).

57 Whittaker, V. P. The structure and function of cholinergic synaptic vesicles. The Third Thudichum Lecture. *Biochemical Society transactions* **12**, 561-576 (1984).

58 Axelrod, D. Total internal reflection fluorescence microscopy in cell biology. *Methods in enzymology* **361**, 1-33 (2003).

59 Demb, J. B. Cellular mechanisms for direction selectivity in the retina. *Neuron* **55**, 179-186, doi:10.1016/j.neuron.2007.07.001 (2007).

60 Gillespie, D. C., Kim, G. & Kandler, K. Inhibitory synapses in the developing auditory system are glutamatergic. *Nature neuroscience* **8**, 332-338, doi:10.1038/nn1397 (2005).

61 Gutierrez, R. *et al.* Plasticity of the GABAergic phenotype of the "glutamatergic" granule cells of the rat dentate gyrus. *The Journal of neuroscience : the official journal of the Society for Neuroscience* **23**, 5594-5598 (2003).

62 Ren, J. *et al.* Habenula "Cholinergic" Neurons Corelease Glutamate and Acetylcholine and Activate Postsynaptic Neurons via Distinct Transmission Modes. *Neuron* **69**, 445-452, doi:Doi 10.1016/J.Neuron.2010.12.038 (2011).

63 El Mestikawy, S., Wallen-Mackenzie, A., Fortin, G. M., Descarries, L. & Trudeau, L. E. From glutamate co-release to vesicular synergy: vesicular glutamate transporters. *Nature reviews. Neuroscience* **12**, 204-216, doi:10.1038/nrn2969 (2011).

64 Herzog, E. *et al.* Expression of vesicular glutamate transporters, VGLUT1 and VGLUT2, in cholinergic spinal motoneurons. *Eur J Neurosci* **20**, 1752-1760, doi:10.1111/j.1460-9568.2004.03628.x (2004).

65 Lamotte d'Incamps, B. & Ascher, P. Four excitatory postsynaptic ionotropic receptors coactivated at the motoneuron-Renshaw cell synapse. *The Journal of neuroscience : the official journal of the Society for Neuroscience* **28**, 14121-14131, doi:10.1523/JNEUROSCI.3311-08.2008 (2008).

66 Chuhma, N. *et al.* Dopamine neurons mediate a fast excitatory signal via their glutamatergic synapses. *Journal of Neuroscience* **24**, 972-981, doi:Doi 10.1523/Jneurosci.4317-03.2004 (2004).

67 Lavin, A. *et al.* Mesocortical dopamine neurons operate in distinct temporal domains using multimodal signaling. *Journal of Neuroscience* **25**, 5013-5023, doi:Doi 10.1523/Jneurosci.0557-05.2005 (2005).

68 Ho, V. M., Lee, J. A. & Martin, K. C. The cell biology of synaptic plasticity. *Science* **334**, 623-628, doi:10.1126/science.1209236 (2011).

69 Holt, C. E. & Schuman, E. M. The central dogma decentralized: new perspectives on RNA function and local translation in neurons. *Neuron* **80**, 648-657, doi:10.1016/j.neuron.2013.10.036 (2013).

70 Flavell, S. W. & Greenberg, M. E. Signaling mechanisms linking neuronal activity to gene expression and plasticity of the nervous system. *Annu Rev Neurosci* **31**, 563-590, doi:10.1146/annurev.neuro.31.060407.125631 (2008).

71 Gebauer, F. & Hentze, M. W. Molecular mechanisms of translational control. *Nature reviews. Molecular cell biology* **5**, 827-835, doi:10.1038/nrm1488 (2004).

72 Besse, F. & Ephrussi, A. Translational control of localized mRNAs: restricting protein synthesis in space and time. *Nature reviews. Molecular cell biology* **9**, 971-980, doi:10.1038/nrm2548 (2008).

73 Scheper, G. C., van der Knaap, M. S. & Proud, C. G. Translation matters: protein synthesis defects in inherited disease. *Nature reviews. Genetics* **8**, 711-723, doi:10.1038/nrg2142 (2007).

74 Storz, G., Opdyke, J. A. & Zhang, A. Controlling mRNA stability and translation with small, noncoding RNAs. *Current opinion in microbiology* **7**, 140-144, doi:10.1016/j.mib.2004.02.015 (2004).

75 Emara, M. M. *et al.* Angiogenin-induced tRNA-derived stress-induced RNAs promote stress-induced stress granule assembly. *The Journal of biological chemistry* **285**, 10959-10968, doi:10.1074/jbc.M109.077560 (2010).

76 Siomi, H. & Siomi, M. C. Posttranscriptional regulation of microRNA biogenesis in animals. *Molecular cell* **38**, 323-332, doi:10.1016/j.molcel.2010.03.013 (2010).

77 Ballarino, M. *et al.* Coupled RNA processing and transcription of intergenic primary microRNAs. *Molecular and cellular biology* **29**, 5632-5638, doi:10.1128/MCB.00664-09 (2009).

78 Bushati, N. & Cohen, S. M. microRNA functions. *Annual review of cell and developmental biology* **23**, 175-205, doi:10.1146/annurev.cellbio.23.090506.123406 (2007).

79 Ameres, S. L. & Zamore, P. D. Diversifying microRNA sequence and function. *Nature reviews. Molecular cell biology* **14**, 475-488, doi:10.1038/nrm3611 (2013).

80 Du, T. & Zamore, P. D. microPrimer: the biogenesis and function of microRNA. *Development* **132**, 4645-4652, doi:10.1242/dev.02070 (2005).

81 Hutvagner, G. & Zamore, P. D. A microRNA in a multiple-turnover RNAi enzyme complex. *Science* **297**, 2056-2060, doi:10.1126/science.1073827 (2002).

82 Martinez, J. & Tuschl, T. RISC is a 5 ' phosphomonoester-producing RNA endonuclease. *Gene Dev* **18**, 975-980, doi:Doi 10.1101/Gad.1187904 (2004).

83 Ivanov, P., Emara, M. M., Villen, J., Gygi, S. P. & Anderson, P. Angiogenin-induced tRNA fragments inhibit translation initiation. *Molecular cell* **43**, 613-623, doi:10.1016/j.molcel.2011.06.022 (2011).

84 Bjork, G. R. *et al.* Transfer-Rna Modification. *Annu Rev Biochem* **56**, 263-287, doi:Doi 10.1146/Annurev.Biochem.56.1.263 (1987).

85 Zhang, S. D., Sun, L. & Kragler, F. The Phloem-Delivered RNA Pool Contains Small Noncoding RNAs and Interferes with Translation. *Plant Physiol* **150**, 378-387, doi:Doi 10.1104/Pp.108.134767 (2009).

86 Wang, Q. *et al.* Identification and functional characterization of tRNA-derived RNA fragments (tRFs) in respiratory syncytial virus infection. *Molecular therapy : the journal of the American Society of Gene Therapy* **21**, 368-379, doi:10.1038/mt.2012.237 (2013).

87 Kohn, M., Pazaitis, N. & Huttelmaier, S. Why YRNAs? About Versatile RNAs and Their Functions. *Biomolecules* **3**, 143-156, doi:10.3390/biom3010143 (2013).

88 Farris, A. D., Puvion-Dutilleul, F., Puvion, E., Harley, J. B. & Lee, L. A. The ultrastructural localization of 60-kDa Ro protein and human cytoplasmic RNAs: association with novel electron-dense bodies. *Proceedings of the National Academy of Sciences of the United States of America* **94**, 3040-3045 (1997).

89 Wolin, S. L. & Steitz, J. A. Genes for 2 Small Cytoplasmic Ro Rnas Are Adjacent and Appear to Be Single-Copy in the Human Genome. *Cell* **32**, 735-744, doi:Doi 10.1016/0092-8674(83)90059-4 (1983).

90 Nicolas, F. E., Hall, A. E., Csorba, T., Turnbull, C. & Dalmay, T. Biogenesis of Y RNA-derived small RNAs is independent of the microRNA pathway. *FEBS letters* **586**, 1226-1230, doi:DOI 10.1016/j.febslet.2012.03.026 (2012).

91 Yu, C., Gershwin, M. E. & Chang, C. Diagnostic criteria for systemic lupus erythematosus: a critical review. *J Autoimmun* **48-49**, 10-13, doi:10.1016/j.jaut.2014.01.004 (2014).

92 Gendron, M., Roberge, D. & Boire, G. Heterogeneity of human Ro ribonucleoproteins (RNPS): nuclear retention of Ro RNPS containing the human hY5 RNA in human and mouse cells. *Clinical and experimental immunology* **125**, 162-168 (2001).

93 Tuček, S. *Choline acetyltransferase and the synthesis of acetylcholine*. Vol. 86 125-165 (Springer, 1988).

94 Erickson, J. D. *et al.* Functional identification of a vesicular acetylcholine transporter and its expression from a "cholinergic" gene locus. *The Journal of biological chemistry* **269**, 21929-21932 (1994).

95 Ren, J. *et al.* Habenula "cholinergic" neurons co-release glutamate and acetylcholine and activate postsynaptic neurons via distinct transmission modes. *Neuron* **69**, 445-452, doi:10.1016/j.neuron.2010.12.038 (2011).

96 Bellocchio, E. E., Reimer, R. J., Fremeau, R. T., Jr. & Edwards, R. H. Uptake of glutamate into synaptic vesicles by an inorganic phosphate transporter. *Science* **289**, 957-960 (2000).

97 Varoqui, H., Schafer, M. K., Zhu, H., Weihe, E. & Erickson, J. D. Identification of the differentiation-associated Na+/PI transporter as a novel vesicular glutamate transporter expressed in a distinct set of glutamatergic synapses. *J. Neurosci.* **22**, 142-155 (2002).

98 Takamori, S., Malherbe, P., Broger, C. & Jahn, R. Molecular cloning and functional characterization of human vesicular glutamate transporter 3. *EMBO reports* **3**, 798-803, doi:10.1093/embo-reports/kvf159 (2002).

99 Shigeri, Y., Seal, R. P. & Shimamoto, K. Molecular pharmacology of glutamate transporters, EAATs and VGLUTs. *Brain Res. Brain Res. Rev.* **45**, 250-265, doi:10.1016/j.brainresrev.2004.04.004 (2004).

100 Axelrod, D., Burghardt, T. P. & Thompson, N. L. Total internal reflection fluorescence. *Annual review of biophysics and bioengineering* **13**, 247-268, doi:10.1146/annurev.bb.13.060184.001335 (1984).

101 Mutch, S. A. *et al.* Determining the number of specific proteins in cellular compartments by quantitative microscopy. *Nature protocols* **6**, 1953-1968, doi:10.1038/nprot.2011.414 (2011).

102 Ohsawa, K., Dowe, G. H., Morris, S. J. & Whittaker, V. P. The lipid and protein content of cholinergic synaptic vesicles from the electric organ of Torpedo marmorata purified to constant composition: implications for vesicle structure. *Brain research* **161**, 447-457 (1979).

103 Jahn, R. & Maycox, P. R. *Protein components and neurotransmitter uptake in brain synaptic vesicles*. 411-424 (1988).

104 Gaffield, M. A. & Betz, W. J. Imaging synaptic vesicle exocytosis and endocytosis with FM dyes. *Nature protocols* **1**, 2916-2921, doi:10.1038/nprot.2006.476 (2006).

105 Agresti, A. & Coull, B. A. Approximate Is Better than "Exact" for Interval Estimation of Binomial Proportions. *The American Statistician* **52**, 119-126 (1998).

106 Tashiro, T. & Stadler, H. Chemical composition of cholinergic synaptic vesicles from Torpedo marmorata based on improved purification. *Eur. J. Biochem.* **90**, 479-487 (1978).

107 Fallon, J. R., Nitkin, R. M., Reist, N. E., Wallace, B. G. & McMahan, U. J. Acetycholine receptor-aggregating factor is similar to molecules concentrated at neuromuscular junctions. *Nature* **315**, 571-574 (1985).

108 Nagwaney, S. *et al.* Macromolecular connections of active zone material to docked synaptic vesicles and presynaptic membrane at neuromuscular junctions of mouse. *J Comp Neurol* **513**, 457-468, doi:10.1002/cne.21975 (2009).

109 Wiedenmann, B. & Franke, W. W. Identification and localization of synaptophysin, an integral membrane glycoprotein of Mr 38,000 characteristic of presynaptic vesicles. *Cell* **41**, 1017-1028 (1985).

110 Mutch, S. A. *et al.* Protein quantification at the single vesicle level reveals that a subset of synaptic vesicle proteins are trafficked with high precision. *J. Neurosci.* **31**, 1461-1470, doi:10.1523/JNEUROSCI.3805-10.2011 (2011).

111 Harlow, M. L. *et al.* Alignment of synaptic vesicle macromolecules with the macromolecules in active zone material that direct vesicle docking. *PloS one* **8**, e69410, doi:10.1371/journal.pone.0069410 (2013).

112 Burnstock, G. Historical review: ATP as a neurotransmitter. *Trends Pharmacol. Sci.* **27**, 166-176, doi:10.1016/j.tips.2006.01.005 (2006).

113 Urazaev, A. K., Magsumov, S. T., Poletayev, G. I., Nikolsky, E. E. & Vyskocil, F. Muscle NMDA receptors regulate the resting membrane potential through NO-synthase. *Physiol. Res.* **44**, 205-208 (1995).

114 Pinard, A., Levesque, S., Vallee, J. & Robitaille, R. Glutamatergic modulation of synaptic plasticity at a PNS vertebrate cholinergic synapse. *Eur. J. Neurosci.* **18**, 3241-3250 (2003).

115 Dale, H. H. The action of certain esters and ethers of choline, and their relation to muscarine. *J. Pharmacol. Exp. Ther.* **6**, 147-190 (1914).

116 Loewi, O. Humoral transferability of the heart nerve effect. I. Announcement. *Pflug Arch Ges Phys* **189**, 239-242, doi:Doi 10.1007/Bf01738910 (1921).

117 Fatt, P. & Katz, B. Spontaneous Subthreshold Activity at Motor Nerve Endings. *J Physiol-London* **117**, 109-128 (1952).

118 Bliss, T. V. P. & Lomo, T. Long-Lasting Potentiation of Synaptic Transmission in Dentate Area of Anesthetized Rabbit Following Stimulation of Perforant Path. *J Physiol-London* **232**, 331-356 (1973).

119 Davis, H. P. & Squire, L. R. Protein-Synthesis and Memory - a Review. *Psychol. Bull.* **96**, 518-559, doi:Doi 10.1037/0033-2909.96.3.518 (1984).

120 Steward, O. & Levy, W. B. Preferential localization of polyribosomes under the base of dendritic spines in granule cells of the dentate gyrus. *J. Neurosci.* **2**, 284-291 (1982).

121 Hawkins, R. D., Kandel, E. R. & Bailey, C. H. Molecular mechanisms of memory storage in Aplysia. *Biol. Bull.* **210**, 174-191 (2006).

122 Pfeiffer, B. E. & Huber, K. M. Current advances in local protein synthesis and synaptic plasticity. *The Journal of neuroscience : the official journal of the Society for Neuroscience* **26**, 7147-7150, doi:10.1523/JNEUROSCI.1797-06.2006 (2006).

123 Smalheiser, N. R. The RNA-centred view of the synapse: non-coding RNAs and synaptic plasticity. *Philosophical transactions of the Royal Society of London. Series B, Biological sciences* **369**, doi:10.1098/rstb.2013.0504 (2014).

124 Bramham, C. R. & Wells, D. G. Dendritic mRNA: transport, translation and function. *Nat. Rev. Neurosci.* **8**, 776-789, doi:Doi 10.1038/Nrn2150 (2007).

125 Pichardo-Casas, I. *et al.* Expression profiling of synaptic microRNAs from the adult rat brain identifies regional differences and seizure-induced dynamic modulation. *Brain Res.* **1436**, 20-33, doi:10.1016/j.brainres.2011.12.001 (2012).

126 Xu, J., Chen, Q., Zen, K., Zhang, C. & Zhang, Q. Synaptosomes secrete and uptake functionally active microRNAs via exocytosis and endocytosis pathways. *J. Neurochem.* **124**, 15-25, doi:10.1111/jnc.12057 (2013).

127 Perreault, J., Perreault, J. P. & Boire, G. Ro-associated Y RNAs in metazoans: evolution and diversification. *Mol. Biol. Evol.* **24**, 1678-1689, doi:10.1093/molbev/msm084 (2007).

128 Whittaker, V. P., Essman, W. B. & Dowe, G. H. The isolation of pure cholinergic synaptic vesicles from the electric organs of elasmobranch fish of the family Torpedinidae. *Biochem. J.* **128**, 833-845 (1972).

129 Hell, J. W., Maycox, P. R., Stadler, H. & Jahn, R. Uptake of GABA by rat brain synaptic vesicles isolated by a new procedure. *EMBO J.* **7**, 3023-3029 (1988).

130 Lamparski, H. G. *et al.* Production and characterization of clinical grade exosomes derived from dendritic cells. *J. Immunol. Methods* **270**, 211-226 (2002).

131 Witwer, K. W. *et al.* Standardization of sample collection, isolation and analysis methods in extracellular vesicle research. *Journal of extracellular vesicles* **2**, doi:10.3402/jev.v2i0.20360 (2013).

132 Montecalvo, A. *et al.* Mechanism of transfer of functional microRNAs between mouse dendritic cells via exosomes. *Blood* **119**, 756-766, doi:Doi 10.1182/Blood-2011-02-338004 (2012).

133 Valadi, H. *et al.* Exosome-mediated transfer of mRNAs and microRNAs is a novel mechanism of genetic exchange between cells. *Nat. Cell Biol.* **9**, 654-659, doi:10.1038/ncb1596 (2007).

134 Kao, T. H. & Crothers, D. M. A Proton-Coupled Conformational Switch of Escherichia-Coli 5s Ribosomal-Rna. *P Natl Acad Sci-Biol* **77**, 3360-3364, doi:Doi 10.1073/Pnas.77.6.3360 (1980).

135 Vanaken, T., Foxallvanaken, S., Castleman, S. & Fergusonmiller, S. Alkyl Glycoside Detergents - Synthesis and Applications to the Study of Membrane-Proteins. *Methods Enzymol.* **125**, 27-35 (1986).

136 Li, H. & Harlow, M. L. Individual synaptic vesicles from the electroplaque of Torpedo californica, a classic cholinergic synapse, also contain transporters for glutamate and ATP. *Physiol Rep* **2**, e00206, doi:10.1002/phy2.206 (2014).

137 Takamori, S., Riedel, D. & Jahn, R. Immunoisolation of GABA-specific synaptic vesicles defines a functionally distinct subset of synaptic vesicles. *J. Neurosci.* **20**, 4904-4911 (2000).

138 Fu, H. *et al.* Stress induces tRNA cleavage by angiogenin in mammalian cells. *FEBS letters* **583**, 437-442, doi:10.1016/j.febslet.2008.12.043 (2009).

139 Yamasaki, S., Ivanov, P., Hu, G. F. & Anderson, P. Angiogenin cleaves tRNA and promotes stress-induced translational repression. *J. Cell Biol.* **185**, 35-42, doi:10.1083/jcb.200811106 (2009).

140 Varshney, U., Lee, C. P. & RajBhandary, U. L. Direct analysis of aminoacylation levels of tRNAs in vivo. Application to studying recognition of Escherichia coli initiator tRNA mutants by glutaminyl-tRNA synthetase. *J. Biol. Chem.* **266**, 24712-24718 (1991).

141 Anger, A. M. *et al.* Structures of the human and Drosophila 80S ribosome. *Nature* **497**, 80-85, doi:10.1038/nature12104 (2013).

142 Takamori, S. *et al.* Molecular anatomy of a trafficking organelle. *Cell* **127**, 831-846 (2006).

143 Hammond, S. M., Bernstein, E., Beach, D. & Hannon, G. J. An RNA-directed nuclease mediates post-transcriptional gene silencing in Drosophila cells. *Nature* **404**, 293-296, doi:10.1038/35005107 (2000).

144 Ahmed, S., Holt, M., Riedel, D. & Jahn, R. Small-scale isolation of synaptic vesicles from mammalian brain. *Nature protocols* **8**, 998-1009, doi:10.1038/nprot.2013.053 (2013).

145 Gruber, A. R., Lorenz, R., Bernhart, S. H., Neubock, R. & Hofacker, I. L. The Vienna RNA websuite. *Nucleic Acids Res.* **36**, W70-74, doi:10.1093/nar/gkn188 (2008).

146 Popenda, M. *et al.* Automated 3D structure composition for large RNAs. *Nucleic Acids Res.* **40**, e112, doi:10.1093/nar/gks339 (2012).

147 Hanada, T. *et al.* CLP1 links tRNA metabolism to progressive motor-neuron loss. *Nature* **495**, 474-480, doi:10.1038/nature11923 (2013).

148 Thompson, D. M. & Parker, R. Stressing out over tRNA cleavage. *Cell* **138**, 215-219, doi:10.1016/j.cell.2009.07.001 (2009).

149 Peng, H. *et al.* A novel class of tRNA-derived small RNAs extremely enriched in mature mouse sperm. *Cell research* **22**, 1609-1612, doi:10.1038/cr.2012.141 (2012).

150 Tan, C. L. *et al.* MicroRNA-128 governs neuronal excitability and motor behavior in mice. *Science* **342**, 1254-1258, doi:10.1126/science.1244193 (2013).

151 Jin, Y. *et al.* MicroRNA-99 family targets AKT/mTOR signaling pathway in dermal wound healing. *PloS one* **8**, e64434, doi:10.1371/journal.pone.0064434 (2013).

152 Jovicic, A., Jolissaint, J. F. Z., Moser, R., Santos, M. D. S. & Luthi-Carter, R. MicroRNA-22 (miR-22) Overexpression Is Neuroprotective via General Anti-Apoptotic Effects and May also Target Specific Huntington's Disease-Related Mechanisms. *PloS one* **8**, doi:ARTN e54222
DOI 10.1371/journal.pone.0054222 (2013).

153 Gardiner, E. *et al.* Imprinted DLK1-DIO3 region of 14q32 defines a schizophrenia-associated miRNA signature in peripheral blood mononuclear cells. *Molecular psychiatry* **17**, 827-840, doi:10.1038/mp.2011.78 (2012).

154 Goodarzi, H. *et al.* Endogenous tRNA-Derived Fragments Suppress Breast Cancer Progression via YBX1 Displacement. *Cell* **161**, 790-802, doi:10.1016/j.cell.2015.02.053 (2015).

155 Ivanov, P. *et al.* G-quadruplex structures contribute to the neuroprotective effects of angiogenin-induced tRNA fragments. *Proc Natl Acad Sci U S A* **111**, 18201-18206, doi:10.1073/pnas.1407361111 (2014).

156 Lagendijk, A. K., Moulton, J. D. & Bakkers, J. Revealing details: whole mount microRNA in situ hybridization protocol for zebrafish embryos and adult tissues. *Biology open* **1**, 566-569, doi:10.1242/bio.2012810 (2012).

157 Wolin, S. L. & Matera, A. G. The trials and travels of tRNA. *Genes Dev* **13**, 1-10 (1999).

158 Cantara, W. A. *et al.* The RNA Modification Database, RNAMDB: 2011 update. *Nucleic acids research* **39**, D195-201, doi:10.1093/nar/gkq1028 (2011).

159 Agris, P. F. Bringing order to translation: the contributions of transfer RNA anticodon-domain modifications. *EMBO Rep* **9**, 629-635, doi:10.1038/embor.2008.104 (2008).

160 Bartel, D. P. MicroRNAs: genomics, biogenesis, mechanism, and function. *Cell* **116**, 281-297 (2004).

161 Shih, J. D. & Hunter, C. P. SID-1 is a dsRNA-selective dsRNA-gated channel. *Rna* **17**, 1057-1065, doi:10.1261/rna.2596511 (2011).

162 Winston, W. M., Sutherlin, M., Wright, A. J., Feinberg, E. H. & Hunter, C. P. Caenorhabditis elegans SID-2 is required for environmental RNA interference. *Proceedings of the National Academy of Sciences of the United States of America* **104**, 10565-10570, doi:10.1073/pnas.0611282104 (2007).

163 Kish, P. E. & Ueda, T. Glutamate accumulation into synaptic vesicles. *Methods in enzymology* **174**, 9-25 (1989).

164 Meister, G. Argonaute proteins: functional insights and emerging roles. *Nature reviews. Genetics* **14**, 447-459, doi:10.1038/nrg3462 (2013).

165 Hutvagner, G. & Simard, M. J. Argonaute proteins: key players in RNA silencing. *Nature reviews. Molecular cell biology* **9**, 22-32, doi:10.1038/nrm2321 (2008).

166 Zhao, H., Lii, Y., Zhu, P. & Jin, H. Isolation and profiling of protein-associated small RNAs. *Methods Mol Biol* **883**, 165-176, doi:10.1007/978-1-61779-839-9_13 (2012).

167 Piskounova, E. *et al.* Determinants of microRNA processing inhibition by the developmentally regulated RNA-binding protein Lin28. *The Journal of biological chemistry* **283**, 21310-21314, doi:10.1074/jbc.C800108200 (2008).

168 Broz, P. & Monack, D. M. Newly described pattern recognition receptors team up against intracellular pathogens. *Nat Rev Immunol* **13**, 551-565, doi:10.1038/nri3479 (2013).

169 Leulier, F. & Lemaitre, B. Toll-like receptors--taking an evolutionary approach. *Nature reviews. Genetics* **9**, 165-178, doi:10.1038/nrg2303 (2008).

170 Heil, F. *et al.* Species-specific recognition of single-stranded RNA via toll-like receptor 7 and 8. *Science* **303**, 1526-1529, doi:10.1126/science.1093620 (2004).

171 Dememes, D., Lleixa, A. & Dechesne, C. J. Cellular and subcellular localization of AMPA-selective glutamate receptors in the mammalian peripheral vestibular system. *Brain research* **671**, 83-94 (1995).